Investigating the role of exosomes in Medulloblastoma and their involvement in metastasis

Hannah Kate Jackson BSc (Hons)

Children's Brain Tumour Research Centre

School of Medicine

The University of Nottingham

Supervisors: Dr Beth Coyle and Dr Ian Kerr

Table of Contents

Acknowledgements v

Abstract vi

List of Tables ix

Abbreviations x

1. Introduction 12

1.1 Medulloblastoma 12

1.1.1 Tumour staging 14

1.1.2 Histology 15

1.1.3 Molecular subgroups 16

1.1.3.1 WNT medulloblastoma 17

1.1.3.2 SHH medulloblastoma 18

1.1.3.3 Group 3 medulloblastoma 20

1.1.3.4 Group 4 medulloblastoma 20

1.1.4 Risk stratification 21

1.1.5 Treatment 22

1.2 Metastasis- one of the hallmarks of cancer 23

1.2.1 Molecular mechanisms of metastasis 26

1.2.2 Metastasis in medulloblastoma 26

1.2.2.1 Markers of metastasis in Medulloblastoma 27

1.3 Extracellular vesicles 32

1.3.1 Exosomes 32

1.3.1.1 Exosomal content 34

1.3.1.2 Biological functions of exosomes 35

1.3.2 Microvesicles 37
1.3.3 Apoptotic bodies 37
1.3.4 Isolation and analysis of exosomes 38
1.3.4.1 Ultracentrifugation 39
1.3.4.2 Exosome precipitation 39
1.3.4.3 Ultrafiltration 40
1.3.4.4 Sucrose gradient 40
1.3.4.5 Western blot analysis 40
1.3.4.6 Transmission electron microscopy 41
1.3.4.7 Nanoparticle tracking analysis 41
1.4 The significance of exosomes in cancer 42
1.4.1 Exosomes as biomarkers in cancer 42
1.4.2 Exosomes as mediators of intercellular communication in cancer 43
1.4.3 Exosomes in medulloblastoma 45
1.5 Hypothesis and aims 47
2. Materials and methods 49
2.1 Materials 49
2.1.1 Antibodies 49
2.1.2 Cell lines 49
2.2 Methods 51
2.2.1 Tissue culture methods 51
2.2.1.1 Recovering cells from liquid nitrogen 51
2.2.1.2 Sub-culturing cell lines 51
2.2.1.3 Freezing cells for stocks 52

2.2.1.4 Snap freezing cell pellets 52
2.2.1.5 Cell counting 52
2.2.2 Extracellular vesicle techniques 52
2.2.2.1 Particle-free FBS 52
2.2.2.2 Isolation of exosomes and microvesicles 53
2.2.3 Protein biochemistry 54
2.2.3.1 Protein isolation 54
2.2.3.2 Protein quantification by Bradford assay 54
2.2.3.3 SDS-PAGE 54
2.2.3.4 Western Blot 56
2.2.4 Electron microscopy 57
2.2.5 Nanoparticle analysis 57
2.2.5.1 NanoSight 57
2.2.5.2 Dynamic light scattering 58
2.2.6 Gene expression analysis 58
2.2.6.1 Total RNA isolation 58
2.2.6.2 DNase treatment 59
2.2.6.3 Measuring RNA concentration and purity 59
2.2.6.4 Complementary DNA (cDNA) synthesis 60
2.2.6.5 Quantitative real-time PCR (qRT-PCR) 60
2.2.7 Statistical analysis 63
3. Results 64
3.1 Medulloblastoma cells release two distinct populations of extracellular vesicles 64

3.1.1 EV samples did not contain foetal bovine serum EV impurities..... 65

3.1.2 Verification of exosomes and microvesicles by NTA..... 66

3.1.3 Verification of exosomes and microvesciles by TEM..... 70

3.1.4 Verification of exosomes by Western Blot analysis..... 73

3.2 Differential profiles of EVs from metastatic tumour cells compared with non-metastatic cells..... 75

3.2.1 NTA detected more metastatic exosomes..... 75

3.2.2 Metastatic exosomes contain more protein cargo..... 76

3.2.3 Metastatic exosomes contain more RNA cargo..... 78

3.3 Markers of metastasis present in extracellular vesicles..... 81

3.3.1 Primer optimisation of candidate markers..... 81

3.3.2 Candidate markers of metastasis are present in EVs..... 84

3.3.2.1 c-Met expression..... 84

3.3.2.2 ABCB1 expression..... 88

3.3.2.3 ITG-A9 expression..... 90

4. Discussion and future work..... 93

4.1 Exosomes and MV differ in their morphology and internal cargo..... 94

4.2 Metastatic tumour cells secrete higher concentrations of exosomes ... 97

4.3 RNA from cells are selectively transferred into extracellular vesicles .. 98

5. Main conclusions 104

6. References 105

Acknowledgements

Firstly, I would like to thank my supervisor's Dr Beth Coyle and Dr Ian Kerr, for giving me the opportunity to undertake this masters, who encouraged, taught and guided me throughout; I am extremely grateful. It has been a privilege to pursue such an interesting research topic, and I am so excited to spend the next three years working alongside you both.

A special thanks are owed to Franziska for always steering me in the right direction, she is the best postdoc I could have ever asked for!

I would also like to thank Sophie, who has been the bestest friend to me for the past 8 years, I certainly wouldn't be where I am now if it wasn't for you. A huge thank you also goes to my lovely lab girls, Macha, Christine and Alice, I am so lucky to have had you all by my side during the tough and happy times.

I thank all my wonderful lab friends for making this lab such a lovely place to work in and for the countless times you have all helped me; Jasper, James, Matt, Aishah, Huda, Josh, Maria, Tim, Catherine, Helen, Becky, Lisa, Jennifer, Dawn and Johnathon.

I gratefully acknowledge Graham Rance and Rhys Lodge at NMRC for all your help and support with NanoSight and electron microscopy analysis.

Most of all, I would like to thank my amazing family and my wonderful boyfriend, whose unconditional love and support has got me through the hardest moments and with whom I am so glad to share all the happy ones with. I am incredibly lucky to have you all.

Abstract

Medulloblastoma, the most prevalent malignant paediatric brain tumour, accounts for around 10% of all cancer-related deaths in children. Medulloblastomas frequently metastasize; over one-third of tumours are metastatic at diagnosis and almost all patients have metastases at relapse. These patients are categorised as high-/very high-risk. Currently there is no curative treatment for patients with metastatic medulloblastoma, any advancements in the underlying biology of medulloblastoma, particularly regarding their metastatic behaviour, could help to improve patient outcome. One area that remains relatively unstudied is medulloblastoma extracellular vesicles.

Extracellular vesicles are a heterogeneous population of nano-sized, cell derived vesicles. They can be categorised into three main classes, exosomes, microvesicles and apoptotic bodies. Accumulating evidence indicates that exosomes play vital roles in cancer progression. They have been shown to transfer oncogenic proteins and nucleic acid cargo to recipient cells, which modulates their activity and plays a decisive role in tumorigenesis. Exosomes have been shown to promote tumour growth and progression, by enhancing tumour cell migration and invasion, drug resistance and immunosuppressive functions.

In this project, a protocol was optimised for the isolation and characterisation of medulloblastoma extracellular vesicles. Success of this was validated by nanoparticle tracking analysis, electron microscopy and western blot analysis. Our data demonstrates that medulloblastoma cells secrete two distinct populations of exosomes and microvesicles, with unique size, morphology and cargo. Our data also shows that more aggressive, metastatic cell lines produce higher quantities of exosomes compared with less aggressive, non-metastatic cell lines. In the final part of the project, candidate genes of medulloblastoma metastasis, identified from the literature, were profiled in cells and their derivative extracellular vesicles.

Our results have shown that RNA of medulloblastoma associated genes are passed from the parent cells to exosomes and microvesicles.

List of Figures

Figure 1. Post-gadolinium MRI 13

Figure 2. Histological variants of Medulloblastoma 16

Figure 3. WNT and SHH signalling pathways schematic 19

Figure 4.Multistep process of metastasis 24

Figure 5. Epithelial to mesenchymal transition and the reversion 25

Figure 6. Release of exosomes and microvesicles 33

Figure 7. Exosome content 35

Figure 8. TEM of microvesicles and exosomes 41

Figure 9. Schematic representation of EV isolation 53

Figure 10. FBS comparison to ultracentrifuge FBS 66

Figure 11. Nanoparticle tracking video frame of extracellular vesicles 67

Figure 12. Nanoparticle tracking showing EV sizes and concentrations 68

Figure 13. Nanoparticle tracking showing EV sizes and concentrations 69

Figure 14.TEM of dried uranyl acetate and exosomes 71

Figure 15. TEM images of exosomes 72

Figure 16. TEM images of microvesicles 73

Figure 17. Western blot analysis of medulloblastoma derived exosomes 74

Figure 18. Particle concentrations of extracellular vesicles 76

Figure 19. Protein amounts in cells 77

Figure 20. Protein amounts in extracellular vesicles 77

Figure 21. Yield and purity of exosomal RNA extracted by 4 methods 79

Figure 22. RNA amount in cells 80

Figure 23. RNA amount in extracellular vesicles 80

Figure 24. PCR amplification results associated with different annealing temperatures 82

Figure 25. Successful primer optimisation of c-Met, ITGA9 and ABCB1 83

Figure 26. c-Met expression levels in cell lysates 86

Figure 27. GAPDH expression in EVs 86
Figure 28. Fold change in c-Met expression 87
Figure 29. c-Met expression in EVs 88
Figure 30. ABCB1 expression in cell lysates 89
Figure 31. ABCB1 expression in EVs 90
Figure 32. ITG-A9 expression in cell lysates 91
Figure 33. ITG-A9 expression in EVs 92

List of Tables

Table 1. The Chang system for medulloblastoma staging 15
Table 2. Molecular subgroups of Medulloblastoma 21
Table 3.Table summarizing different extracellular vesicles 38
Table 4. Antibodies 49
Table 5. Cell lines 50
Table 6. Resolving gel components 55
Table 7. Stacking gel components 55
Table 8. Electrode buffer 56
Table 9. Transfer buffer 56
Table 10. PCR reaction mix 61
Table 11. PCR programme 61
Table 12. Primer design parameter for web tool NCBI Primer-BLAST 62
Table 13. Primer optimisation 84

Abbreviations

ABC	ATP-binding cassette
CAFs	cancer-associated fibroblasts
cDNA	Complementary DNA
CNS	Central Nervous System
COS	Costal
CSCs	Cancer stem cells
CSF	Cerebral spinal fluid
CTNNB1	Catenin beta 1
CT	Computer tomography
Ct	Cycle threshold
CSRT	Craniospinal radiotherapy
DMEM	Dulbecco's modified eagle's medium
DMSO	Dimethyl N3-sulfoxide
DNA	Deoxyribonucleic acid
DSH	Dishevelled
ECM	Extracellular matrix
EGFR	Epidermal growth factor receptor
EMT	Epithelial to mesenchymal transition
EVs	Extracellular vesicles
FBS	Foetal bovine serum
FP	Forward prime
FU	Fused
FRZ	Frizzled
GAPDH	Glyceraldehyde 3phosphate dehydrogenase
GLI	Glioma associated oncogene
HBSS	Hank's Balanced Salt Solution
HGF	Hepatocyte growth factor

HRP	Horse radish peroxidase
H4	Histone 4
PTCH	Patched
M+	Metastatic
MErT	Mesenchymal to epithelial reverting transition
MMP	Matrix-metalloproteinases
MRI	magnetic resonance imaging
MVB	Mulitvesicular bodies
MVE	Mulitvesicular endosomes
MVs	Microvesicles
NTA	Nanoparticle Tracking Analysis
PTCH	Patched
ROCK	RHO-associated serine/threonine kinase
RNAi	RNA interference
RNA	Ribonucleic acid
SEM	Standard error of the mean
SHH	Sonic Hedgehog
SMO	Smoothened
SUFU	Suppressor of fused
TEM	Transmission electron microscopy
Tsg101	Tumour susceptibility gene 101
WHO	World Health Organisation
WNT	Wingless

1. Introduction

1.1 Medulloblastoma

Brain tumours are the most common cause of morbidity and mortality in childhood cancer. Medulloblastomas are the most prevalent malignant paediatric brain tumours. Medulloblastoma arises in the cerebellum and accounts for around 10% of all cancer-related deaths in children (Pizer and Clifford, 2009). It is an embryonal tumour and is classified as a highly malignant grade IV tumour according to the World Health Organisation (WHO), implying a high proliferative potential and aggressive nature (Louis *et al.*, 2007).

Medulloblastoma tumours occur in patients of all ages; however, they are most prevalent in children aged between 3- and 9-years, with around 70% under the age of 16-years. The ratio of boys compared to girls with medulloblastoma tumours is roughly 1.6:1.

Approximately 75% of paediatric medulloblastomas arise within the cerebellar vermis and median part of the cerebellum. These tumours then often progressively invade and destroy the fourth ventricle (Figure 1). Further invasion into the brainstem can also occur (Chiou *et al.*, 2006). A smaller proportion of medulloblastoma tumours, around 25%, arise in one of the cerebellar hemispheres. Medulloblastoma have a propensity of leptomeningeal spread via the cerebral spinal fluid (CSF) circulation. Approximately 30-35% of patients with medulloblastoma have evidence of metastasis at diagnosis, and almost all at relapse (Bailey *et al.*, 1995).

Medulloblastomas are rapidly growing tumours and classical symptoms of patients presenting with medulloblastoma tumours include, morning headaches, nausea and vomiting (associated with elevated intracranial pressure), double vision (associated with cranial nerve dysfunction), ataxic gait with unsteadiness and papilledema (associated with dysfunction of the cerebellar vermis) (Gerber *et al.*,

2012; Sadighi, Vats and Khatua, 2012). Patients with medulloblastoma tumours are typically diagnosed using computer tomography (CT) scans and magnetic resonance imaging (MRI) (Figure 1) MRI scans are performed to detect metastatic dissemination. It has also more recently been shown that MRI scans can be used to distinguish histological variants and molecular subgroups of medulloblastoma and can be used to aid tumour staging (Kombogiorgas *et al.*, 2011).

Current therapies for these cancers consist of surgical resection followed by adjuvant post-operative craniospinal radiotherapy (CSRT) and chemotherapy. The current treatment protocols have significantly improved survival rates and have achieved a 5-year overall survival rate of above 60% (Coluccia *et al.*, 2016). However, these therapies cause substantial health, neurological, behavioural and developmental sequelae for those who survive the tumour and their treatments (Polkinghorn and Tarbell, 2007).



Figure 1. Post-gadolinium MRI
MRI of a 4 year old with a medulloblastoma tumour. The enhancing mass is within the cerebellar vermis and has invaded and destroyed the fourth ventricle. Image taken from Polkinghorn and Tarbell, 2007.

1.1.1 Tumour staging

The original tumour staging system (T-stage), established by Chang *et al.* in 1969, was developed dependent on the size and location of the tumour (Chang, Housepian and Herbert, 1969).. Although the original system has been updated, a modified system is still in place today to stage medulloblastoma tumours. The adapted system considers both the extent (tumour stage) and metastatic spread (metastatic stage) of the tumour (Cassidy et al. 2010).

T-stage groups tumours into four different stages T1-T4 (summarised in Table 1). T1 accounts for tumours which have a diameter less than 3cm whilst tumours with a diameter greater than 3cm are staged T2-T4, depending on the extent of tumour growth. T2 tumours have a diameter greater than 3cm, tumours classified as T3a show extension into the cerebral aqueduct (area between the third and fourth ventricle), T3b are tumours showing extension into the brainstem and T4 show extend above the aqueduct and/or into the foramen magnum (opening into the cranium leading to the spinal cord).

Metastatic staging (M-stage) of tumours is based on the presence, and extent of, metastases. Patients who have no evidence of metastases are characterised as M0 whereas patients positive for metastatic spread (M+) are classified as M1-M4 dependent upon the extent of metastatic spread (summarised in Table 1). Stage M1 indicates the presence of tumour cells in the CSF. M2 stage represents patients with nodular seeding in either the cerebellar subarachnoid space, cerebral subarachnoid space, third ventricle or the lateral ventricle. Metastases into the spinal subarachnoid space is classified as M3 stage. The highest metastatic stage is M4 and indicates the presence of metastases outside of the cerebrospinal axis. Patients presenting with metastatic disease have a worse prognostic outcome compared to patients without metastatic disease (Brugières *et al.*, 2012).

Table 1. The Chang system for medulloblastoma staging

Tumour stage		Metastatic stage	
T1	<3cm diameter	M0	No metastasis
T2	>3cm diameter	M1	Evidence of microscopic tumour cells in CSF
T3a	>3cm diameter with extension into the cerebral aqueduct	M2	Macroscopic tumour seeding in: - Cerebellar subarachnoid space - Cerebral subarachnoid space - Third or lateral ventricle
T3b	>3cm diameter extension into the brainstem	M3	Metastases into spinal subarachnoid space
T4	>3cm diameter extend above the aqueduct and/or into the foramen magnum	M4	Metastases outside of the cerebrospinal axis

Adapted from Chang *et al.,* 1969 and Cassidy *et al.,* 2010

1.1.2 Histology

The most recent edition of the World Health Organisation (WHO) classification of CNS tumours defines four different histological variants of medulloblastoma:

1. Classic subtype, which represents the majority of medulloblastoma tumours (68%), are characterised by sheets of small cells with a high nuclear to cytoplasmic ratio. Rosettes are present in some classic tumours and indicate high mitotic activity and nuclear pleomorphism (Figure 2A).

2. Desmoplastic subtype represents approximately 25% of tumours and are characterised by reticulin-free nodules surrounded by proliferating cells which produce an extracellular matrix rich in reticulin (Figure 2B).

3. Medulloblastoma with extensive nodularity (MBEN) subtype represents around 3% of tumours and is most common in children under the age of three. Like desmoplastic subtype, MBEN is also characterised by reticulin-free nodules, however in this instance these are larger and populated with small rounded cells (Figure 2C).

4. Large cell/anaplastic (LC/A) subtype compromises the most undifferentiated tumours and consists of around 5% of tumours. This subtype displays characteristic cells with prominent nucleoli and large nuclei embedded in a background of cells (Figure 2D). Several reports have suggested that LC/A medulloblastoma correlates with poor prognostic outcome (Taylor *et al.*, 2012).

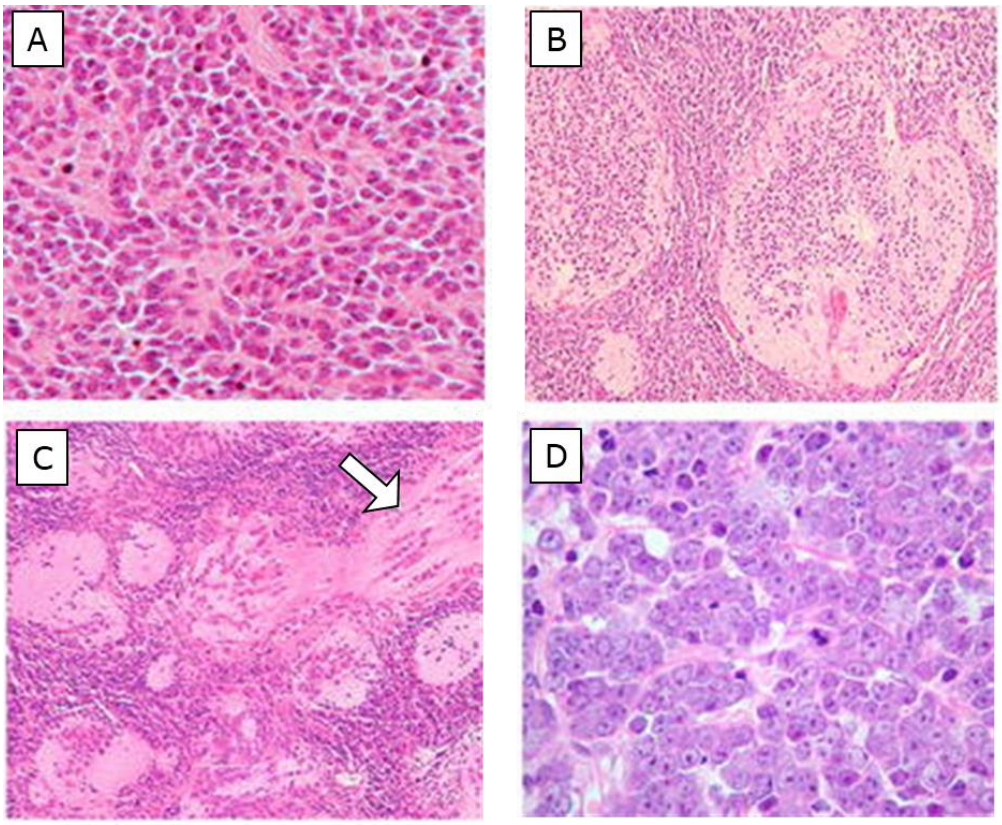

Figure 2. Histological variants of Medulloblastoma
Microphotographs showing (a) classic medulloblastoma, characterised by sheets of small cells with a high nuclear to cytoplasmic ratio. (b) Desmoplastic subtype, characterised by reticulin-free nodules surrounded by proliferating cells which produce an extracellular matrix rich in reticulin. (c) Medulloblastoma with extensive nodularity, characterised by large reticulin-free nodules populated with small rounded cells (arrow). (d) Large cell/anaplastic subtype, displaying characteristic cells with prominent nucleoli and large nuclei embedded in a background of cells. Image adapted from Ellison, 2010.

1.1.3 Molecular subgroups

Medulloblastoma was primarily regarded as a single tumour entity, with prognosis being based on clinical factors including, metastatic status, histology and extent of resection. It was first identified in 2006 that medulloblastoma can be sub-

classified according to their molecular profile (Thompson *et al.*, 2006). This finding lead to further genomic and transcriptomic characterisation of medulloblastoma tumours, and in 2012 a consensus was reached, by members of various laboratories publishing on this topic, agreeing that there were four distinct genetic (molecular) subtypes of medulloblastoma; WNT-activated, SHH-activated, Group 3 and Group 4. The WNT and SHH (Sonic Hedgehog) were named from the signalling pathways playing the most significant roles in the pathogenesis of that subgroup. The underlying biology driving the remaining two subgroups is less understood therefore the agreement was to retain generic names for these groups. The four groups are distinct in terms of histology, prognosis, driver mutations and demographics, summarised in Table 2.

1.1.3.1 WNT medulloblastoma

WNT subgroup is the most understood of the medulloblastoma tumours, however is the least common, accounting for only 10% of all MB tumours. Tumours typically reside in the midline region of the fourth vertical and infiltrate the brain stem. Almost all WNT tumours studied have classic histology (Figure 2) and rarely metastasize. The WNT subgroup has a very good long term prognosis in comparison to other subgroups, with survival rates likely to exceed 90% (Taylor *et al.*, 2012).

Under normal circumstances the WNT pathway is activated by WNT binding to the cell surface receptor frizzled (FRZ), this activates dishevelled (DSH), which then blocks the phosphorylation-activated (by glycogen synthase kinase-3β (GSK3β) in a complex with APC and axin) degradation of β-catenin. β-catenin translocates to the nucleus and activates transcriptional events (Figure 3). WNT medulloblastoma tumours frequently have somatic mutations of *CTNNB1* which encodes β-catenin, this leads to an accumulation of nuclear β-catenin which is a characteristic observed in WNT patients and can be analysed by immunohistochemical staining for β-catenin. Alternatively, patients can be

screened for hotspot mutations in exon 3 of CTNNB1 by sequencing. WNT tumours are also frequently described as having deletion of one copy of chromosome 6 (monosomy six). Other than monosomy six, it is uncommon to see other regions of genetic amplification or deletion in the genome of patients with WNT tumours (Nelson and Nusse, 2004).

1.1.3.2 SHH medulloblastoma

The SHH subgroup of medulloblastomas are named after the Sonic Hedgehog signalling pathway which drives tumour initiation in almost all cases. SHH tumours account for around 30% of MB tumours. They arise in the midline in paediatric patients, whilst in adults these tumours are more frequently seen in the cerebellar hemispheres (Remke *et al.*, 2011). The incidence of SHH tumours is dichotomous, in that they are frequently observed in infants (0-3 years) and adults (>16 years) but much less common in children between the ages of 3 to 16. Around 15-20% of patients with SHH tumours present with metastatic disease. The SHH group has an intermediate prognosis compared with group 3 and 4, with a 5 year survival rate of approximately 75% (Kool *et al.*, 2012)

SHH signalling is normally responsible for cerebellum development and the pathway is activated by SHH binding to the cell surface receptor patched (PTCH), this binding inhibits the function of PTCH which in turn releases smoothened (SMO). SMO represses the cleavage of glioma associated oncogene family (GLI), resulting in its release from a complex of fused (FU) and costal (COS). GLI is translocated to the nucleus and activates target genes. Suppressor of fused (SUFU) can repress the SHH pathway by promoting nuclear export of GLI (Figure 3). Germline mutations in SUFU or PTCH can predispose patients to develop medulloblastoma. Somatic mutations of PTCH, SMO (occurs most frequently in adults) and SUFU (most commonly observed in adults) have been found in patients with SHH medulloblastoma, as well as amplifications of GLI.

SHH medulloblastomas have mostly been identified by transcriptional profiling (Kim *et al.*, 2011; Northcott *et al.*, 2011; Kool *et al.*, 2012). Immunohistochemistry staining for SFRP1 is another approach widely used (Thompson *et al.*, 2006). Virtually all desmoplastic medulloblastomas belong to the SHH group, unfortunately around 50% of SHH subgroup are not desmoplastic thus this is not an effective marker for SHH.

Therapy to target the SHH pathway has been attempted in the form of small molecular inhibitors targeting smoothened (SMO) which are highly effective, with patients showing a positive response, however they later relapsed after developing resistance to SMO (Rudin *et al.*, 2009; Buonamici *et al.*, 2010).

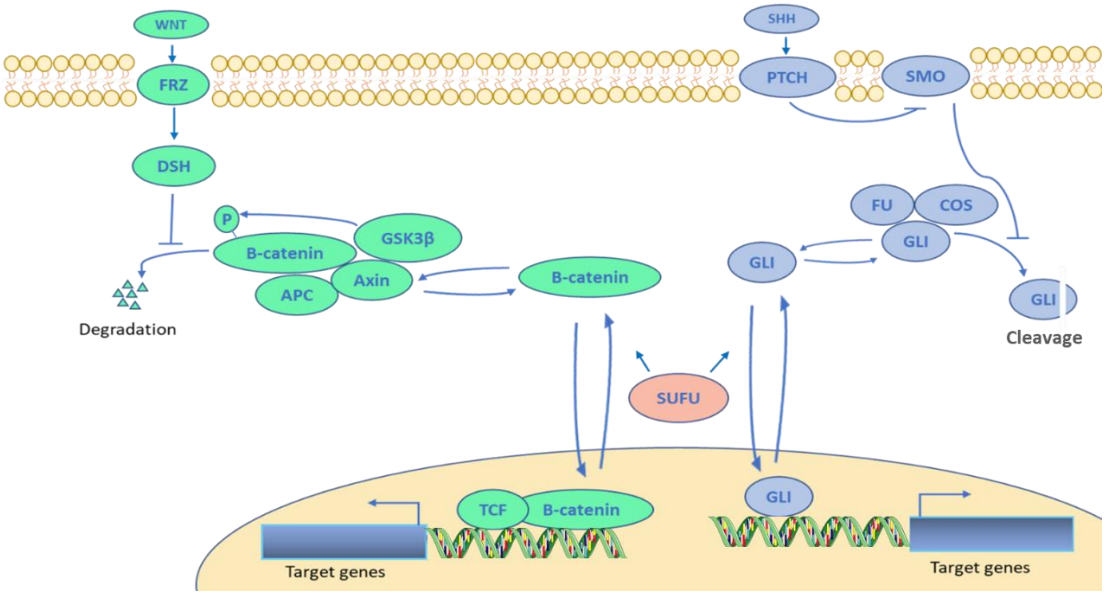

Figure 3. WNT and SHH signalling pathways schematic
WNT pathway is activated by WNT binding to the cell surface receptor frizzled (FRZ), this activates dishevelled (DSH), this then inhibits the phosphorylation-activated (by glycogen synthase kinase-3β (GSK3β) in a complex with APC and axin) degradation of β-catenin. β-catenin translocates to the nucleus and activates transcriptional events. The SHH pathway is activated by SHH binding to the cell surface receptor patched (PTCH), this binding inhibits the function of PTCH which in turn releases smoothened (SMO). SMO represses the cleavage of glioma associated oncogene family (GLI), causing its release from a complex of fused (FU) and costal (COS). GLI is translocated to the nucleus and activates target genes. Suppressor of fused (SUFU) can repress SHH pathway by promoting nuclear export of GLI. Adapted from Scotting, Walker and Perilongo, 2005.

1.1.3.3 Group 3 medulloblastoma

Group 3 tumours have the worst prognosis of the four subgroups, with less than 50% 5-year survival. 45% of patients with Group 3 present with metastatic disease, which correlates with poor prognosis in medulloblastoma (Northcott *et al.,* 2011). Group 3 tumours occur most frequently in males in comparison to females and are present in both children and infants, but are seldom seen in adults. The majority of Group 3 tumours are classic medulloblastomas, however Group 3 also encapsulates the majority of LCA tumours. (Kool *et al.*, 2008; Kim *et al.*, 2011).

Currently no germline mutations associated with group 3 are known, however MYC has been identified as a somatic driver of group 3 tumours (Kool *et al.*, 2008; Kim *et al.*, 2011; Northcott *et al.*, 2011). Unfortunately, MYC expression alone is not a prognostic indictor of Group 3 as MYC is downstream target of the WNT pathway, thus is also observed in WNT tumours (Rudin *et al.*, 2009). MYC amplification has been observed in around 17% of Group 3 tumours and is indicative of a high risk of recurrence and low survival rates. Amplification of the medulloblastoma oncogene OTX2 is also common in group 3 tumours (Adamson *et al.*, 2010). A high level of isochromosomes (gain of chromosomes) are frequently observed in Group 3 patients including 1q, 7 and 17q as well as deletions of 10q, 11, 16q and 17p (Kool *et al.*, 2008). NPR3 has been proposed as an immunohistochemical marker for Group 3 tumours (Northcott *et al.*, 2011).

1.1.3.4 Group 4 medulloblastoma

Patients with Group 4 medulloblastoma tumours have an intermediate prognosis, comparable to the SHH subgroup. Despite the fact Group 4 tumours account for over 30% of all medulloblastomas, the molecular pathogenesis of these tumours are less understood and are least represented among the current established cell lines (Ivanov *et al.*, 2016). The majority of Group 4 patients are children or adults

with cases in infants being rare. Patients with Group 4 tumours have an intermediate prognosis with a 5 year survival rate of approximately 70% (Northcott *et al.*, 2011). As seen in Group 3 patients, isochromosome 17q is also observed in Group 4 tumours, however it is more frequent in Group 4 (66%) compared with Group 3 tumours (26%). Deletions of chromosome 17p is also seen in Group 4 tumours, however has rarely been observed in WNT or SHH subgroups.

Group 4 tumours are currently identified through transcriptional profiling and KCNA1 has been proposed as the marker for immunohistochemistry (Kim *et al.*, 2011; Northcott *et al.*, 2011).

Table 2. Molecular subgroups of Medulloblastoma

	WNT (10%)	**SHH** (30%)	**Group 3** (25%)	**Group 4** (35%)
Age group	Children/Adults	Infants/Adults	Infants/Children	Children
Gender	:	:	:	:
Histology	Classic	Desmoplastic, classic, LC/A	Classic, LC/A	Classic, LC/A
Gene expression	Wnt signaling	SHH signaling	Photoreceptor/GABAergic	Neuronal/Glutamatergic
Driver mutation	CTNNB1	PTCH/SMO/SUFU mutations GLI amplification	MYC amplification	MYCN amplification
Metastasis	Rare	Uncommon	Very frequent	Frequently
Prognosis*	90%	75%	50%	70%

*5 year overall survival

Adapted from Taylor *et al.,* 2012 and Northcott *et al.,* 2012a

1.1.4 Risk stratification

Traditionally, prognosis of a patient with medulloblastoma relied primarily on extent of resection, age, histological subtypes and presence of metastases. However, more recently a consensus was reached defining four risk groups of medulloblastoma;

1. Low risk defines patients with a survival rate of more than 90%. The WNT subgroup and non-metastatic Group 4 tumours with whole chromosome 11 loss

or whole chromosome 17 gain are categorised as low-risk tumours. Patients with low risk tumours may be given reduced therapy.

2. Average/standard risk defines patients with a survival rate between 75-90%. Non-metastatic, TP53 wildtype or non-MYC amplified SHH medulloblastoma are characterised as standard risk.

3. High risk defines patients with a survival rate between 50-75%. Patients with metastatic SHH or Group 4 tumours are categorised as high risk.

4. Very high risk defines patients with a survival rate of <50%. Patients with metastatic Group 3 or SHH with TP53 mutations are defined as very high risk.

1.1.5 Treatment

The current treatment of medulloblastoma is based on risk stratification. Patients characterised as standard risk involves complete surgical resection, followed by craniospinal radiotherapy (CSRT) and maintenance chemotherapy. Despite the fact CSRT is an effective therapy and has dramatically increased overall survival, it leads to irreparable damage to the surrounding cells and numerous adverse clinical effects including neurocognitive and psychological health impairments, hearing loss infertility and hormonal imbalances. Clinical trials have tested combination adjuvant chemotherapy or multimodal therapies to limit these adverse effects (Bar and Stearns, 2008).

Patients with high-risk medulloblastoma require more aggressive treatments. High-risk patients above the age of three are treated with high-dose chemotherapy and radiotherapy. Patients below the age of three are considered high-risk due to the avoidance of radiotherapy, this is to prevent neurocognitive impairment which could likely have devastating long term effects. Therefore, adjuvant chemotherapy is the main treatment used in children, examples include Methotrexate, Carboplatin Vincristine and Etoposide (Bar and Stearns, 2008).

1.2 Metastasis- one of the hallmarks of cancer

Metastasis describes the dissemination of tumour cells to distant organs or parts of the body resulting in the formation of secondary tumours. It is defined as one of the six hallmarks of cancer (Hanahan and Weinberg, 2000). The occurrence of metastases often confers a devastating clinical fate and is responsible for over 90% of cancer-related deaths (Gupta and Massagué, 2006).

Metastasis is a complex, multistep process (Figure 4) dependent on intrinsic and external environmental factors. The initial steps of the metastatic process requires the cells to acquire an invasive phenotype and lose their adhesion to the stroma (Provenzano, Eliceiri and Keely, 2009), this results in degradation of the surrounding tissue at the primary tumour site, followed by breakdown of the basement membranes of blood or lymphatic vessels or the leptomeningies (Chambers, Groom and MacDonald, 2002). This process is termed intravasation and allows tumour cells to migrate around the body via the lymph or circulatory system or along surfaces across body cavities. After successful intravasation, some of the tumour cells eventually adhere to blood vessel walls and can invade (extravasation) and migrate into the local tissue, here they are capable of forming a secondary tumour. The process of metastasis is considered highly inefficient as only 0.01% of tumour cells which reach the blood stream succeed in establishing a secondary metastatic tumour (Fidler, 1970). A recent study in mice has also suggested that cancer cells rarely form metastatic tumours alone, and travelling in groups increases their chances of survival and forming a new metastasis (Cheung *et al.*, 2016).

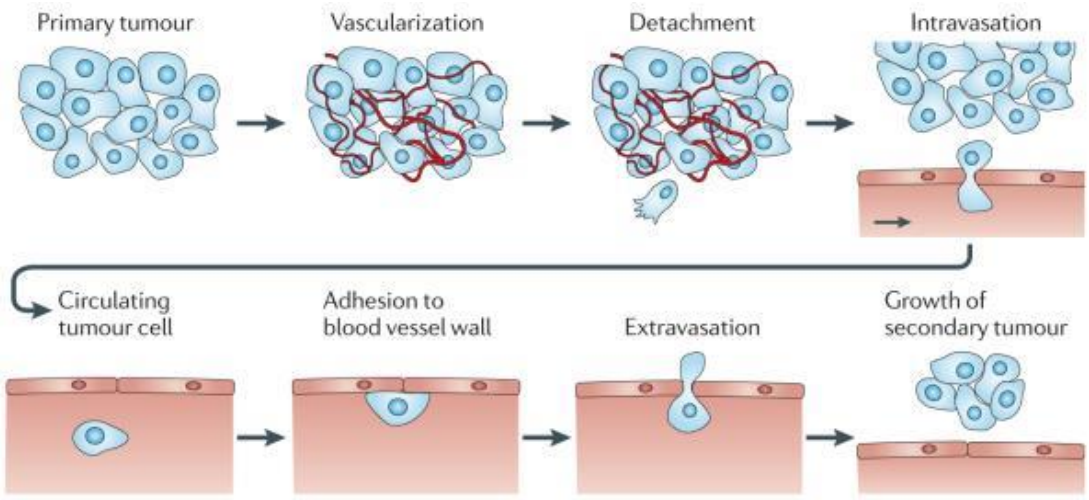

Figure 4.Multistep process of metastasis
Cells with an invasive phenotype detach from the primary vascularized tumour, they infiltrate the surrounding tissue and invade nearby blood vessels in a process termed intravasation. This allows tumour cells to circulate the blood and lymph systems. Eventually tumour cells adhere to blood vessel walls and can invade (extravasation) and migrate into the local tissue, here they are capable of forming a secondary tumour. Taken from Wirtz, Konstantopoulos and Searson, 2011.

Epithelial to mesenchymal transition (EMT) often initiates the multistep metastatic process. EMT refers to epithelial tumour cells acquiring a mesenchymal phenotype under the influence of cancer-associated fibroblasts (CAFs). Tumour cells undergoing EMT lose their cell-cell junctions and epithelial polarity and turn to a low proliferative state with an increased invasive and migratory capacity (Diepenbruck and Christofori, 2016). Molecular markers of EMT include an increased expression of vimentin as a mesenchymal marker and loss of E-cadherin and β-cadherin as epithelial markers (Figure 5). A spindle-like cell shape is also characteristic of cells undergoing EMT (Dudas *et al.*, 2017). These morphological changes are regulated by three transcriptional factors, Snail, Zeb and Twist. Once the tumours have reached the distant metastatic site the reverse process takes place. Mesenchymal to epithelial reverting transition (MErT) returns tumour cells to a high proliferative state and allows for the formation of secondary tumours (Steinbichler *et al.*, 2017).

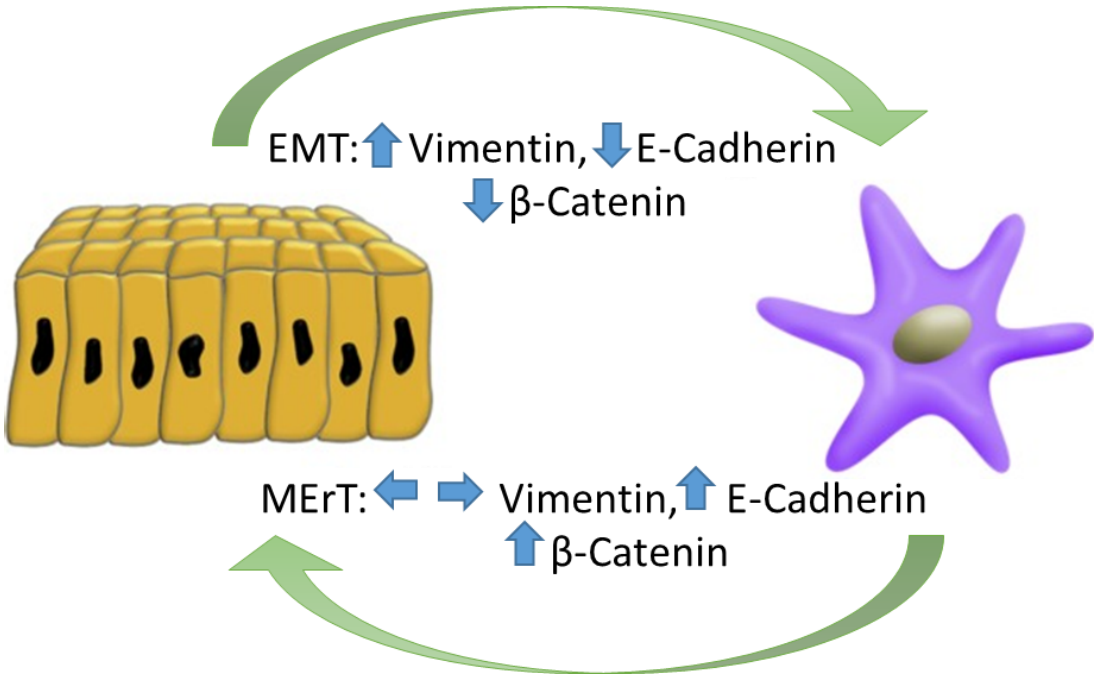

Figure 5. Epithelial to mesenchymal transition and the reversion
Epithilial to mesenchymal transition (EMT) refers to epithelial tumour cells acquiring a mesenchymal phenotype under the influence of cancer-associated proteins (CAFs). EMT is characterised by an increased expression of vimentin as a mesenchymal marker and loss of E-cadherin and β-cadherin as epithelial markers. Mesenchymal to epithelial reverting transition (MErT) returns tumour cells to a high proliferative state and allows for the formation of secondary tumours. MErt is characterised by a constant expression of vimentin and increased expression of E-cadherin and β-cadherin. Adapted from Steinbichler *et al.,* 2017.

It is also important to note that metastatic sites are not chosen randomly and that different types of cancers appear to favour particular organs as metastatic sites (Lu and Kang, 2007). This idea was originally postulated by Stephen Paget in 1889 as the 'seed and soil' hypothesis when he observed that breast cancer patients have distinct metastatic patterns to the liver, ovaries, lung and bone. The analogy encompasses the idea that initiating cancer cells "seed" require a certain affinity to a particular organ "soil" to establish tumour growth, because they offer a compatible microenvironment (Paget, 1889). This has allowed for metastatic patterns to be predicted for almost all cancer types. Fidler *et al.,* supported this hypothesis in 1970, showing metastatic cancer cells from certain tumour sites displayed high incidence of metastatic ability to specific organs, independent of the anatomy of the blood and lymphatic vessels which drain the primary tumour (Fidler, 1970).

1.2.1 Molecular mechanisms of metastasis

Migrating tumour cells exhibit many characteristics of normal cell migration, as seen in embryonic morphogenesis, wound healing and immune cell migration. The moving cell becomes polarized and elongates, the leading edge of the cell forms an extension called a pseudopod, which attaches to the extracellular matrix (ECM) of the surrounding tissue. This process is driven by actin polymerization (Beviglia and Kramer, 1999). Adherence to the ECM is regulated by integrins, including α5β1 which binds fibronectin or α6β1 which binds laminin. Integrins interact with the ECM via clustering, forming focal contacts between the cell body cytoskeleton and the ECM, this allows cells to adhere and move along the ECM surface. The engagement of integrins leads to the recruitment of surface proteases, such as matrix metalloproteinases (MMPs), which degrade ECM components. ECM degradation provides space for cell expansion and migration. Contractions are generated inside the cell by the actin/myosin cytoskeleton causing the cells to slowly glide forward. Contractions are induced by G-protein RHO and its downstream effector RHO-associated serine/threonine kinase (ROCK).

Many studies have shown that the multistep process of cell migration applies to cancer cells and ECM-degrading enzymes, such as MMPs and cathepsins, are frequently upregulated in tumour cells and have been shown to facilitate migration *in vitro* as well as dissemination *in vivo* (Liotta & Paweletz, 2005; Rosenthal, *et al.,* 1999). Equally, the overexpression or activation of RAC, RHO and ROCK signalling pathways have been associated with *in vitro* tumour-cell migration, and *in vivo* invasion.

1.2.2 Metastasis in medulloblastoma

Medulloblastoma arises in the cerebellum and has a propensity for leptomeningeal spread. Over 30% of patients with medulloblastoma present with evidence of metastatic disease and almost all at relapse (Taylor *et al.*, 2005). Once the cancer cells have breached the leptomeningies they reach the CSF and float along the

CSF pathways, here they can settle and grow along the neuroaxis. The tumour can remain here or infiltrate the parenchyma of the brain, spinal cord, cranial nerves, or peripheral nerve roots (Posner, 1996). Leptomeningeal metastasis (LM) is diagnosed through MRI imaging and cytological CSF assessment. Treatment may consist of chemotherapy as well as radiotherapy. The median survival of patients with LM is around a week without treatment and only months with treatment. LM can also occur during surgery via the placement of shunts which are used to drain CSF. This is because tumours can block the flow of CSF resulting in an increased intracranial pressure. The shunt often drains the CSF into the abdominal cavity, which can result in peritoneal metastasis (Greenfield and Bilsky, 2005).

In some instances medulloblastoma tumour cells can also disseminate from the cerebellum and invade into the adjacent substance of the brain tissue, this is termed parenchymal metastasis (Rochkind *et al.*, 1991).

1.2.2.1 Markers of metastasis in Medulloblastoma

The molecular mechanisms which potentiate medulloblastoma metastasis remains elusive, however expression changes of some proteins have been suggested to correlate with medulloblastoma metastasis. Examples include factors involved in epithelial to mesenchymal transformation including integrins and matrix-metalloproteinases. Overexpression of the receptor tyrosine kinase c-Met has been correlated with cell proliferation, invasion and migration. Increased expression of the multidrug resistance transporter ABCB1 has also been correlated with drug resistance and metastasis in medulloblastoma.

1.2.2.1.1 Integrins

Integrins are heterodimer transmembrane receptors which facilitate ECM adhesion. The integrin family of proteins consist of alpha and beta subtypes, forming heterodimers. Upon ligand (collagen, vitronectin, fibronectin etc.) binding, integrins activate signal transduction pathways which facilitate cellular

signals including organisation of the cytoskeleton, movement of new receptors to the cell membrane and regulation of the cell cycle. The presence of integrins allows dynamic responses to events at the cell surface (Danen, 2013).

The significance of integrins in metastasis is due to the fact that metastasis requires cellular activities such as cell proliferation, invasion and apoptosis. These processes require regulation of cell attachment and detachment, which requires the recruitment of integrins (Gassmann *et al.*, 2010). There have been several migration and metastasis studies which correlated the expression levels of integrins in human tumours with pathological outcomes and have identified numerous integrins which have an important role in disease progression. For example, the expression of α5, β1 and β3 integrins has been suggested as prognostic marker of survival in non-small cell lung cancer. The same group also showed that the expression of the same three integrins could be used as a marker for lymph node metastasis and recurrence (Kren *et al.*, 2007).

As previously mentioned medulloblastoma spreads via leptomeningeal metastasis, this involves the tumour cells migrating from the primary site, flow through the CSF, adherence to the secondary site and establishment of a metastatic tumour (Bracke, Roy and Mareel, 1996). A study by Fiorilli *et al* showed that integrins α9 and β1 mediate medulloblastoma adhesion to the leptomeningies with ECM tenascin. Tenascin is a ligand for integrins α9 and β1 and is a component of the ECM. They also suggested that α9 and β1 adhesion to the ECM activates the MAPK pathway which is vital for medulloblastoma cell survival and proliferation (Fiorilli *et al.*, 2008).

1.2.2.1.2 Matrix-metalloproteinases

Matrix-metalloproteinases (MMPs) are calcium-dependent zinc-containing endopeptidases and are capable of degrading almost all proteins found in the ECM (Egeblad and Werb, 2002). MMPs can either be bound to the cell membrane or secreted from the cytosol into the extracellular matrix. They are synthesised as

inactive zymogens and once secreted must be activated by proteolytic cleavage in order to become functional (Sternlicht and Werb, 2001; Isaacson *et al.*, 2017).

MMPs are known to be involved in every stage of metastasis and increased expression of MMPs has been related to pathological outcomes, such as patient survival and metastasis. MMPs have been shown to convert E-cadherin (adhesion protein) into a soluble form in tumours, this allowed cells to detach from the bulk tumour and become mobile (Fingleton *et al.*, 2010). MMPs have the ability to degrade proteins in the ECM, and in prostate cancer they have been shown to create a migratory pathway for tumour cell invasion (Chen *et al.*, 2011). Since MMPS are involved in all stages of the metastatic process, MMPs would make an ideal target for chemotherapy as all stages of metastasis would be targeted.

Studies of regional distributions of MMPs in medulloblastoma tumours showed that MMP-2 and MMP-9 had the highest expression. Several studies have shown that increased expression levels of MMP-2 and MMP-9 correlate with metastasis and advanced tumour stage (Bodey *et al.*, 2000; Vince *et al.*, 2001). A study by Rao *et al* concluded that targeting MMP-9 by RNA interference (RNAi) inhibited medulloblastoma tumour growth *in vitro* and decreased cell viability (Rao *et al.*, 2007). The same group also inhibited MMP-2 in medulloblastoma cells which resulted in repression of stem cell tropism towards tumour cells (Bhoopathi *et al.*, 2011).

1.2.2.1.3 c-Met

c-Met is a receptor tyrosine kinase, which, following engagement with its ligand, hepatocyte growth factor (HGF), activates several different cellular signalling pathways. During embryogenesis c-Met/HGF signalling is essential for the development of the kidney, placenta, liver and neuronal tissue and has also been implicated in the directional migration of skeletal muscle cells (Birchmeier and Gherardi, 1998). In adults, the c-Met/HGF pathway is essential for wound healing and regeneration (Bevan *et al.*, 2004). HGF is secreted as a precursor which is

activated by proteolytic cleavage by the serine protease hepatocyte growth factor activator.

Dysregulation of the c-Met/HGF pathway has emerged as a significant player in several cancers as it can promote tumorigenesis through proliferation, cell migration and invasion, angiogenesis and prevention of apoptosis. The evidence for this is abundant, for example overexpression of c-MET and/or HGF in both mouse and human cell lines results in them becoming more tumorigenic and metastatic in animal models (Rong *et al.*, 1994). Oppositely, decreased expression of c-MET and or HGF in glioma tumour cells decreases their metastatic and growth potential (Abounader and Laterra, 2005). In a more recent study it was noted that renal cancer stem cells (CSC's) overexpress c-Met and CSC's are key players in metastasis to the bone. Analysis of patients with renal cancer revealed an increased expression in bone metastatic lesions. The group inhibited c-Met, which blocked bone metastasis development induced by renal CSC's *in vivo* (D'Amico *et al.*, 2016).

The role of the c-Met/HGF pathway in brain tumour growth and development is well-established (Abounader and Laterra, 2005). It also plays a vital role in the development of the cerebellum, the knockdown of HGF or c-Met are embryonic lethal in mouse models (Mitchell *et al.,* 2001). Medulloblastoma cell lines and patient tumour samples express HGF and c-Met and overexpression of c-Met is associated with poor patient outcome (Kongkham *et al.*, 2008). 14 human medulloblastoma samples were analysed by comparative hybridization which revealed c-Met amplification on 7q in 38.5% of cases (Tong *et al.*, 2004). Another study revealed that upregulation of the c-Met/HGF pathway induced cell cycle progression, proliferation, resistance to chemotherapy, anchorage independent growth and induced apoptosis in medulloblastoma cell lines. (Li *et al.*, 2005). *SPINT2* is a tumour suppressor gene and has been identified in several cancer types as being an inhibitor of the c-Met/HGF pathway. Kongkham *et al* conducted

an epigenome-wide screening and revealed that *SPINT2* was downregulated in 73.2% of primary medulloblastoma samples whilst c-Met was upregulated in 45% of cases (Kongkham *et al.*, 2008). Experimental studies with medulloblastoma cells transfected with *SPINT2* displayed decreased proliferation, migration and anchorage independent growth *in vitro* and increased survival in animal models (Kongkham *et al.*, 2008).

1.2.2.1.4 ABCB1 transporter

ABCB1 transporter is a member of the superfamily ATP-binding cassette (ABC) transporter. ABC proteins transport different molecules across cellular and organellular membranes. Eukaryotic ABC genes can be divided into seven discrete subfamilies (ABC1, ABCA-G, MRP, ALD, OABP, GCN20 and White) (Gottesman and Ambudkar, 2001). ABCB1 is a member of the ABCA-G subfamily, and is one of three human ABC transporters involved in multidrug resistance. ABCB1 is required to decrease drug accumulation in multidrug resistant cells and has been implicated in the development of resistance to anticancer drugs. ABCB1 physiological function is thought to be primarily protective and its localization to many epithelia (Kimura *et al.*, 2007).

ABCB1 has been implicated as a marker for aggressive subpopulations in several different cancers, including lung, gastrointestinal and cutaneous melanoma (Haraguchi *et al.*, 2006; Kimura *et al.*, 2007; Landreville *et al.*, 2011). A study on uveal melanomas revealed that clinical samples of primary uveal melanomas contained subpopulations of cells which expressed high levels of ABCB1. This subpopulation of cutaneous melanoma cells was highly metastatic and tumorigenic compared to cells with low or no expression of ABCB1 (Landreville *et al.*, 2011). A more recent study by Sensorn *et al* indicated that breast cancer patients with high expression levels of ABCB1 and ABCC2 were significantly associated with specific disease recurrence such as bone metastasis (Sensorn *et al.*, 2016).

Increased expression levels of ABCB1 transporters has been implicated with chemo resistance and poor clinical outcome in several brain tumours such as glioma (von Bossanyi *et al.*, 1997), ependymoma and medulloblastoma (Chou *et al.*, 1995). This was confirmed in a more recent study by Hussein *et al* in 2011 when they showed that a subpopulation of cells from a cancer stem cell model expressed ABCB1 (Hussein *et al.*, 2011). ABCB1 has also been associated with metastasis and invasion in medulloblastoma tumours. ABCB1 protein expression from 347 patients showed 74% of high risk (large cell or anaplastic tumours with metastatic disease) medulloblastoma tumours were positive for ABCB1 compared to 22% in standard risk groups (no evidence of metastasis) (Othman *et al.*, 2014).

1.3 Extracellular vesicles

Intercellular communication is a vital hallmark of multicellular organisms and can be facilitated through direct cell to cell contact or through the transfer of secreted molecules. Extracellular vesicles (EVs) are circulating, cell derived nano-particles containing proteins and nucleic acids. Over the last two decades EVs have emerged as important mediators of intercellular communication (Holme *et al.*, 1997; Hess *et al.*, 1999). They are involved in the transmission of biological signals between cells to regulate a diverse range of biological processes. More recently, pathological roles of EVs have been recognised in diseases such as cancers, neurodegenerative disorders, and infectious diseases. Three different types of EV populations have been identified including exosomes, microvesicles and apoptotic bodies (summarised in Table 3). Exosomes will be the main focus of my project; however, the remaining two subtypes will also be explained in more detail below.

1.3.1 Exosomes

Exosomes are small, secreted membrane-bound vesicles, with sizes ranging between 30-100nm in diameter. Exosomes were first described in 1987 in studies on reticulocyte differentiation (Harding, Heuser and Stahl, 1983). They are derived

from internal vesicles (IV) stored in mulitvesicular endosomes (MVE). MVE are part of the endosomal compartment and contain internalized proteins, mRNA and miRNAs (Gruenberg and Stenmark, 2004). In general, MVE can be processed via two different routes; they can either fuse with lysosomes, leading to the degradation of their cell contents, or they can fuse with the cellular plasma membrane and release their cargo as exosomes into the extracellular space (Gruenberg and Stenmark, 2004) (Figure 6). Upon reaching their destination, which is usually determined by specific ligands on their surface, exosomes can enter the target cells in one of two ways; either taken up directly via the recipient cell's endocytic pathway or by fusion with the target cell membrane and release of their cell contents directly into the cytoplasm. This fusion results in the exchange of membrane proteins and cytosol between two cell types.

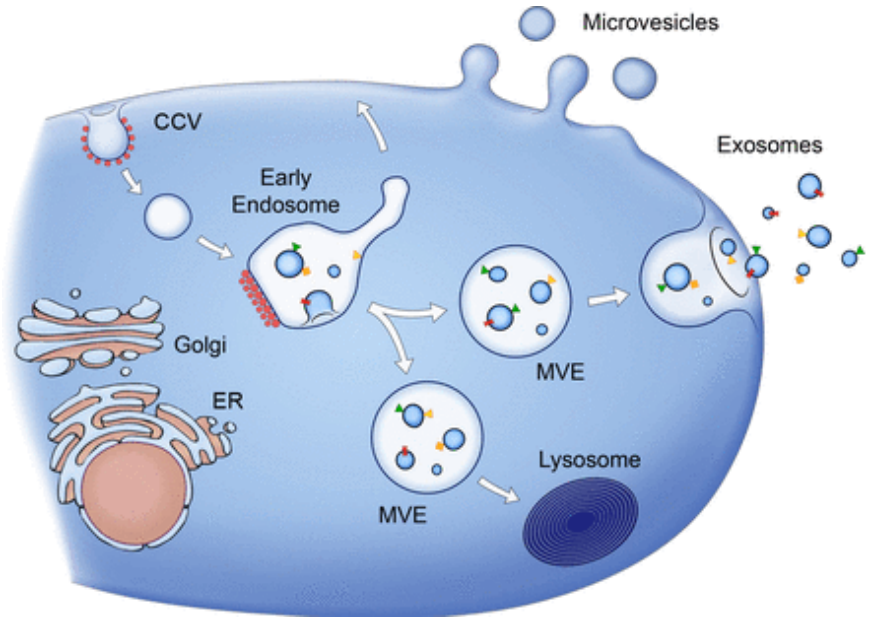

Figure 6. Release of exosomes and microvesicles
Exosomes are derived from internal vesicles (IV) stored in mulitvesicular endosomes (MVE). MVE are part of the endosomal compartment and contain internalized proteins, mRNA and miRNAs. MVE can be processed via two different routes; they can either fuse with lysosomes, leading to the degradation of their cell contents, or they can fuse with the cellular plasma membrane and release their cargo as exosomes into the extracellular space. The biogenesis of microvesicles occurs at the surface of the cells by outward budding of the membrane. Golgi: Golgi apparatus; ER: endoplasmic reticulum; CCV: clathrin-coated vesicles. Image taken from Raposo and Stoorvogel, 2013.

1.3.1.1 Exosomal content

Prior to exosome secretion, but during biogenesis, numerous molecules are loaded into the lumen of exosomes. Exosomes have a lipid bilayer and contain multiple biomolecules including proteins, lipids, RNAs (mRNA, miRNA, ncRNA) and DNA (Colombo, Raposo and Théry, 2014) (Figure 7). The available proteomic studies define a subset of 17 cellular proteins that are targeted specifically to exosomes. One of the most abundant protein families found in exosomes comprises the tetraspanins, including CD9, CD63, CD81 and CD82 (Théry *et al.*, 2006). Typical marker proteins which are also present in exosomes from most cell types include chaperones, such as constitutive isoforms of HSP70 and HSP90 (de Gassart *et al.*, 2003) and Rab proteins, Rab2 and Rab7 (Février and Raposo, 2004). Currently, thousands of different proteins have been identified as cargo of exosomes (ExoCarta). Whilst exosomes contain cytosolic proteins, proteins of the nucleus, Golgi-apparatus, mitochondria and endoplasmic reticulum are absent.

The exosome transport of proteins has widely been accepted by the research community and has been analysed by western blot and proteomic analysis. However, the demonstration that exosomes contained miRNA and mRNA, which could be translated into protein by the target cell, was not shown until much later (Ratajczak *et al.*, 2006; Lotvall and Valadi, 2007). More recently unbiased deep sequencing approaches demonstrated that exosomes also contain a large variety of other small non-coding RNA species including small interfering RNA, structural RNAs and tRNA fragments (Bellingham, Coleman and Hill, 2012).

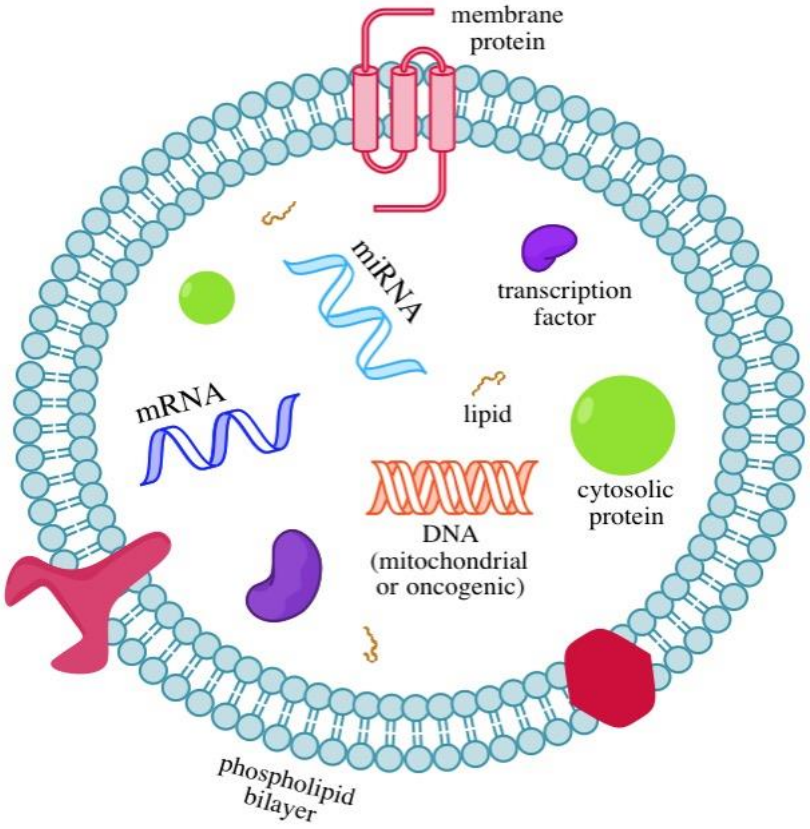

Figure 7. Exosome content
Exosomes have a double-lipid membrane and contain multiple proteins, lipids, RNAs (mRNA, miRNA, ncRNA), DNA and have even been shown to contain biomolecules for viruses and prions. Image taken from cancerquest.org/cancer-biology.

1.3.1.2 Biological functions of exosomes

Exosomes have been shown to be secreted by all cell types in culture including B cells, T cells, dendritic cells, platelets, epithelial cells, adipocytes etc. Exosomes have also been found *in vivo* from diverse bodily fluids including semen (Ronquist and Brody, 1985), blood (Caby *et al.*, 2005), urine (Pisitkun, Shen and Knepper, 2004), saliva (Ogawa *et al.*, 2011) breast milk (Admyre *et al.*, 2007), amniotic fluid (Asea *et al.*, 2008), bile (Masyuk *et al.*, 2010) and cerebral spinal fluid (Vella *et al.*, 2008). All exosomes, secreted by either cells in culture or by organs into bodily fluids, have been suggested to play a function in intercellular communication, either assisting or disturbing different physiological processes (van Niel *et al.*, 2006; Schorey and Bhatnagar, 2008).

Originally, it was thought that exosomes' only role was to allow cells to excrete unnecessary proteins; however, exosomes are now viewed as specifically secreted vesicles enabling intercellular communications. Consequently, interest in exosomes has expanded considerably, and efforts to utilize exosomes for diagnostic and therapeutic purposes are underway.

Depending on their cell of origin, exosomes have been shown to have varying functions. For example, exosomes have been extensively studied as facilitators of the immune response. In 1996, it was observed that B lymphocytes utilize exosomes for antigen presentation to enhance the immune cell response (Raposo *et al.*, 1996). More recently it was noted that exosomes derived from intestinal epithelial cells contain a high concentration of MHC class II/peptides which are able to elicit an immune response by direct antigen presentation to T-cells in mice (van Niel *et al.*, 2006). Exosomes have been associated with normal development and physiology of the nervous system. Fruhbeis *et al*, described the signal-mediated transfer of exosomes from oligodendrocytes to neurones, contributing to neuronal integrity (Frühbeis *et al.*, 2013). Aside from normal development of the nervous system, exosomes have been implicated in the generation and progression of neurodegenerative diseases, including Parkinson's disease. α-synuclein mutated proteins form intracellular oligomers, which can be passed by exosomes into nearby cells, thus spreading the disease from cell to cell within the brain (Danzer *et al.*, 2012). An interesting study comparing post-mortem brain samples from patients with Schizophrenia and bipolar disease, demonstrated the expression of certain exosomal miRNA compared to those from normal control samples (Banigan *et al.*, 2013). Over the last few years, it has been well documented that exosomes have a role in infectious diseases. For example, exosome shuttling of miRNA has been demonstrated to be involved in HIV-associated neuronal dysfunction and susceptibility to viral infection (Hu, Drescher and Chen, 2012). In Human T-lymphotropic virus type 1 (HTLV-1), exosomes

have been shown to deliver proteins and mRNA transcripts, which protect them from apoptosis (Jaworski *et al.*, 2014). Exosomes have also been reported to have a role in programmed coagulation (Huber and Holvoet, 2015), cell death (Janowska-Wieczorek *et al.*, 2005), inflammation and angiogenesis (Li *et al.*, 2016). They have also been implicated as morphogen transporters in the creation of polarity during embryonic development (Lakkaraju and Rodriguez-Boulan, 2008).

1.3.2 Microvesicles

Unlike in exosomes, the biogenesis of microvesicles occurs at the surface of the cells by outward budding of the membrane. Microvesicles constitute a more heterogeneous and larger population of extracellular vesicles, ranging from 100-1000nm in diameter. Like exosomes, microvesicles have also been shown to deliver functional protein and RNA to recipient cells. Studies of pure microvesicles populations are limited as they were originally pelleted together with exosomes at the 100,000 *x g* ultracentrifugation step. It is only more recently that microvesicles have been accepted as a distinct extracellular vesicle population and isolated separately from exosomes at around 10,000-20,000 *x g* (van der Pol *et al.*, 2012).

1.3.3 Apoptotic bodies

Of the three different subpopulations of extracellular vesicles, apoptotic bodies are the least well characterised. They range from around 800-5,000nm in diameter and are released by cells undergoing programmed cell death/apoptosis. Cells undergo several steps during apoptosis including cell shrinkage, chromatin condensing, nuclear fragmentation, membrane blebbing and then the cells break down into apoptotic bodies (Reed, 2000). Apoptotic bodies can be isolated at 2,000 *x g* (Crescitelli *et al.*, 2013). They consist of cytoplasm with tightly packed organelles and sometimes contain a nuclear fragment which can be visualised by electron microscopy. The organelle integrity is maintained and is enclosed by an

intact plasma membrane. After release, apoptotic bodies are quickly phagocytosed by neoplastic cells, macrophages or parenchymal cells and degraded inside phagolysosomes (Reed, 2000).

Table 3.Table summarizing different extracellular vesicles

Characteristics	Exosomes	Microvesicles	Apoptotic bodies
Size (nm)	30-100	200-1000	800-5,000
Shape	Spheroid	Irregular	Heterogeneous
Sedimentation (*xg*)	100,000	10,000-20,000	2,000
Markers	CD63, CD81, CD9, tsg101, Alix	Integrins, EMMPRIN, Selectins	Histones
Lipids	Cholesterol, ceramide, lipid rafts	Phophatidylserine	Not determined
Origin	Multivesicular endosomes	Plasma membrane	Plasma membrane

1.3.4 Isolation and analysis of exosomes

To facilitate the application and study of extracellular vesicles, it is vital to specifically isolate exosomes from interfering components and cellular debris. There is currently no clear consensus on the most efficient method of isolating high yields of pure exosomes from conditioned cell culture medium or bodily fluids.

The International Society of Extracellular Vesicles (ISEV) has recently proposed the minimal experimental requirement for the definition of extracellular vesicles and their functions (Lötvall *et al.*, 2014). The requirements state that vesicles must be purified in a cell disruption limiting manner, three or more proteins enriched in exosomes (as well as proteins not expected) should be identified in a semi-quantitative manner, and at least two different technologies of characterising exosomes should be used. Methods for the isolation and characterisation exosomes which are routinely used will be discussed below.

1.3.4.1 Ultracentrifugation

Ultracentrifugation is considered the gold-standard and is one of the most widely applied method for separating exosomes from cells, apoptotic bodies, and microvesicles. This approach is used by many due to its ease and high yield of relatively homogeneous population of exosomes. Isolation of exosomes by ultracentrifugation consists of several centrifugation steps to sediment cell debris, microvesicles and apoptotic bodies, followed by a high-speed ultracentrifugation step ranging from 100,000 to 120,000 *x g* (Théry *et al.*, 2006). Unfortunately, ultracentrifugation is not always appropriate from clinical samples due to large starting volumes required and user-dependent recovery rates. In support of this, a recent study determined that 100% exosome recovery in certain biological fluids could not be achieved, despite the addition of spike-in exosome controls (Kalra *et al.*, 2013).

1.3.4.2 Exosome precipitation

Several commercial kits are available to precipitate exosomes which are easy to use, do not require specialised equipment and do not require large starting volumes, allowing for easy integration into the clinic. Examples include ExoQuick™ (System Bioscience, California, USA) and Exo-Spin™ (Cell guidance Systems, Cambridge, UK.) The exact mode of action of these kits has not yet been verified or disclosed (Huang *et al.*, 2013), however these kits rely on polymer interactions to precipitate exosomes out of solution (Zarovni *et al.*, 2015). A big disadvantage of using exosome precipitation kits is the co-precipitation of other non-exosome contaminants, including polymeric materials and proteins, which greatly biases downstream RNA analysis of exosomal cargo (Zarovni *et al.*, 2015). Contamination from the reagents used in these kits could also affect assays of exosomal activity.

1.3.4.3 Ultrafiltration

Ultrafiltration is one of the most popular size-based exosome isolation techniques. Several groups have developed ultrafiltration as an alternative and rapid method of isolating exosomes. Ultrafiltration has also recently been recommended as an additional step within the ultracentrifugation protocol, to further purify exosome populations by removal of non-exosomal proteins or larger particles (Muller *et al.*, 2014). Ultrafiltration is much less time consuming than ultracentrifugation and no specialist equipment is required. Nevertheless, the use of force can cause breakage of larger vesicles which has the potential to skew the results of downstream analysis (Zarovni *et al.*, 2015).

1.3.4.4 Sucrose gradient

Sucrose gradient isolation is seen as both a purification and detection method. Briefly, this method involves two centrifugation steps at 1,000 *x g* followed by addition of a 30% sucrose cushion, followed by differential ultracentrifugation. This yields exosome pellets with fewer contaminating large proteins or aggregates (Zhang *et al.*, 2015). This method relies on the floating densities of exosomes which range from 1.13 g ml-1 to 1.19 g ml-1 (Hugel *et al.*, 2005). A recent study by Muller *et al*., identified a large loss in total numbers of exosomes recovered using a sucrose gradient cushion, however a lower ratio of contaminating protein, suggesting a purer isolation method (Muller *et al.*, 2014).

1.3.4.5 Western blot analysis

There is currently no specific marker for exosomes, but rather a panel of "exosome-enriched" proteins. A recently published proteomics study defined novel markers to characterize heterogenous population of extracellular vesicles (Kowal *et al.*, 2016). They recommended that transmembrane proteins, like the tetraspanin CD63 (alongside CD81 and CD9) should be used as general exosome markers. Tsg101 was also highlighted as a marker of small exosomes (<100nm).

However, the main disadvantage of western blot analysis is that large starting volumes are required for effective protein detection.

1.3.4.6 Transmission electron microscopy

Transmission electron microscopy (TEM) forms an image when a beam of electrons is transmitted through a sample. When exosomes are examined under electron microscopy, they show a characteristic cup-shaped morphology (Figure 8A), with diameters ranging from 30-100nm (Raposo *et al.*, 1996). It is believed the cup-shaped morphology originates from the sample processing, during which exosomes suffer extensive dehydration and often collapse. When microvesicles are examined under TEM, they show a typical irregular shape (Figure 8B) (Menck *et al.*, 2013).

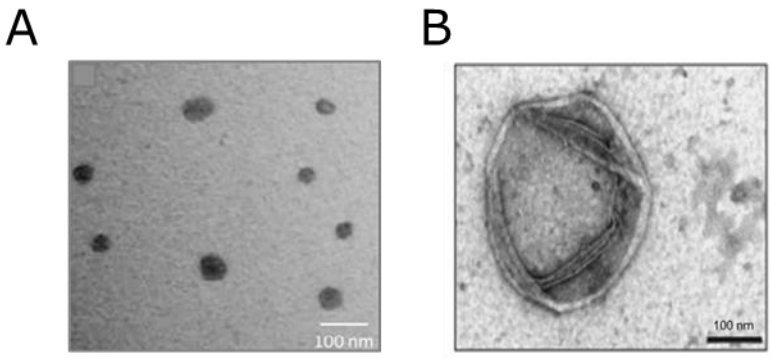

Figure 8. TEM of microvesicles and exosomes
Transmission electron microscopy determines morphological characteristics of microvesicles and exosomes. (A) Exosomes show typical spherical cup-shaped morphology. (B) Microvesicles show typical irregular shape and yield membrane-bound particles. Image taken from Menck et al., 2013.

1.3.4.7 Nanoparticle tracking analysis

Nanoparticle Tracking Analysis (NTA) is a relatively new method used for the visualisation and analysis of nanometre particles in liquids ranging from a size of 10-1000nm. The size of the particles is related to the rate of Brownian motion, temperature and the viscosity of the liquid and is not influenced by particle density or refractive index. In this method, a laser beam is directed through the sample chamber and the vesicles in suspension in the path of the beam scatter light in a

manner which can easily be detected via a microscope onto which a video camera is mounted. The camera captures a video file of vesicles moving under Brownian motion. The NTA software tracks particles individually using Stokes Einstein equation, calculating their diameters and concentration (Soo *et al.*, 2012).

1.4 The significance of exosomes in cancer

Accumulating evidence indicates that exosomes play vital roles in cancer progression. They have been shown to transfer oncogenic proteins and nucleic acid cargo to recipient cells which modulates their activity and plays a decisive role in tumorigenesis, promoting tumour growth and progression, enhancing tumour cell migration and invasion, developing drug resistance and performing immunosuppressive functions.

1.4.1 Exosomes as biomarkers in cancer

As previously mentioned, exosomes are not only present *in vitro* cell culture models, they have been detected and are readily accessible in almost all bodily fluids including blood and cerebrospinal fluid. Exosomes contain RNA and protein cargo which reflects the pathological state of their parent cell. Therefore, since exosomes closely represent the state of their originated cell and can be easily collected from nearly all bodily fluids exosomes would be ideal biomarkers for cancer. It has already been shown that the levels of exosomes are elevated in the plasma of some cancer patients as compared to healthy controls. For example, a study by Graves *et al* demonstrated increased levels of extracellular vesicles in ascites fluid of ovarian cancer patients and that their amounts correlated with disease progression (Graves *et al.*, 2004). This was also confirmed for extracellular vesicles found in peripheral blood of gastric cancer patients (Baran *et al.*, 2010). The increased levels of exosomes have been correlated with the hypoxic, acidic microenvironment around tumours, which is hypothesised to stimulate the release of exosomes but also their cell fusion capabilities (Parolini *et al.*, 2009).

Profiling of exosomes secreted into the urine of patients with bladder cancer, revealed an upregulation of 8 proteins in patient samples, with five of them being part of oncogenic EGFR signalling compared to healthy controls (Smalley *et al.*, 2008). The identification of exosomal proteins derived from prostate cancer compared to control cells also resulted in the discovery of four proteins, PDCD6IP, FASN, XPO1 and ENO1, as novel candidate biomarkers for prostate cancer (Duijvesz *et al.*, 2013). Analysis of exosomal RNA has also been used in various studies, for example in serum samples of patients with oesophageal squamous cell carcinoma, elevated expression levels of miR-21 were revealed compared with patients with benign diseases (Toiyama *et al.*, 2016). miRNA let-7, a tumour suppressor gene, was reported in exosomes derived from metastatic gastric cancer cells. The study suggests that secretion of exosomal let-7 may have a role in promoting metastasis (Ohshima *et al.*, 2010). Exosomes from patients with metastatic prostate cancer were compared to a cohort of normal individuals. It was identified that two miRNA's were markedly upregulated and several candidates were significantly downregulated in metastatic samples compared to normal controls (Bhagirath *et al.*, 2017). In addition to miRNA, long non-coding RNA has also been isolated from exosomes (Kogure *et al.*, 2013). Long non-coding RNA which was protected from exosomes isolated from blood plasma of gastric cancer patients has been suggested as a novel stable biomarker (Yu *et al.*, 2007). Together, these studies show the potential use of exosomes as easily accessible targets for disease detection, monitoring or prognosis establishment in cancer.

1.4.2 Exosomes as mediators of intercellular communication in cancer

Several studies have also shown that exosomes not only serve as potential biomarkers in cancer, they have been implicated in numerous physiological and pathological processes, such as tumour initiation, growth, progression and metastasis. These affects are mainly attributed to their role as mediators of

intercellular communication, as exosomes can transfer oncogenic proteins and RNA from their cell of origin to recipient cells. Exosomes from malignant cells have been shown to have the potential to induce transformation of normal cells. For example, Elmageed *et al*, showed exosomes derived from prostate cancer cells induced clonal expansion of tumours through neoplastic reprogramming of patient derived adipose stem cells (Abd Elmageed *et al.*, 2014). It has also been demonstrated that exosomes derived from breast cancer patient serum induced tumour formation in mice, this was not seen with exosome derived from healthy donors (Melo *et al.*, 2014). The promoting effects of exosomes on tumour growth has been widely reported; exosomes isolated from mutant KRAS-expressing colon cancer cells enhance tumour cell growth of recipient cells relative to exosomes purified from wild-type KRAS-expressing cells (Beckler *et al.*, 2013). Exosomes also contribute towards tumour metastasis by increasing cell migration and invasion through establishing a pre-metastatic niche. Highly metastatic melanoma-derived exosomes "educate" bone marrow progenitor cells towards a pre-metastatic phenotype via the MET receptor, enhancing the metastatic ability of primary tumours (Zhu *et al.*, 2013). Similar results were also seen in gastrointestinal stromal tumour cell derived exosomes containing protein tyrosine kinase, which converted progenitor smooth muscle cells to a pre-metastatic phenotype (Atay *et al.*, 2014). More recently, exosomes have also been shown to be critical for invadopodia biogenesis and activity. Invadopodia are actin-based protrusions formed in cancer and normal cells and are involved in multiple steps of the metastatic cascade. Knock-down of exosome secretion by Rab27a (critical for MVB docking) resulted in decreased numbers of invadopodia per cell, reducing cell migration (Paterson *et al.*, 2017). Therefore, there is clear, compelling evidence to support a role of exosomes in tumour biology and disease progression.

1.4.3 Exosomes in medulloblastoma

Exosomes isolated from brain tumour cells have been shown to affect signalling capacities, interrupt immunity and promote migration and invasion. For example, in 2008 it was first revealed that glioblastoma extracellular vesicles stimulated proliferation of human glioma cells, suggesting a self-promoting aspect of extracellular vesicles. In the same study, they also identified the enrichment of mutant epidermal growth factor receptor (EGFRvIII) in plasma exosomes present in 7 out of 25 glioblastoma patients, but not in 30 healthy subjects. Mutant EGFRvIII is the most common mutation found in glioblastoma multiform patients and plays a prominent role in tumorigenesis (Skog *et al.*, 2008; Al-Nedawi *et al.*, 2009). A study by Haug *et al* showed that MYCN-amplified neuroblastoma cell lines secrete exosome-like extracellular vesicles containing miRNA's. MYCN is a proto-oncogene which correlates with high-risk neuroblastoma. The vesicles were taken-up by recipient cells, releasing miRNA's with potential roles in cancer progression (Haug *et al.*, 2015). This study identified a novel method for MYCN-amplified neuroblastoma cells to co-operate with the tumour microenvironment.

To date, only two studies reporting a potential role for exosomes in medulloblastoma have been published (Epple *et al.*, 2012; Bisaro *et al.*, 2015). In 2012 a study by Epple *et al*., analysed exosomes in medulloblastoma cell lines with proteomic analysis (Epple *et al.*, 2012). Examination of the proteomic data suggested functional roles of exosomes which are relevant to medulloblastoma tumour progression, including their roles as proliferation stimulants and attractants for tumour cell migration. They also confirmed the presence of common vesicular molecules, such as tetraspanins CD9 and CD63 and identified the tumour transcription factor HNF4A. They suggested HNF4A could be a tumour suppressor and inhibited it with the known drug inhibitor MEDICA 16, which resulted in an increase in cell proliferation. This work showed that medulloblastoma derived exosomes may have a role in tumour growth and

progression. A more recent study also analysed medulloblastoma cell lines by proteomic analysis and revealed that some medulloblastoma derived extracellular vesicles contained iron carrier proteins. They found that treating medulloblastoma cells grown as spheres with iron chelators reduced the number and sizes of spheres (Bisaro *et al.*, 2015). Therefore, this study suggested a role of extracellular vesicle mediated iron metabolism in medulloblastoma progression and invasion. Both studies reported a potential role for exosomes in medulloblastoma cell line proliferation, invasion and progression, however, there was relatively little indication of the underlying processes involved. Any advancements in our understanding of medulloblastoma derived exosomes may lead to novel ways to target these tumours.

1.5 Hypothesis and aims

Cancer extracellular vesicles are seen as very promising biomarkers as well as therapy targets. Existing data has shown that the release of exosomes from many tumour types contributes to tumour growth and increases likelihood of migration and invasion. Hence, the capacity of secreted extracellular vesicles to mediate progression in terms of increased therapy resistance, metastasis or cell proliferation is under investigation in an abundance of cancer types. We hypothesize that small vesicles, such as exosomes, are an important means of communication between medulloblastoma cells and their surroundings. However, little is known about how exosomes potentiate disease progression in medulloblastoma tumours. Therefore, the focus of this project will be to isolate extracellular vesicles from medulloblastoma cell lines from different subgroups that are characterized by different metastatic and survival rates. The RNA cargo of these extracellular vesicles will then be investigated for candidates of medulloblastoma metastasis. This will enable the following questions to be addressed:

1. Which extracellular vesicle populations are released by medulloblastoma cells?

The initial aim of the project is to optimise a protocol for the isolation of exosomes and microvesicles from medulloblastoma cells lines. Success of this step will be validated by nanoparticle tracking analysis, electron microscopy and western blot analysis.

2. Is there a difference between the subgroups and metastatic stages?

This will be answered in two separate parts:

i. Is there a difference between amounts of isolated EVs between the medulloblastoma cell lines?

Increased levels of extracellular vesicles released has been correlated in other cancer types with poor prognosis and survival outcome. Therefore, we hypothesise that metastatic cell lines produce more EVs in comparison to non-metastatic cell lines.

ii. Are candidate markers of metastasis present in cells also present in extracellular vesicles?

Exosomal RNA will be examined to determine if there is any correlation between the metastatic stage of the tumour of origin and the presence of RNA known to influence invasion and metastasis.

In summary, the project aims to explore the presence of, and the biomarker potential of, medulloblastoma exosomes.

2. Materials and methods

2.1 Materials

2.1.1 Antibodies

The antibodies used in this study are listed in Table 4.

Table 4. Antibodies

Target	Host species	Application	Company
CD63	Mouse	Western blot (1:1000)	Santa cruz biotechnology, INC
EMMPRIN	Mouse	Western blot (1:500)	Santa cruz biotechnology, INC
tsg-101	Mouse	Western blot (1:500)	Santa cruz biotechnology, INC
Histone 4	Mouse	Western blot (1:1000)	Cell signalling

2.1.2 Cell lines

The cell lines used in this study are listed in Table 5.

Table 5. Cell lines

Cell line	Obtained from	MB subgroup	Tumour type	Growth type	Reference
UW228-3	John R. Silber, University of Washington, Seattle	Group 3	Non-metastatic (M0)	Adherent	Keles *et al*., 1995
DAOY	ATCC®HTB-186™	SHH	Non-metastatic (M0)	Adherent	Jacobson *et al*., 1985
CHLA-01-MED*	Professor Geoff Pilkington (University of Portsmouth, UK)	Group 4	Non-metastatic (M0)	Suspension	Xu *et al.,* 2012
CHLA-01R-MED*	Professor Geoff Pilkington (University of Portsmouth, UK)	Group 4	Metastatic (M3)	Suspension	Xu *et al*., 2012
D283 Med	ATCC® HTB-185™	Group 3/4	Metastatic	Semi-adherent	Friedman *et al.,* 1985
HD-MB03	Dr Till Milde (DKFZ, Heidelberg, Germany)	Group 3	Metastatic	Semi-adherent	Milde *et al.,* 2012

*Matched pair

2.2 Methods

2.2.1 Tissue culture methods

2.2.1.1 Recovering cells from liquid nitrogen

Cell stocks were recovered from liquid nitrogen stores by rapidly thawing vials in a 37°C water bath. Cells were transferred into a 25cm^2 standard tissue culture flask (Eppendorf) containing 10ml of pre-warmed culture media. Cells were grown at 37°C and 5% CO_2 in a humidifier incubator for 24 hours prior to a media change.

2.2.1.2 Sub-culturing cell lines

Cell lines were grown at 37°C and 5% CO_2 in a humidifier incubator. Cell lines were passaged when sub-confluent (70-80% confluence)

2.2.1.2.1 Sub-culturing adherent cell lines

Media was removed and cells were washed twice in Hann's Balanced Salt solution (HBSS) (Gibco). The cells were detached by incubation with 2ml Trypsin-EDTA (Sigma, LH-SIG2044) for 5 minutes. The detached cells were collected and centrifuged at 700 *x g* for 5 minutes. Cell pellets were resuspended in fresh media and were split into standard treated tissue culture flasks in a ratio of 1:3-1:20 depending on their respective doubling times. Cell lines were tested regularly for Mycoplasma infection (VenorGem Kit Minerva Labs, Cambio).

2.2.1.2.2 Sub-culturing semi-adherent cell lines

Media containing suspension cells was transferred into a Falcon tube. The remaining cells were washed twice in HBSS to detach remaining semi-adherent cells, HBSS was transferred into the falcon tube with the suspension cells. The remaining adherent cells were detached by incubation with Trypsin-EDTA. Detached cells were collected with suspension cells and centrifuged at 700 *x g* for 5 minutes. Cell pellets were resuspended in fresh media and were split into standard treated tissue culture flasks in a ratio of 1:2-1:5.

2.2.1.2.3 Sub-culturing suspension cell lines

Suspension cells were subcultured by removing volumes of media containing suspension cells and replenishing with volumes of fresh media. Once a week the media containing suspension cells was transferred into a Falcon tube and centrifuged at 100 *x g* for 5 minutes. Cell pellets were resuspended in ¼ conditioned media and ¾ fresh media and split into non-treated tissue culture flasks in a ratio of 1:2-1:5.

2.2.1.3 Freezing cells for stocks

To maintain cells for long periods of time, they were frozen in freezing media, consisting of 10% DMSO (Gibco) and 90% FBS, and stored in liquid nitrogen (-150°C).

2.2.1.4 Snap freezing cell pellets

Cells were harvested in falcon tubes and centrifuged at 200 *x g* for 5 minutes. Cell pellets were resuspended in 1ml of sterile PBS, transferred into a 1.5ml Eppendorf and further centrifuged. The supernatant was discarded and the remaining cell pellet was placed into a Dewar flask of liquid nitrogen (snap freeze) and then stored at -80°C.

2.2.1.5 Cell counting

Cells were routinely counted using either the EVE™ automatic cell counter (Nanotech), according to the cell counter manual, or using a haemocytometer.

2.2.2 Extracellular vesicle techniques

2.2.2.1 Particle-free FBS

Particle-free FBS was generated by the pelleting of extracellular vesicles by overnight ultracentrifugation at 100,000 *x g* at 4°C.

2.2.2.2 Isolation of exosomes and microvesicles

To isolate exosomes and microvesicles from adherent and semi-adherent cell populations, cells were cultured in 10 T75 flasks up to 30% confluence, washed twice with HBSS and incubated in media supplemented with particle-free FBS for 48 hours.

The optimised method used for the isolation of extracellular vesicles is outlined below, initial methods will be discussed in section 3.1.

Cell culture supernatants were collected and centrifuged for 5 minutes at 750 *x g* at 4°C to pellet cells. This was followed by centrifugation of the supernatant for 15 minutes at 1,500 *x g* at 4°C to pellet debris. The supernatant was then centrifuged for 35 minutes at 14,000 *x g* at 4°C to pellet the microvesicles. The microvesicle pellet was resuspended in PBS and centrifuged again for 35 minutes at 14,000 *x g* at 4°C to wash the pellet. The microvesicle pellet was then resuspended in PBS or lysis buffer and stored at -20°C for up to one week or -80°C for several months. For the isolation of exosomes, the supernatant from the 14,000 *x g* centrifugation step was filtered through a 0.22 µm filter to further purify exosome populations by removal of non-exosomal proteins or larger particles. The supernatant was then centrifuged for 2 hours at 100,000 *x g* at 4°C. The pellet was washed by resuspending in PBS and centrifuged again for 2 hours at 100,000 *x g* at 4°C (Figure 9). The remaining pellet was then resuspended in PBS or lysis buffer and stored at -20°C for up to one week or -80°C for several months.

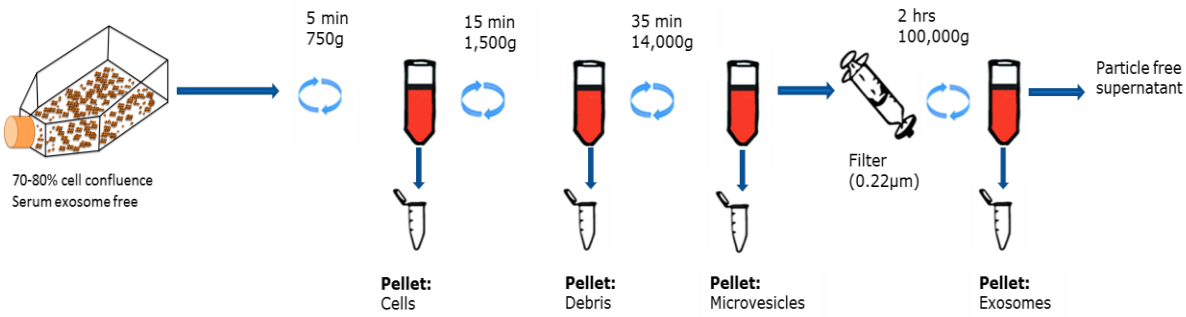

Figure 9. Schematic representation of EV isolation
Exosome and microvesicle isolation method is based on differential centrifugation and filtration steps, followed by a final ultracentrifugation step.

2.2.3 Protein biochemistry

2.2.3.1 Protein isolation

For the isolation of protein from microvesicles, exosomes, and cells, pellets were resuspended in 25-100ul of lysis buffer (150 mM NaCl, 50 Mm Tris Ph 7.4, 0.1% SDS, 1% Triton X-10, supplemented with protease inhibitors) incubated for 20 minutes on ice and centrifuged for 30 minutes at 13,000 *x g* at 4°C. The supernatants were transferred to a clean Eppendorf and subject to protein quantification as described in 2.2.3.2. Supernatants were collected and stored at -80°C.

2.2.3.2 Protein quantification by Bradford assay

The protein concentration in whole cell lysates and the amount isolated from microvesicles and exosomes were quantified using a Bradford assay in relation to a BSA standard curve (Bradford 1976). Bradford assay was confirmed using the Protein Assay Dye Reagent (Biorad, 500-0006). This was diluted 1:4 in distilled water in a volume dependent on the number of samples to be tested (1ml/sample). A 0.2% solution of Bovine serum albumin (Sigma-Alrich, A7906) was used to prepare standards from a concentration range of 0-40µg/ml. Aliquots of unknown samples and BSA standards were loaded into a 96-well plate (Eppendorf) and loaded into the plate reader (FLUOstar Omega, BMG Labtech). The Bradford assay programme was selected and measurements of absorbance at 595nm were determined.

2.2.3.3 SDS-PAGE

To analyse the protein expression of extracellular vesicles or whole cell lysates by western blotting, proteins were separated according to their molecule weight by discontinuous SDS polyacrylamide gel electrophoresis (SDS-PAGE) (Laemuli *et al.,* 1971). This consists of two separate gels cast at different pH values. The resolving gel (15%) (Table 6) was prepared and after its polymerization (30-60 minutes)

the stacking gel (4%) (Table 7) was layered on top and left to set for 60 minutes. Protein samples (20µg for extracellular vesicles and 10µg for whole cell lysates) were mixed with sample buffer, containing 5% β-mercaptoethanol, and heated for 5 minutes at 99°C. The prepared samples were then loaded onto the gel and resolved in electrode buffer (Table 8) for 60 minutes at 140 V. To determine the protein sizes a standard blue protein marker was applied.

Table 6. Resolving gel components

Chemicals	Volume
Tris (0.5M) +0.4% SDS (pH 6.7)	1 ml
Distilled H_2O	2 ml
Acrylamide (30%) (Sigma, A3699)	1 ml
APS (10%)	25 µl
TEMED (Sigma, T7024)	3.3 µl

Table 7. Stacking gel components

Chemicals	Volume
Tris (1.5M) +0.4% SDS (pH 8.8)	2.5 ml
Distilled H_2O	1,248 µl
Acrylamide (30%) (Sigma, A3699)	6 ml
APS (10%)	50 µl
TEMED (Sigma, T7024)	10 µl

Table 8. Electrode buffer

Chemicals	Volume
Tris 25mM	3.03g
Glycine 193mM	14.4g
SDS (10%)	10ml
Distilled H_2O	990ml

2.2.3.4 Western Blot

After electrophoresis, proteins were blotted onto a nitrocellulose membrane (Hybond P Membrane) where they could then be detected by specific antibodies. The stacking gel was removed and the resolving gel was placed on top of the nitrocellulose membrane. The blot was covered in two sheets of filter paper on each side followed by two sponges, arranged in a transfer cassette. Blotting was performed in transfer buffer (Table 9) in a transfer system and ran overnight at 25V at 4°C. The membrane was routinely stained with Ponceau to confirm effective transfer and as a loading control.

Table 9. Transfer buffer

Chemicals	Volume
Tris 25mM	3.03g
Glycine 193mM	14.4g
Methanol	200ml
SDS (10%)	10ml
Distilled H_2O	790ml

For the protein detection, the membrane was blocked in blocking solution (Tris buffer saline, 0.1% Tween and 5% non-fat milk powder) for at least 60 minutes at room temperature on a rocker, to saturate non-specific antigen binding sites. The membrane was then rinsed in two changes of TBS-T and subsequently

incubated in the appropriate primary antibody in TBST overnight at 4°C. The membrane was then rinsed several times in TBS-T (Tris buffer saline and 1% Tween) over a 20 minute period. The membrane was then incubated with horseradish peroxidase (HRP) conjugated goat anti-mouse, secondary antibody, in TBS-T (1:10,000) for 1 hour at room temperature on the rocker. The membrane was then rinsed several times in TBS-T over a 20 minute period.

Protein signals were detected using Prime reagent (Sigma Aldrich) in the LAS-2000 imager (GE Life Sciences). HRP is an enzyme which catalyses the oxidation of luminol, producing a chemiluminescence signal which can be detected in a biomolecular imager.

2.2.4 Electron microscopy

To visualise exosomes and microvesicles, vesicle pellets were resuspended in 2% paraformaldehyde and applied to a Cu-Rh formvar-coated 200 mesh grids (Agar Scientific) for 3 minutes. Absorbing paper was used to gently remove any excess suspension. Negative contrast was achieved by incubating the grid for 30 seconds in 1% uranyl acetate, excess liquid was blotted off. Subsequent analysis of vesicles were carried out by JEOL 2100+ Transmission Electron Microscope (Philips) and iTEM software (Olympus).

2.2.5 Nanoparticle analysis

2.2.5.1 NanoSight

Nanoparticle Tracking Analysis (NTA) is a method used for the visualisation and analysis of nanometre particles in liquids ranging from a size of 10-1000nm. The size of the particles are related to the rate of Brownian motion, temperature and the viscosity of the liquid and are not influenced by particle density or refractive index (Malvern). Each extracellular vesicle preparation was taken and particle counts and size distribution were determined using NTA (NanoSight Ltd, Amesbury, UK). The instrument was configured with a 488nm LM14 laser module

and a high sensitivity digital camera system (OrcaFlash2.8, Hamamatsu C11440, NanoSight Ltd, Amesbury, UK). Prior to analysis of extracellular vesicle samples, 100nm standard latex beads were tested as a control to confirm the NTA measurements were accurate. Samples were diluted in PBS, to a concentration between $2x10^6$ and $5x10^7$ particles/ml within the linear range of the instrument. Five replicate videos of 20 seconds were taken at 25°C, with samples under controlled flow, and analysed using NTA software (version 2.5), with the minimal expected particle size set to automatic, and camera sensitivity set at 12-16. The detection thresholds was set at 1-3, to reveal small particles.

2.2.5.2 Dynamic light scattering

Dynamic light scattering (DLS) is used to determine the size distribution profile of small particles in solution. The particle size distribution was determined by a Nicomp 370 submicron particle sizer. The fluctuation rate of scattered light for each sample is analysed by means of intensity by the Nicomp software, and the final size distribution for each sample was calculated using the number-weight Gaussian setting within the software.

2.2.6 Gene expression analysis

2.2.6.1 Total RNA isolation

The isolation of total RNA from cultured cells and from extracellular vesicles was carried out with spin column based miRNeasy Micro Kit (Qiagen) according to the manufacturer's instructions. Briefly, pellets were lysed in 700µl of lysis reagent. The samples were vortexed for 15 seconds to help cell lysis and then incubated at room temperature for 5 minutes to allow dissociation of nucleoprotein complexes. 140µl of chloroform was added to the samples for removal of cellular components. Samples were shaken vigorously for 15 seconds and incubated at room temperature for 3 minutes. Samples were centrifuged at 12,000 *x g* for 5 minutes at 4°C. After centrifugation, the sample separates into 3 distinct phases; an upper colourless aqueous phase containing RNA, a white interphase and a lower pink

organic phase. The upper aqueous phase was transferred into a new collection tube and 1.5 volumes of 100% ethanol was added and mixed thoroughly by pipetting up and down several times and subsequently applied onto a spin column containing glass fibre fleece. Columns were centrifuged at 8000 x g for 15 seconds at room temperature, this leads to the binding of nucleic acids to the column, whilst proteins and cellular debris are eluted. The columns containing the remaining RNA were washed once with RPE buffer then with 80% ethanol. The column was dried by a further centrifugation at 13,000 *x g* for 5 minutes, before 14µl of nuclease-free water was added to the column for the elution of the isolated RNA. Concentration and purity of the RNA was measured by NanoDrop ND-1000 (2.2.6.3).

2.2.6.2 DNase treatment

To remove contaminating DNA, isolated RNA samples from cell lysates were treated with DNase enzyme. For every 100µl of RNA 14µl of DEPC treated water, 12µl of RQ1 DNase and 14µl of 10x RQ1 DNase buffer were added. The samples were then vortexed briefly and incubated for 30 minutes at 37°C. 14µl of RQ1 stop solution was then added to inhibit DNase enzyme activity and the samples were incubated for a further 10 minutes at 65°C.

2.2.6.3 Measuring RNA concentration and purity

Concentration and purity of RNA was determined using a NanoDrop 2000c spectrophotometer. The upper and lower pedestals were cleaned with nuclease-free water before being blanked at zero with 1µl elution solution. 1µl of RNA sample to be analysed was pipetted onto the lower pedestal and the concentration was derived from the absorbance at 260nm. The ratio of absorbance at 260nm and 280nm was used to verify the purity of the RNA sample. A ratio of ~1.8-2.0 is ideal. The ratio of absorbance at 260nm and 230nm was used to verify the purity of nucleic acids. A ratio between ~2.0-2.2 is ideal. For exosomes and microvesicles, a 260/280 >1.7 was considered acceptable for further analysis.

2.2.6.4 Complementary DNA (cDNA) synthesis

To allow for the analysis of gene expression by qRT-PCR, the isolated RNA was transcribed into complementary DNA (cDNA). 100ng of RNA was mixed with 1 µl of random primers (3µg/µl), 1µl of oligoT_{25} (50µM) and 1µl of dNTPs, made up to a total volume of 14µl with dH_2O. The mixture was briefly centrifuged an incubated for 5 minutes at 65°C, followed by 1 minute incubation on ice. Reverse transcriptase binds to the random primers. 1µl of Superscript III Reverse Transcriptase was added to the mixture, along with 1µl of Dithiothreitol (DTT) and 4µl of 5x first strand buffer. The prepared reaction mixture was incubated in a thermal cycler for 5 minutes at 25°C, 45 minutes at 50°C followed by 15minutes at 70°C to inactivate the reaction. For RNA extracted from whole cell lysates, the samples were diluted in a ration of 1:10 with dH_2O and stored at -20°C.

2.2.6.5 Quantitative real-time PCR (qRT-PCR)

Changes in gene expression were analysed by quantitative real-time PCR (qRT-PCR) using SYBR green detection. The PCR technique amplifies DNA using DNA polymerase to synthesise new DNA from a template strand. PCR typically involves 35-40 cycles in which the gene of interest is amplified. Each PCR cycle consists of three main steps; initial DNA denaturation, followed by the annealing step of gene specific primers, and finally extension in which DNA polymerase synthesises the complementary DNA strand. The amount of DNA doubles for each cycle and every cycle involves a measurement of the fluorescence of SYBR green which emits a fluorescent signal when bound to double-stranded DNA. Therefore, the fluorescence increases with every cycle completed. The number of the cycle in which the fluorescence reaches the threshold level is called Ct value and was normalized on the expression of the house-keeping gene GAPDH (=ΔCt value).

The primers used in this study were designed as described in 2.2.6.6 and are listed in Table 13. samples were normalized on GAPDH expression. For each gene 13µl from the prepared PCR reaction mix (Table 10) were pipetted into a 96-well plate

in triplicates. To each well 1µl cDNA (10ng) diluted in nuclease-free water were added. The plate was sealed, centrifuged (2 min, 750 *x g*) and RT-PCR was carried out according to the following protocol (Table 11), at the optimised annealing temperatures, in the CFX96 Real-Time PCR machine detection system (BIO-RAD). To confirm the specificity of the product a melt curve was also added.

Table 10. PCR reaction mix

Reagent	Amount added/well (µl)
SYBR green master mix*	7.5
Forward-primer	1.5
Reverse-primer	1.5
ddH_2O	2.5
TOTAL	13

*SYBR-Green master mix: iTaq DNA polymerase, dNTP mix, $MgCl_2$, SYBR green dye, enhancer and fluorescein.

Table 11. PCR programme

Number of cycles	Duration	Temperature (°C)
1	3 minutes	95
Denaturation	10 seconds	95
x40 Annealing	30 seconds	Variable temp (see Table 10)
Extension	30 seconds	72
Melt curve	Increments of 0.5°C increase every 5 seconds	65-95

2.2.6.5.1 Primer design

Gene specific primer pairs for qRT-PCR analysis were designed using the open-source web tool NCBI Primer-BLAST. The gene of interest mRNA sequence was

identified through NCBI RefSeq and submitted for primer selection. A stringent selection criteria was applied to find primer sequences (Table 12) Once primer sequences were identified, a second selection process was applied to the sequences using OligoAnalyzer 3.1 (Integrated DNA technologies) to predict oligo secondary structures using mFold algorithm, report possible duplexes and their stabilities when oligo hybridizes to itself and examine possible duplexes when the oligo can anneal to any target sequence. Published primers were also assessed to check their suitability.

Table 12. Primer design parameter for web tool NCBI Primer-BLAST

Primer Parameters	Parameter range
PCR product size	70-150
Target size (bp)	150
Intron length (bp)	Min 200
Melting temperature (T_m) (°C)	Min 57 (default) Optimum 60 (default) Max 63 (default)
Max T_m difference (°C)	3 (default)
GC%	40-60
Max 3' self-complementarity	3
Max self-complementarity	5

2.2.6.5.2 Primer optimisation

To determine the optimal annealing temperature for qRT-PCR, gradient PCRs were performed. A cell line with high expression of the gene of interest was determined from ProteinAtlas database and a RT-PCR was set up to test a range of annealing temperatures. 1µl of cDNA was added to 14µl of master mix (Table 10) for each temperature tested. Internal controls, NRT (no reverse transcription) and NTC (no template control), were included to check for genomic DNA contamination. The

RT-PCR was carried out according to the protocol (Table 11). The PCR products for each temperature were visualised on a 2% agarose gel to verify a single gene product at the appropriate molecular weight and to determine the optimal annealing temperature.

2.2.6.5.3 qRT-PCR product analysis by gel electrophoresis

Agarose Gel Electrophoresis of DNA was performed using a gel unit. The agarose gel was preparing 1% agarose in TAE buffer (40mM Tris (pH 7.6), 20mM acetic acid and 1mM EDTA) followed by heating. Once cooled ethidium bromide was added at 0.5µg/ml, the gel was then poured and the comb put into place. 1KB DNA ladder was used as a reference to estimate the size of the DNA fragment. Samples were supplemented with loading buffer (Cell signalling) (6% SDS, 30% glycerol and 0.03% bromophenol blue) were run with a constant voltage of 120V for 45minutes. DNA was visualised by UV trans-illumination and a digital photograph was taken.

2.2.7 Statistical analysis

All experiments were performed at least in biological duplicates. Data are presented as means ±SEM. Multiple comparisons were analysed by one or two-way ANOVA. A value of $p < 0.05$ was considered statistically significant. All statistical analysis were performed using GraphPad Prism 7.0 software.

3. Results

The aim of this project was to optimise a protocol for the reproducible isolation of extracellular vesicles from medulloblastoma cells and to investigate the role of exosomes and microvesicles in medulloblastoma metastasis. Therefore, the first part of this project focuses on the establishment of a protocol for the isolation of total microvesicles and exosomes from medulloblastoma cell lines, followed by verification of extracellular vesicle populations based on size, specific exosomal protein markers, and morphology. The second part of this project was to use this protocol to isolate and characterize exosomes and microvesicles from a series of medulloblastoma cell lines representing different subtypes and metastatic capacity. The final part of the project was to investigate whether when cells expressed candidate markers of metastasis, would the derived extracellular vesicles also express these markers.

3.1 Medulloblastoma cells release two distinct populations of extracellular vesicles

The majority of methods recommended culturing cells in exosome-depleted FBS (see section3.1.1) for 48 hours after cells reached 70-80% confluence. Several observations revealed that leaving our cell lines for an extra 48 hours after they had reached 70-80% confluence resulted in large numbers of cells becoming detached and dying off. This would result in the release of apoptotic bodies from tumour cells. Thus, we altered the culture conditions to limit cell death by culturing cells in exosome depleted FBS after they reached 30% confluency.

Exosomes and microvesicles can be isolated from cell culture by various methods including, exosome precipitation kits, ultrafiltration and ultracentrifugation. We initially tried isolating medulloblastoma exosomes using the exosome precipitation kit ExoQuick™ (System Bioscience, California, USA) according to the manufactures guidelines. We then analysed our isolated exosome samples by

western blot analysis using exosome markers CD9, CD63 and tsg-101. Unfortunately, after several isolation attempts, no bands were detected in any of our isolated exosome samples. We therefore tried an ultracentrifugation isolation method based on previously published protocols (Thery *et al.,* 2006, Menck *et al.,* 2014). The final multistep centrifugation protocol used produced a reproducible final pellet containing exosomes (as will be demonstrated below), and an earlier lower g-force speed pellet believed to include larger microvesicles (summarised in 2.2.2.2).

In order to identify if our isolation method produced two distinct vesicle populations, exosomes and microvesicles were isolated from the six different medulloblastoma cell lines; non-metastatic UW228-3, DAOY, CHLA-01 and metastatic CHLA-01-R, D283 and HD-MB03. Since extracellular vesicle cargo can be regulated by the state of the parental cell, all cells were grown under basal conditions, without any prior stimulation of the cells which could alter the protein expression of the extracellular vesicles.

3.1.1 EV samples did not contain foetal bovine serum EV impurities

To ensure our extracellular vesicle preparations from medulloblastoma cell culture media only contained the extracellular vesicles from our cells, and not from FBS in the media, we used exo-depleted FBS. This was achieved by overnight ultracentrifugation of FBS at 100,000 *x g*. Dynamic light scattering (DLS) analysis revealed that standard FBS samples shows a large amount of bovine exosome and microvesicle sized particles, whereas the FBS exo-depleted sample has a significant reduction in these particles (Figure 10).

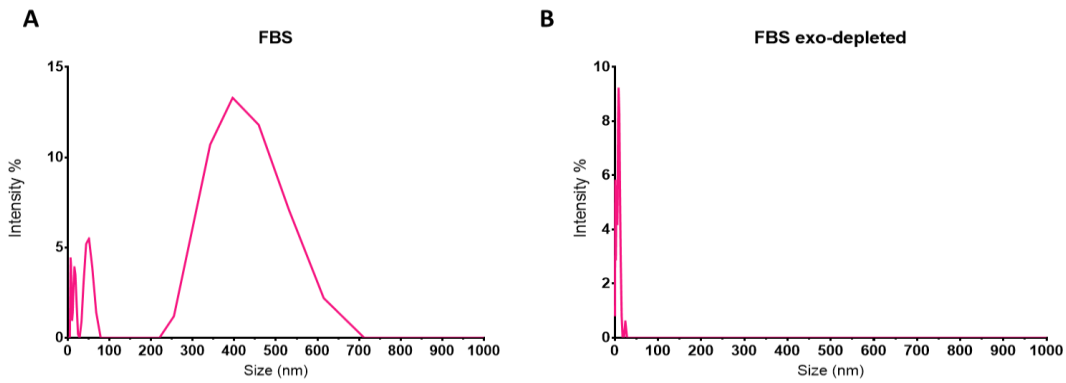

Figure 10. FBS comparison to ultracentrifuge FBS
Foetal bovine serum (FBS) is a rich source of exosomes. To ensure we only studied medulloblastoma derived exosomes, FBS was subject to overnight ultracentrifugation, 100,000 *x g*. Normal FBS was then compared with exo-depleted FBS by dynamic light scattering. (A) Normal FBS showing a range of different particle sizes (B) FBS after ultracentrifugation, showing no measurable bovine exosomes.

3.1.2 Verification of exosomes and microvesicles by NTA

Nanoparticle tracking analysis (NTA) has the capability to resolve and accurately measure different size particles concurrently within the same solution. In comparison to DLS, NTA also allows for the direct estimation of particle concentration. Figure 11 shows an example of a video capture from NTA of exosomes and microvesicles isolated from UW228.3 cells. From the capture the exosome sample appears much more homogenous in size compared to the microvesicle sample (Figure 11).

NTA was used to determine particle numbers and sizes. In order to find the optimal parameter settings for extracellular vesicle measurements, the amount of individual readings taken was optimised. We initially tried running three distinct readings of 30 seconds for our samples. However, after analysis of the results, there appeared to be a lot variation between the three different tracks. Therefore, we tried five distinct readings of 60 seconds for our samples. This reduced the previously observed variation between the different tracks. The final reading we tried was ten readings for 60 seconds, however there was little difference between this and the five readings, therefore we decided to use five readings of 60 seconds for all extracellular vesicle isolations.

A series of exosome and microvesicle isolates were measured by NTA using our optimised parameters. The resulting data were highly consistent and revealed two distinct population of extracellular vesicles, exosomes with a modal particle size of ~100nm and microvesicles with a modal particle size of >150nm. Exosome samples have several other peaks at larger sizes, however these are seen at much lower concentrations. In comparison, microvesicle samples have a much more heterogenous spread of peaks at larger sizes (above 300nm). The concentration of exosomes ranged between $6x10^6$ -$5x10^7$ particles/ml whereas microvesicles ranged between $5x10^5$–$1.5x10^7$ particles/ml. This was consistent across the six different medulloblastoma cell lines (Figure 12 and Figure 13).

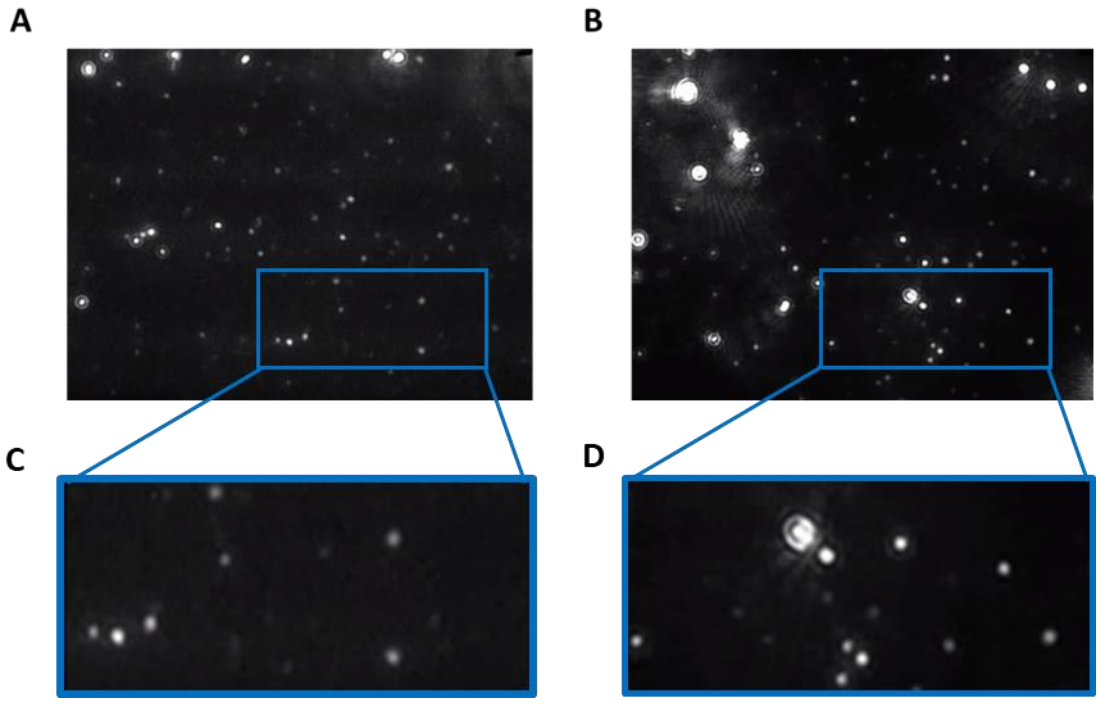

Figure 11. Nanoparticle tracking video frame of extracellular vesicles
Example of NanoSight NTA video frame capture. (A) Exosomes isolated from UW228-3 medulloblastoma cells (B) Microvesicles isolated from UW228-3 cells (C) Magnification of video capture showing homogeneity of exosome sample (D) Magnification of video capture showing heterogeneity of microvesicle sample.

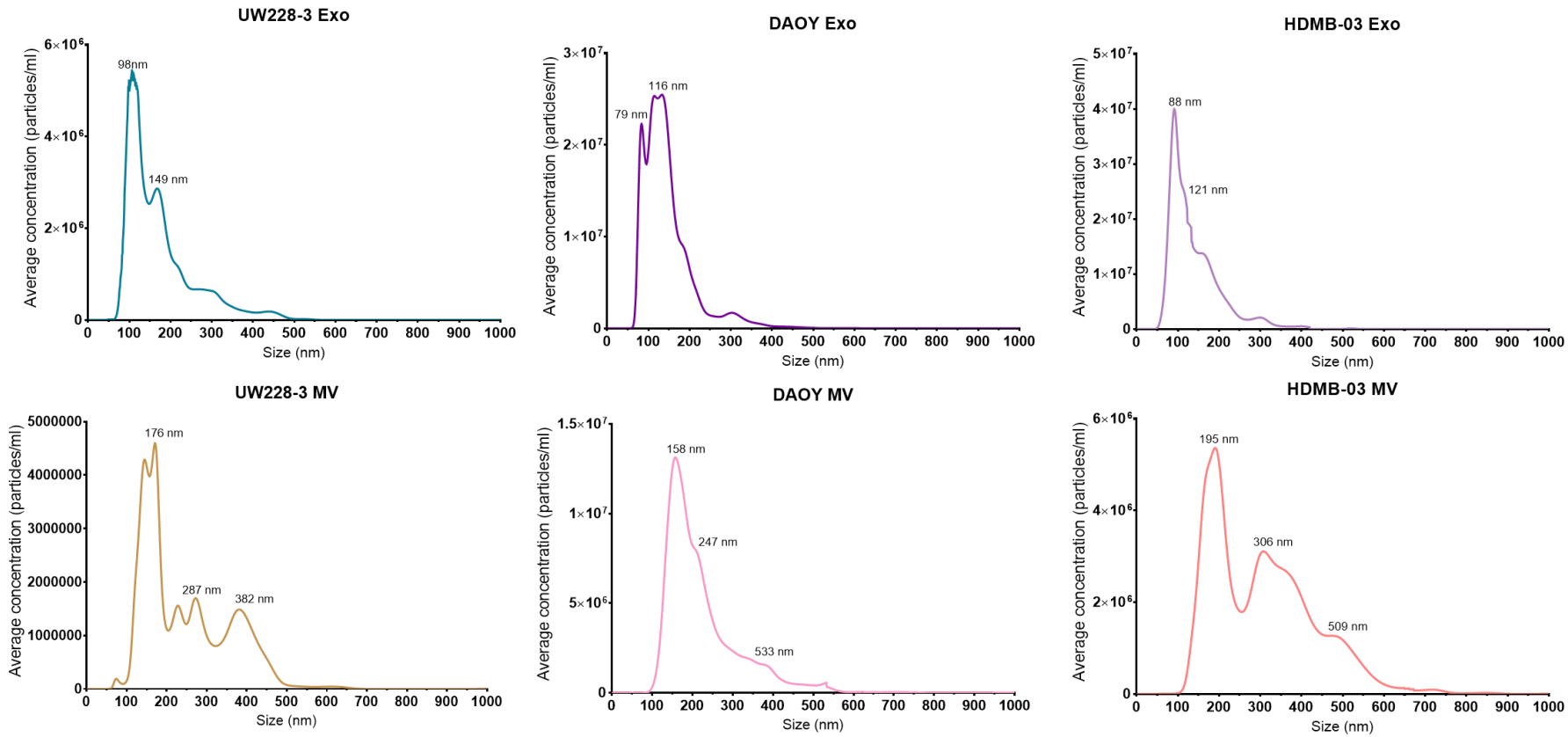

Figure 12. Nanoparticle tracking showing EV sizes and concentrations
Vesicle concentrations and size distributions were verified using Nanoparticle tracking analysis (NTA) from UW228-3, DAOY, and HD-MB03 cells. Sizes of identified peaks are indicated. The modal size of isolated Exosomes (Exo) is <100 nm, which is consistent across the six cells lines. The modal range of microvesicle (MV) is >150 nm. Based on optimisation a total of 5 readings of 60 seconds were taken for each of the samples. (n=2)

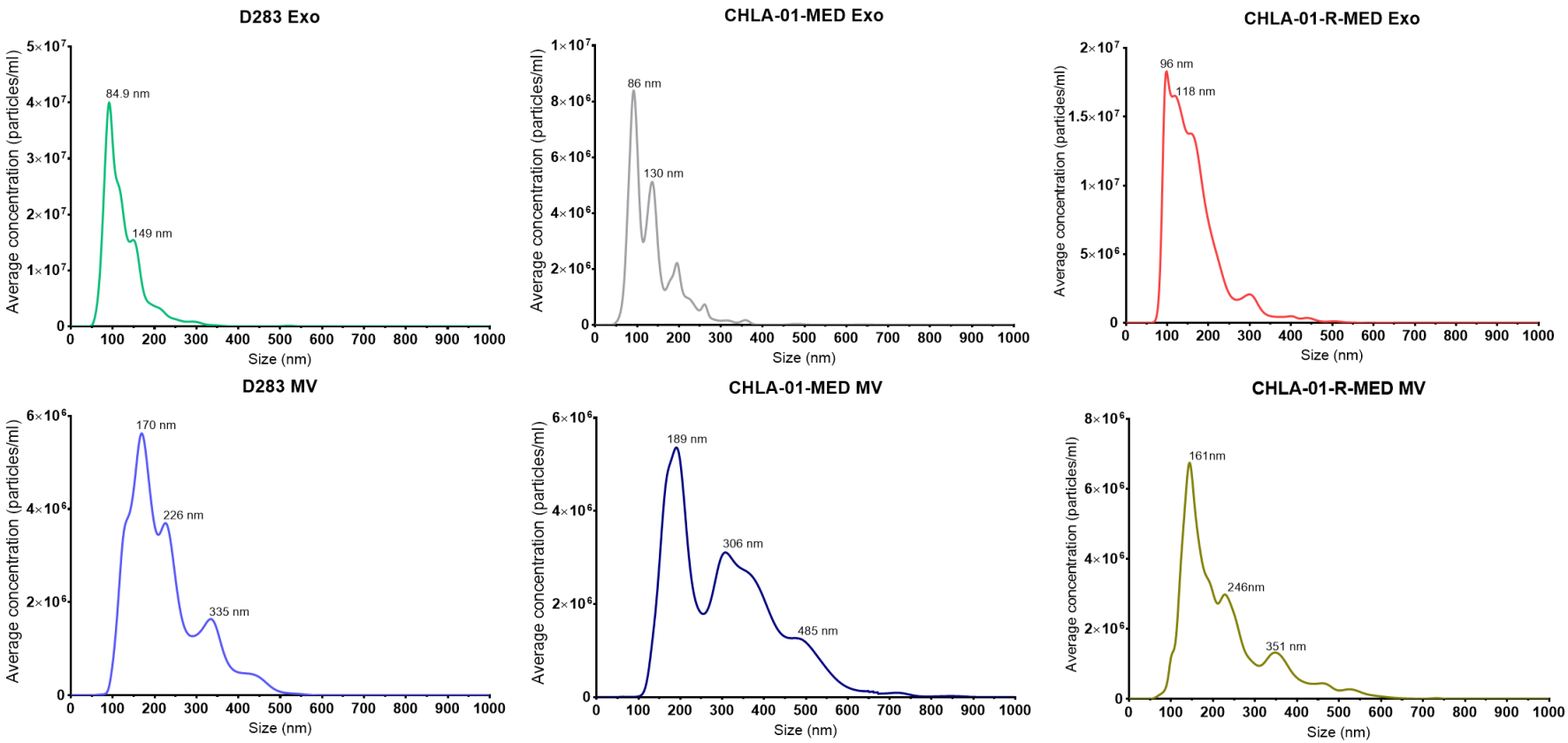

Figure 13. Nanoparticle tracking showing EV sizes and concentrations
Vesicle concentrations and size distributions were verified using Nanoparticle tracking analysis (NTA) from D283, CHLA-01-MED and CHLA-01-R-MED cells. Sizes of identified peaks are indicated. The modal size of isolated Exosomes (Exo) is <100 nm, which is consistent across the six cells lines. The modal range of microvesicle (MV) is >150 nm. Based on optimisation a total of 5 readings of 60 seconds were taken for each of the samples. (n=2)

3.1.3 Verification of exosomes and microvesicles by Electron Microscopy

Transmission electron microscopy (TEM) was used to measure diameters of isolated vesicles. However, as extracellular vesicles are small and low in concentration several optimisation steps were needed. Initially, samples were fixed and loaded onto carbon coated grids, however after examination in the electron microscope the grids appeared to be empty. This was probably due to the very low concentration of extracellular vesicles in our initial samples. Next, we tried negatively staining the samples with 1% uranyl acetate. Unfortunately, uranyl acetate dried on the grids producing water bubbles which appeared to share similar morphological features and diameter sizes to exosomes (Figure 14). It was apparent that in order to visualize exosomes and microvesicles by TEM, we needed to increase their concentrations on the grid. To do this we used glow discharge on the carbon-coated grids, the purpose of this was to make the carbon grids more hydrophilic so the samples in PFA will stick to the grid and not be removed during the drying process.

Results from TEM revealed distinct populations of exosomes and microvesicles. Their sizes were determined directly from electron microscopy. Exosomes typically displayed a clustered appearance, however where single exosomes were found they were spherical in morphology with vesicle diameters <100nm (Figure 15), this is consistent with exosome verification by NTA (Figure 12). Exosomes appeared extremely homogenous in appearance. Several studies have described exosomes to contain a lipid-bilayer (Thery *et al.,* 2006, Kowal *et al.,* 2016), however due to the small sizes and density the expected bilayer appears indistinguishable. Microvesicles consisted of a much more heterogenous population of large vesicles with an average diameter of >150nm (Figure 16), this is also consistent with results seen from NTA (Figure 13). As microvesicles are much larger than exosomes, the lipid bilayer was easily distinguishable

(highlighted by blue arrows Figure 16). Microvesicles were typically geometric in appearance. They also appear to have regions of high and low density (highlighted by yellow arrows Figure 16); however, this could be a side-effect from the vacuum inside the TEM, which puts pressure on the vesicles causing them to ripple, thus resulting in higher density regions.

It was important to note that neither population contained either cell organelles or fragmented DNA, thus excluding the presence of apoptotic bodies. Unfortunately, due to the extensive optimisation of sample preparations needed, TEM images were only produced for extracellular vesicles isolated from CHLA-01 and CHLA-01-R cells.

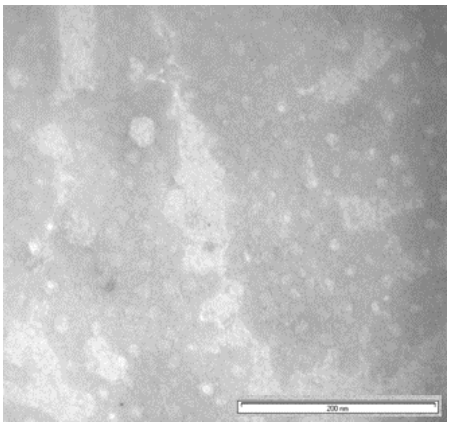

Figure 14.TEM of dried uranyl acetate and exosomes
Isolated exosomes were loaded onto copper-coated TEM grids and stained with 1% uranyl acetate. Grids were examined by TEM. Unfortunately, uranyl acetate dried on the grids producing water bubbles which appeared to share similar morphological features and diameter sizes to exosomes.

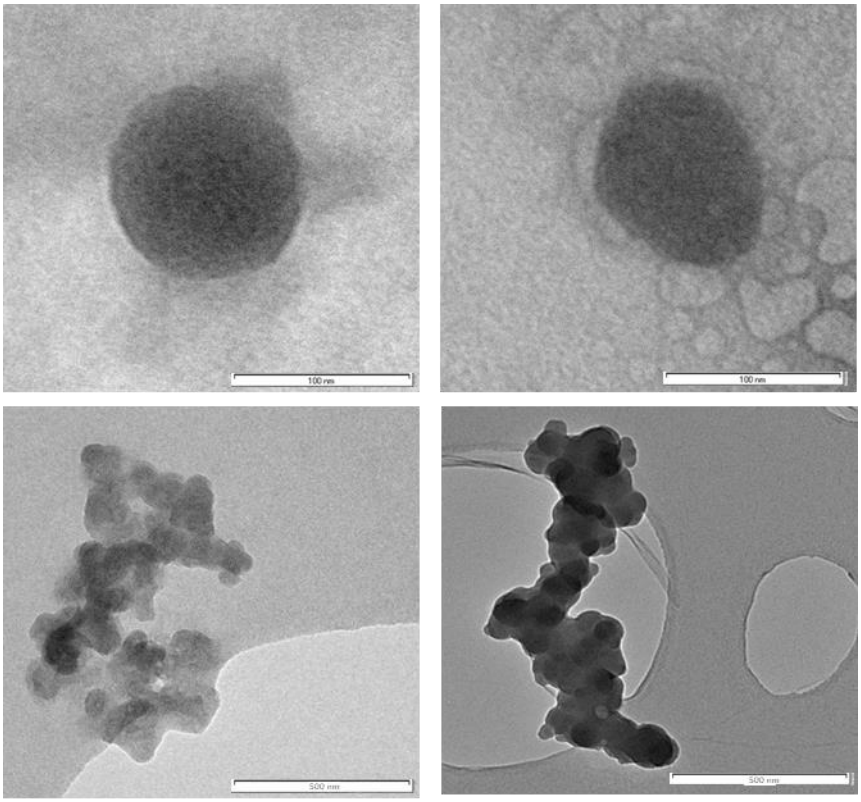

Figure 15. TEM images of exosomes
Exosomes isolated from CHLA-01 (left column) and CHLA-01-R (right column) medulloblastoma cells were loaded onto copper-coated grids which had been pre-treated by glow-discharge. Grids were examined by transmission electron microscopy (TEM). Exosomes typically displayed a clustered appearance (lower panel), however where single exosomes were found (top panel) they were spherical in morphology with vesicle diameters <100nm.

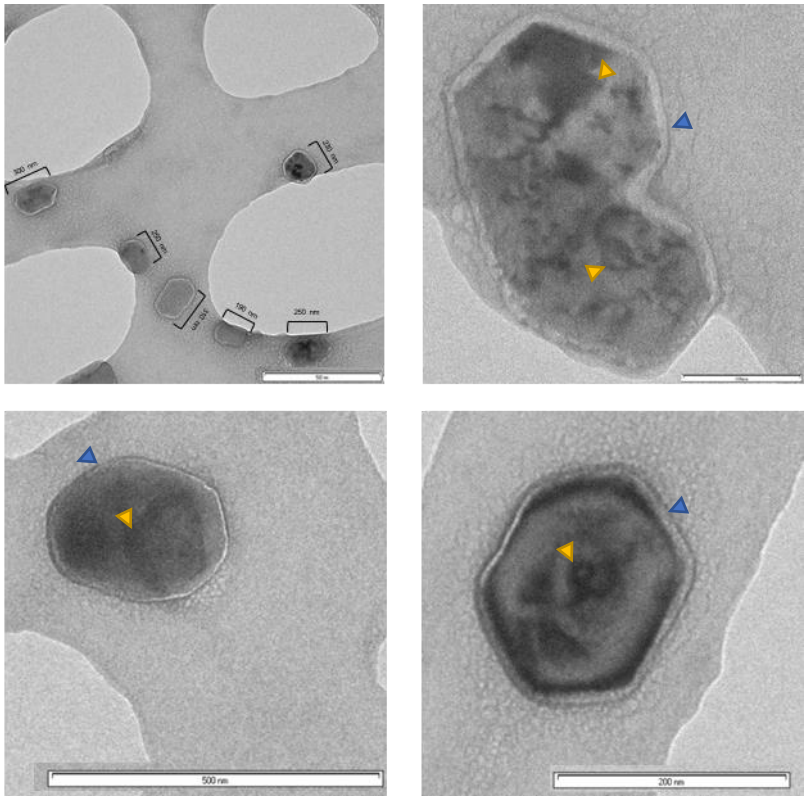

Figure 16. TEM images of microvesicles
Microvesicles isolated from CHLA-01 (left column) and CHLA-01-R (right column) medulloblastoma cells were loaded onto copper-coated grids which had been pre-treated by glow-discharge. Grids were examined by transmission electron microscopy (TEM). Microvesicles consisted of a very heterogenous population of large vesicles with an average diameter of >200nm. Microvesicle lipid bilayers are easily distinguishable (highlighted by blue arrows). Microvesicles are typically geometric in appearance. They also appear to have regions of high density (highlighted by yellow arrows).

3.1.4 Verification of exosomes by Western Blot analysis

The final step of extracellular vesicle characterisation involved analysing protein extracts from exosomes by western blot for the expression of known exosomal markers. Markers included Tsg101, a well-known exosomal marker associated with multivesicular bodies, and one of the most abundant intracellular tetraspanins found in exosomes, CD63 (Kowal *et al.,* 2016). The final marker used was the transmembrane protein EMMPRIN, which has been detected in some exosome samples (Redzic *et al* 2013). Western blotting detected both CD63 and Tsg101 in the exosomes as well as in the cell lysates from all six medulloblastoma cell lines. EMMPRIN was detected in all cell lysates, and was enriched in CHLA-01 and CHLA-01-R cells. EMMPRIN was only detected in exosomes derived from

CHLA-01 and CHLA-01-R cells. Histone 4 (H4) is a negative marker for exosome samples (Lotvall *et al.,* 2014). Exosome samples were negative for the nuclear marker, H4, however all cell lysates were positive for H4, showing that our final pellet was not just nuclear debris (Figure 17).

Initially, the aim was to analyse protein from both exosomes and microvesicles, however not enough protein was isolated from microvesicles for western blot analysis (section 3.2.1).

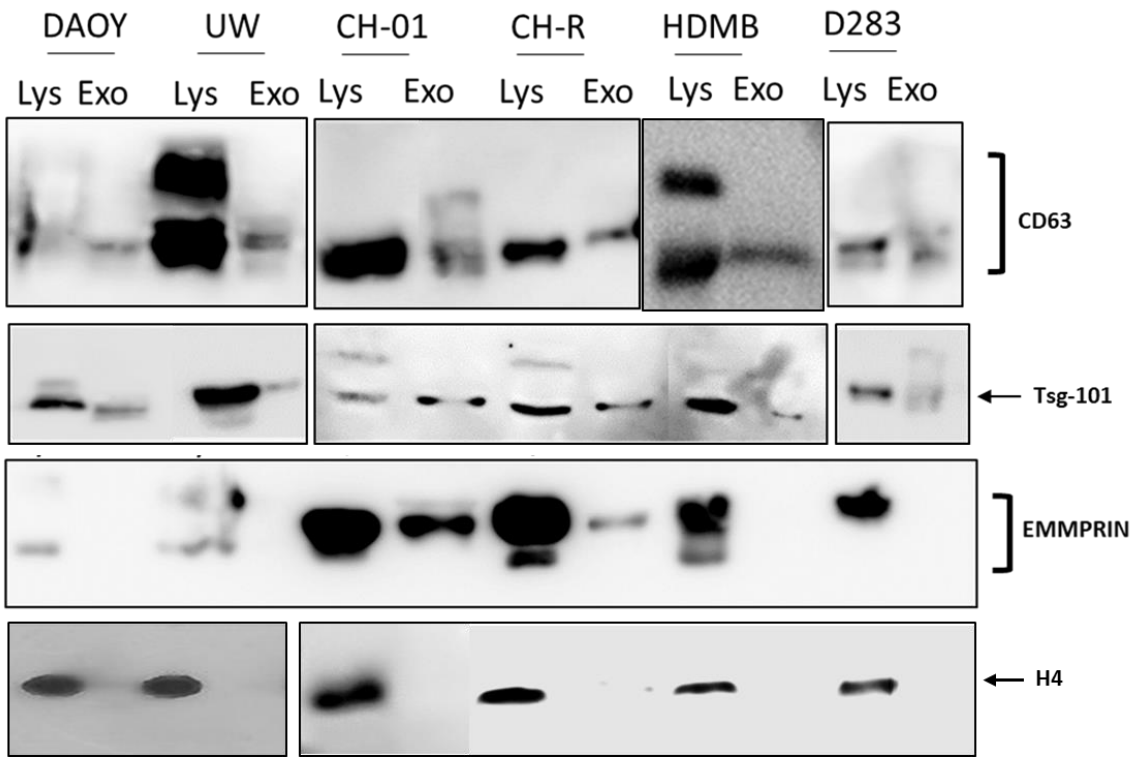

Figure 17. Western blot analysis of medulloblastoma derived exosomes
Exosomes were harvested from DAOY, UW228-3 (UW), CHLA-01 (CH-01), CHLA-01-R (CH-R), HDMB03 (HDMB) and D283 cell lines and were compared to cell lysates. Exosomes and cells were lysed and the protein content was measured by Bradford assay. 20µg of exosome lysates and 10µg of cell lysates were loaded onto gels. Samples were then probed with exosome specific antibodies CD63, Tsg101 and EMMPRIN. The absence of Histone 4 (H4) in exosome samples demonstrates a pure exosome preparation. Lys: cell lysate; Exo: exosome lysate.

3.2 Differential profiles of EVs from metastatic tumour cells compared with non-metastatic cells

Several studies have shown that exosome numbers are elevated in the plasma of cancer patients compared to healthy controls, and increased levels of extracellular vesicles released correlates with poor prognosis and survival outcome (Baran *et al.,* 2010, Gercel-Taylor *et al.,* 2012). Therefore, we wanted to investigate whether there was a difference between amounts of extracellular vesicles released from a series of medulloblastoma cell lines representing different subgroups and metastatic capacity.

Exosomes and microvesicles were successfully isolated from both metastatic (M+) and non-metastatic (M0) medulloblastoma cell lines, their properties were characterised by NTA, TEM and western blot analysis. Next, we wanted to compare the properties of the exosomes and microvesicles isolated from our six medulloblastoma cell lines and characterise their relative numbers, protein concentration and RNA concentration.

3.2.1 NTA detected more metastatic exosomes

As well as determining size, NTA also has the capacity to measure particle concentrations in a given volume. NTA detected a significant increase in exosomal concentrations between metastatic exosomes compared with non-metastatic exosomes ($p \leq 0.01$) (Figure 18). The lowest concentration of exosomes was produced from UW228-3 cells. Similar results were seen in microvesicles, where UW228-3 cells produced the lowest concentration of microvesicles (Figure 18).

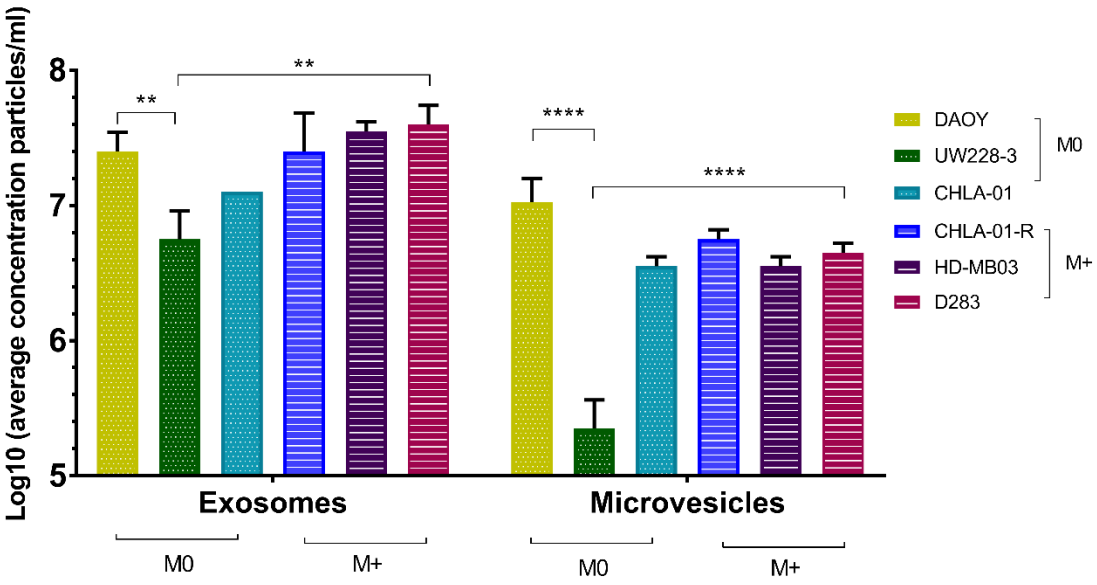

Figure 18. Particle concentrations of extracellular vesicles
Nanoparticle tracking analysis (NTA) was used to determine the log10 of the average concentration of particles/ml isolated from six different medulloblastoma cell lines. Metastatic cell lines, HD-MB03 and D283 produced the largest number of particles. (** p ≤0.01 **** p ≤0.0001) (n=2)

3.2.2 Metastatic exosomes contain more protein cargo

Protein concentration of extracellular vesicles were analysed by Bradford assay, and protein yields were compared between the cells different metastatic status. We observed that whilst there is no significant difference between the amount of protein isolated from cell lysates from the varying different cell lines (Figure 19), exosomes isolated from metastatic cell lines (D283 and HD-MB03) produced significantly higher levels of proteins compared to the non-metastatic cell lines (p≤0.001). The least amount of protein isolated was consistently seen in exosomes from CHLA-01 cells, and the highest amounts were isolated from D283 exosomes (Figure 18). These differences were not represented in the amount of protein isolated from microvesicles (Figure 20), where the yield was consistently low.

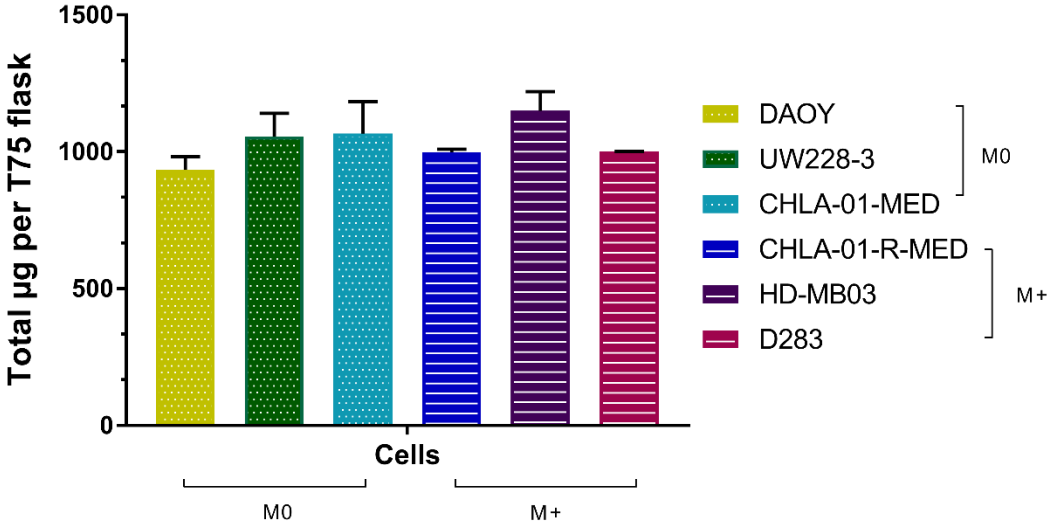

Figure 19. Protein amounts in cells
Cell pellets of six different medulloblastoma cell lines were lysed and protein was extracted. Protein concentrations were determined by Bradford assay. There were no significant differences between cell lines and protein amounts. M+: Metastatic; M0: non-metastatic (p=>0.05) (n=3)

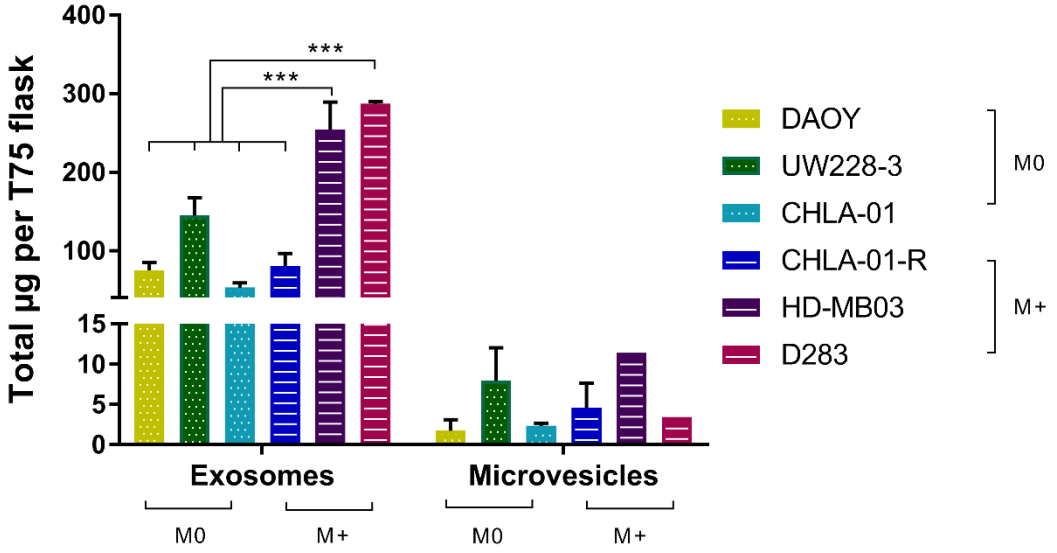

Figure 20. Protein amounts in extracellular vesicles
Exosome and microvesicle pellets from six different medulloblastoma cell lines were lysed and protein was extracted. Protein concentrations were determined by Bradford assay. Metastatic cell lines (M+) were compared with non-metastatic cell lines (M0). Metastatic cell lines, HD-MB03 and D283, consistently produced greater yields of protein. (***p≤0.0001) (n=3)

3.2.3 Metastatic exosomes contain more RNA cargo

In order to analyse exosomal and microvesicle RNA cargo, we first needed to optimise a protocol for RNA extraction which would give a high yield and purity of RNA suitable for gene expression analysis.

Cellular and exosomal RNA was extracted using four different RNA isolation methods. To assess the RNA yield of exosomes, total RNA was analysed with a Nanodrop. The RNA yield differed substantially between the different isolation methods. The total RNA amounts ranged between 10 ng per T75 flask (Agilent) to 500 ng per T75 flask (Qiagen). For the three cell lines (DAOY, UW228-3 and D283) the Qiagen kit resulted in the highest yield of total RNA. The mirVana and Agilent showed the lowest total RNA yield in exosomes (Figure 21A). When comparing purity of the isolated RNA, results ranged from 1.148 for 260/280 and 0.06 for 260/230 to 2.04 for 260/280 (mirVana) and 1.69 for 260/230 (Qiagen) (Figure 22B). From these results, it is clear that the Qiagen kit produced the highest yield and purity of RNA required for gene expression analysis. Therefore, for all RNA isolations the Qiagen kit was used.

The RNA amounts between the different cell lines were also measured. Cell pellets were lysed and RNA was extracted, cell pellets were from cell lines grown in T75 flask to 70-80% confluency. RNA concentrations were determined by Nanodrop. Metastatic (M+) CHLA-01-R cells consistently produced the greatest yield of RNA and non-metastatic (M0) UW228-3 consistently produced the lowest yields of RNA. There was no significant difference between the amount of RNA isolated from, DAOY, CHLA-01-R, HD-MB03 and D283 cells (Figure 22). When comparing RNA isolated from extracellular vesicles, very similar results were seen, as to what was observed in protein levels. Where the metastatic cell line, HD-MB03, consistently produced higher yields of RNA (Figure 23) and there were no significant differences observed in the remaining exosomes. There was no significant difference between the amounts of RNA produced between the microvesicles.

A

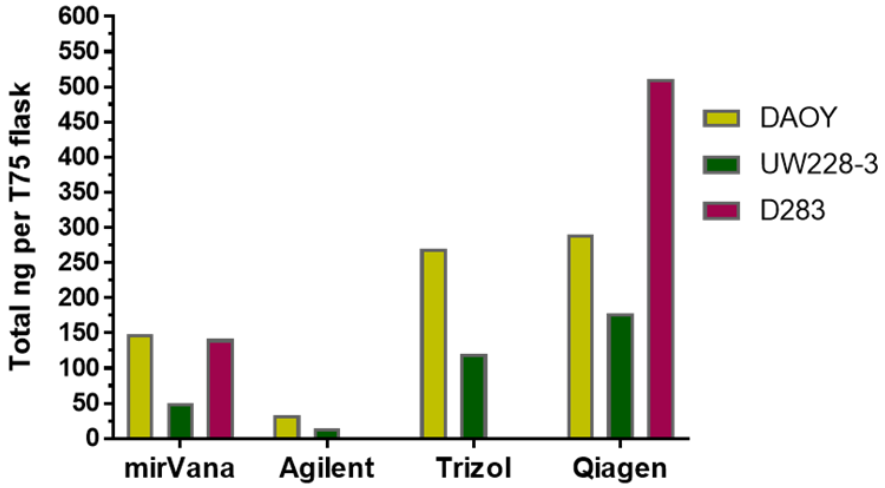

B

Isolation method	260/280	260/230
mirVana	1.48	0.06
Agilent	1.51	0.21
Trizol	1.95	0.98
Qiagen	2.04	1.69

Figure 21. Yield and purity of exosomal RNA extracted by 4 methods
Total RNA from exosome pellets from three different cell lines, DAOY, UW228-3 and D283, was isolated using either a mirVana kit, an Agilent kit, Trizol reagent or a Qiagen kit. RNA yields and purity were determined by Nanodrop. (A)The Qiagen kit resulted in the highest yield of total RNA compared with mirVana, Agilent and Trizol. (B) Qiagen kit produced the best RNA purity.

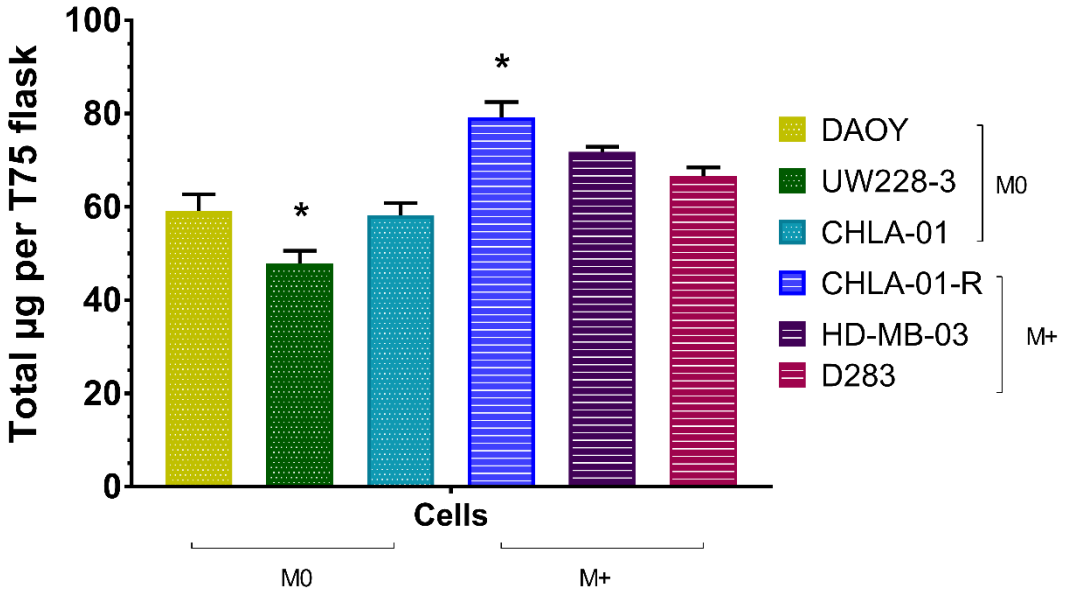

Figure 22. RNA amount in cells
Cell pellets of six different medulloblastoma cell lines were lysed and RNA was extracted. RNA concentrations were determined by Nanodrop. Metastatic (M+) CHLA-01-R cells consistently produced the greatest yield of RNA and non-metastatic (M0) UW228-3 consistently produced the lowest yields of RNA. (* p ≤0.05) (n=3)

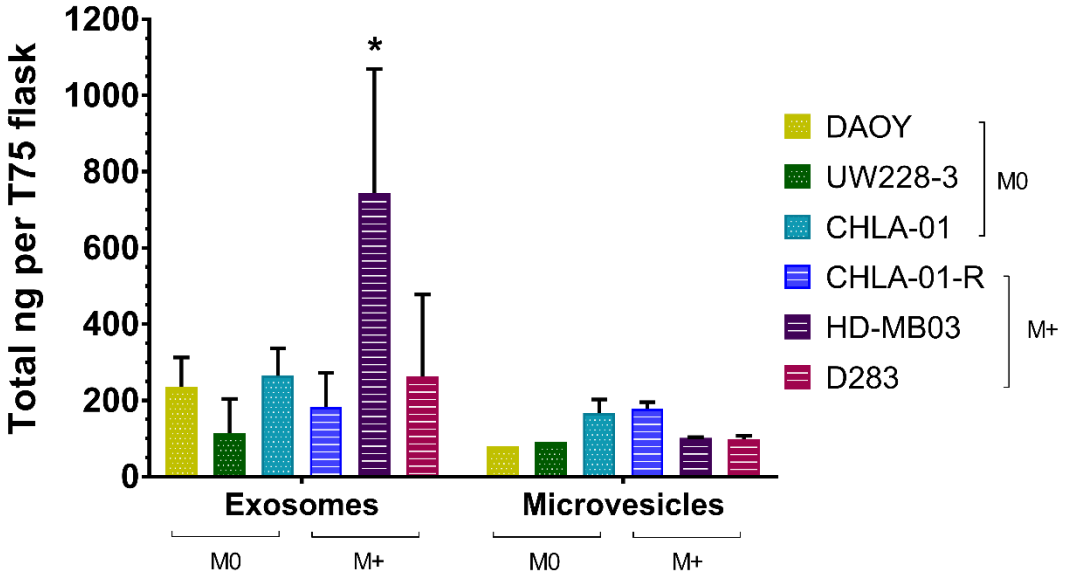

Figure 23. RNA amount in extracellular vesicles
Total RNA was extracted from extracellular vesicles derived from six different medulloblastoma cell lines. RNA concentrations were determined by Nanodrop. Metastatic cell line, HD-MB03, consistently produced the greatest yields of RNA. M+: Metastatic; M0: non-metastatic (* p ≤0.05) (n≥2)

3.3 Markers of metastasis present in extracellular vesicles

Several studies have shown that exosomes would be ideal biomarkers for cancer as they closely represent the state of their originated cell, therefore we hypothesised that if cells expressed candidate markers of metastasis the derived extracellular vesicles would also express these markers.

3.3.1 Primer optimisation of candidate markers

Annealing temperatures of QRT-PCR is a critical parameter for reaction specificity. Setting an annealing temperature too low can result in amplification of non-specific PCR products. Equally, setting the annealing temperature too high can result in a reduced yield of the desired PCR product. Therefore, primers used for QRT-PCR reactions were analysed to determine their optimal annealing temperatures. This involved running a series of amplification processes at different annealing temperatures ranging from 56-64 in a gradient PCR for primers c-Met and ITG-A9. Analyses of amplification products after 35 cycles were performed and results are shown below (Figure 24). Higher intensities of the desired product band was seen at 64°C, therefore the annealing temperature of c-Met and ITG-A9 primers were set at 64°C. Three additional primers were also tested, mmp-2, ITG-B1 and mmp-9, however the desired product band was not seen, therefore, these primers were not taken forward.

Successful QRT-PCR requires efficient and specific amplification of the desired product. To determine reaction efficiency standard curves were constructed using a dilution series. The efficiency of the assay should range between 90-110%, indicating that the percentage of target cDNA doubles with each PCR cycle. The R2 of the standard curve identifies the consistency of amplification at the different serial dilutions and should be >0.980. Finally, the slope of the standard curve can be directly correlated to the efficiency of the reaction. An efficiency value of 100% produces a slope of -3.32. Slopes between -3.0 and -3.8 are deemed efficient. c-

Met, ITG-A9, ABCB1 and GAPDH primers are all within the acceptable ranges. Melt curve analysis was used to determine specificity of the PCR products. Single melt curve peaks show that a single specific product was produced (Figure 25). For c-Met and ITG-A9 peaks were also identified in the control reactions when no template cDNA was added. These second peaks indicate that when no cDNA is added to the reaction mix the primers can self-dimerize. However, when cDNA is added the primer dimer peaks disappear and do not interfere with results (Figure 24). Sequences of primers along with annealing temperatures and primer efficiency values can be found in Table 13.

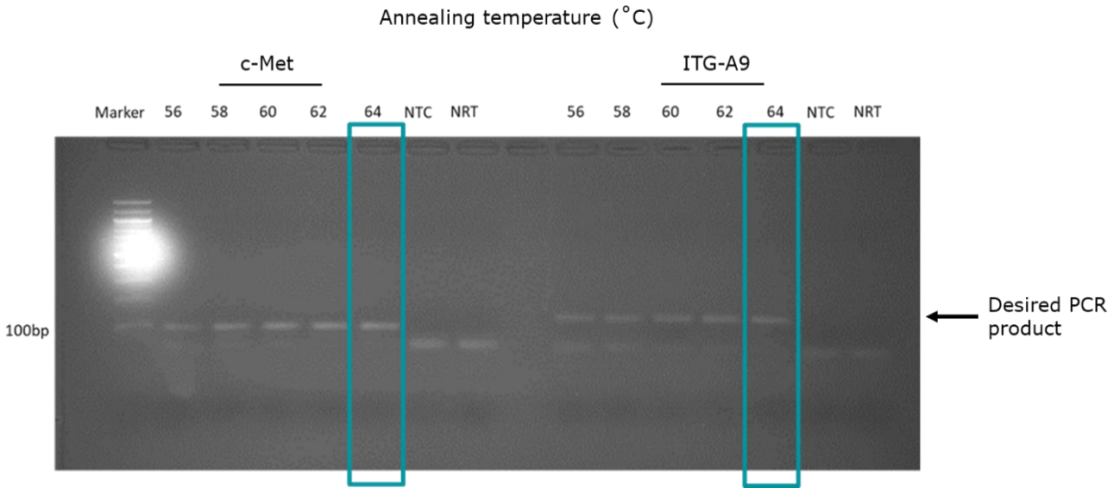

Figure 24. PCR amplification results associated with different annealing temperatures
A series of amplification processes were run at different annealing temperatures ranging from 56-64°C in a gradient PCR for c-Met and ITG-A9 primers. Analyses of amplification products after 35 cycles were performed and results are shown above. Higher intensities of the desired product band were seen at 64 (highlighted by blue boxes), therefore the annealing temperature of c-Met and ITG-A9 primers were set at 64°C. NTC: no template control; NRT: no reverse transcriptase

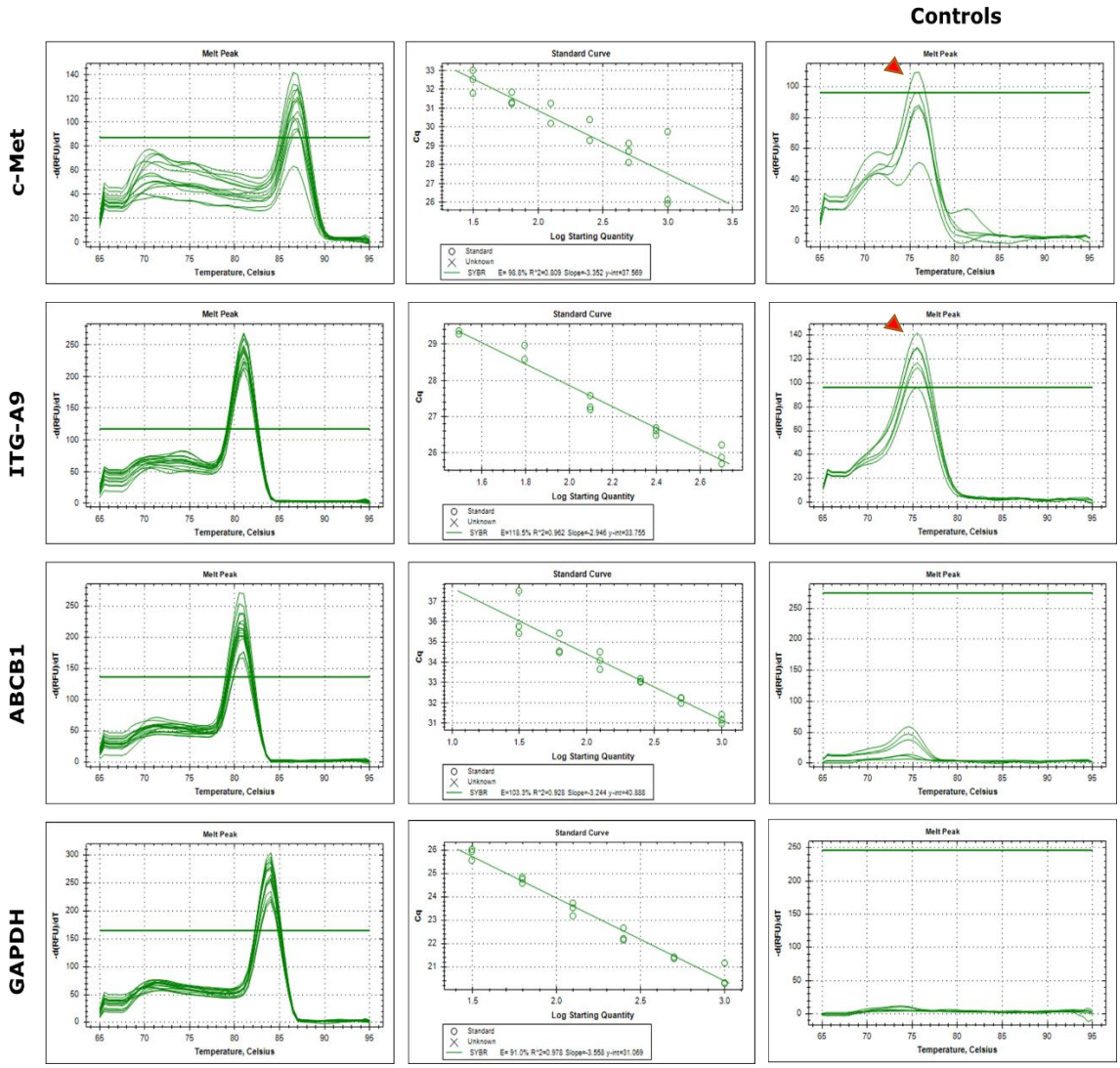

Figure 25. Successful primer optimisation of c-MET, ITGA9 and ABCB1
To optimise for a dilution series, c-Met, ITG-A9 and ABCB1 melt curves and standards curves were calculated. Singular melt peaks show that a single specific product was produced. For c-Met and ITG-A9 primer dimer peaks (highlighted by red arrows) were also identified in the control reactions when no template cDNA was added. These were absent from reactions where cDNA template was included (left column).

Table 13. Primer optimisation

Gene		Primers	Aannealing temperature	Efficiency (%)	R	Slope
c-Met	FP (5'-3')	GCTGACTTGCTGAGAGGAGG	64	98.8	0.809	-3.352
	RP (5'-3')	AGGTTTATCTTTCGGTGCCCA				
ITG-A9	FP (5'-3')	CAAAGGCATCGGCAAGGTTT	64	118.5	0.962	-2.946
	RP (5'-3')	TCCCCATTCAGGTCAACTGC				
ABCB1	FP (5'-3')	TGGGAAGAGCACAACAGTCC	62	103.3	0.928	-3.244
	RP (5'-3')	GGGTCTAGCTCGCATCATCC				
ITG-B1	FP (5'-3')	GCTCAGTGGAGAACAGATTGG	n/a	n/a	n/a	n/a
	RP (5'-3')	CCCACCTGATGGAATACGTT				
MMP 2	FP (5'-3')	GTTGTCTTGTGAGCGTGCG	n/a	n/a	n/a	n/a
	RP (5'-3')	TCAGGTATTGGCAACACTGCG				
MMP 9	FP (5'-3')	TTCAGGGAGACGCCCATTTC	60	28.5	0.155	-9.194
	RP (5'-3')	AACCGAGTTGGAACCACGAC				
GAPDH	FP (5'-3')	ATGTTCGTCATGGGTGTGAA	60-64	91.0	0.978	-3.558
	RP (5'-3')	GTCTTCTGGGTGGCAGTGAT				

FP- forward primer RP- reverse primer

3.3.2 Candidate markers of metastasis present in cells are present in EVs

Once the purity of the recovered exosomes and microvesicles was confirmed, we proceeded with RNA isolation using the optimised RNA isolation method. We followed this protocol to isolate RNA from exosomes, microvesicles and the respective cells. We then analysed the expression levels of c-Met, ABCB1 and ITG-A9 in exosomal and microvesicle RNA by qRT-PCR. Based on Ct values, 25-36 for all analyses, RNA isolation was efficient and the amount of RNA recovered is ample for standard PCR analysis (Figure 23).

3.3.2.1 c-Met expression

Using qRT-PCR we compared expression level of c-Met between the different medulloblastoma cell lines with varying migration capacities. We detected expression of c-Met in all six cell lines. High expression of c-Met was detected in

the metastatic cell lines (CHLA-01-R, HD-MB03 and D283). High c-Met expression was also detected in non-metastatic DAOY cell line. The lowest levels of c-Met expression were detected in non-metastatic cell lines, UW228-3 and CHLA-01 (Figure 26)

When detecting expression levels in extracellular vesicles, it became extremely challenging. This is because there is currently no known housekeeping gene for extracellular vesicles, therefore results became extremely skewed when analysing expression levels in extracellular vesicles in the same manner as they had been analysed in the cell lysates, and it became impossible to compare the two because GAPDH expression was not consistent across the extracellular vesicles and enrichment changed over several isolations (Figure 27). Next, we tried to analyse fold change in expression levels of extracellular vesicles compared to the cell lysates, however it then seemed that even if c-Met expression was detected in extracellular vesicles, if their levels were lower than in the cell lysates they appeared to have no expression (Figure 28). Finally, we felt the only way to show expression levels in extracellular vesicles was to look at their Ct values and show firstly, if exosomes or microvesicles express c-Met and secondly, if it was low or high expression. Results showed that highest expression of c-Met was detected in exosomes derived from the metastatic cell line HD-MB03. High levels of expression were detected in D283, CHLA-01, CHLA-01-R and DAOY. No expression of c-Met was detected in exosomes or microvesicles derived from UW228-3 cells. In microvesicles, very high expression was detected in DAOY microvesicles, medium expression in HD-MB03 and D283 microvesicles and low expression in CHLA-01 and CHLA-01-R microvesicles (Figure 29).

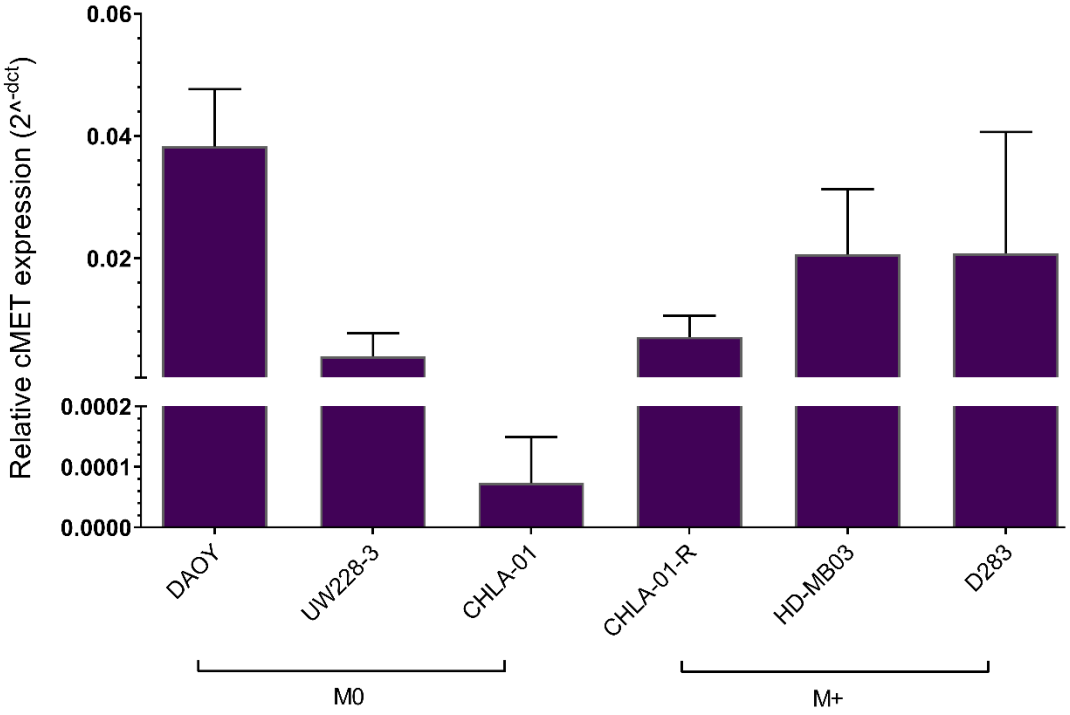

Figure 26. c-Met expression levels in cell lysates
qRT-PCR was used to determine the relative expression levels of c-Met in six medulloblastoma cell lines with varying migration capabilities, non-metastatic (M0) DAOY, UW228-3 and CHLA-01, metastatic (M+) CHLA-01-R, HD-MB03 and D283. Gene expression was calculated using 2Δdct relative to GAPDH. Data represents the mean ±SEM with (n=3).

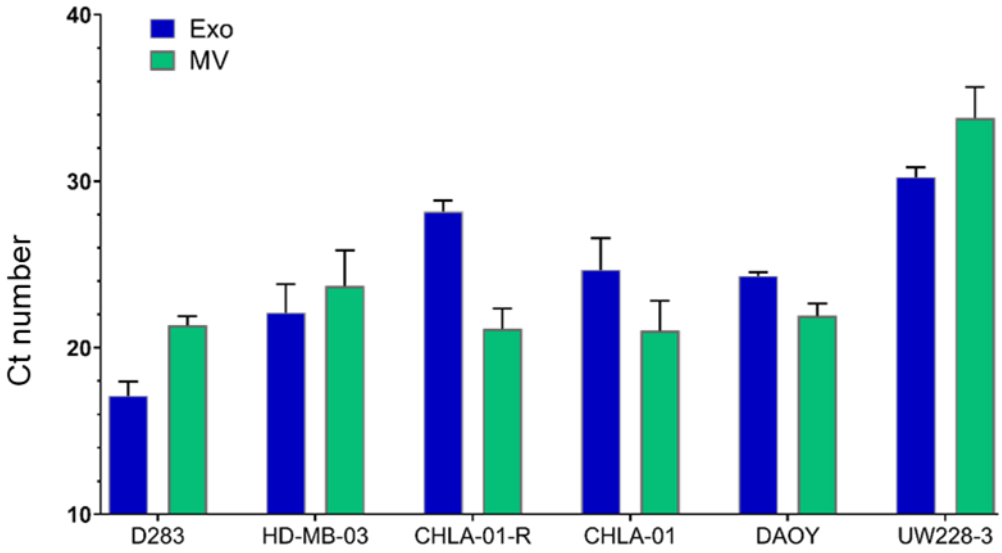

Figure 27. GAPDH expression in EVs
Following qRT-PCR the raw mean Ct values of reactions were acquired. Ct mean values for exosomes and microvesicles from six different medulloblastoma cell lines were used to compare the expression rates of housekeeper GAPDH. The data shows that GAPDH expression was not consistent across the extracellular vesicles, Ct values ranged from 17-36. Data represents the mean ±SEM with (n=3) Exo: exosomes; MV: microvesicles

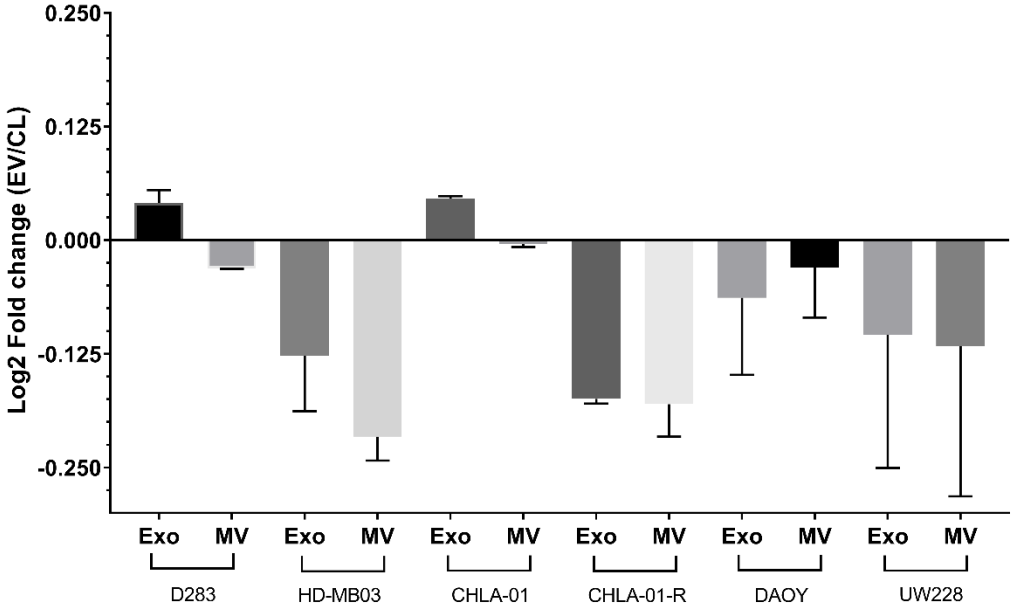

Figure 28. Fold change in c-Met expression
Comparison of expression levels of c-Met measured by qRT-PCR. Log2 transformed fold change in expression levels of extracellular vesicles compared with their derived cell lysates. Fold change in expression levels of extracellular vesicles compared to the cell lysates, showed that even if c-Met expression was detected in extracellular vesicles, if their levels were lower than in the cell lysates they appeared to have no expression. Exo: exosomes; MV: microvesicles

A

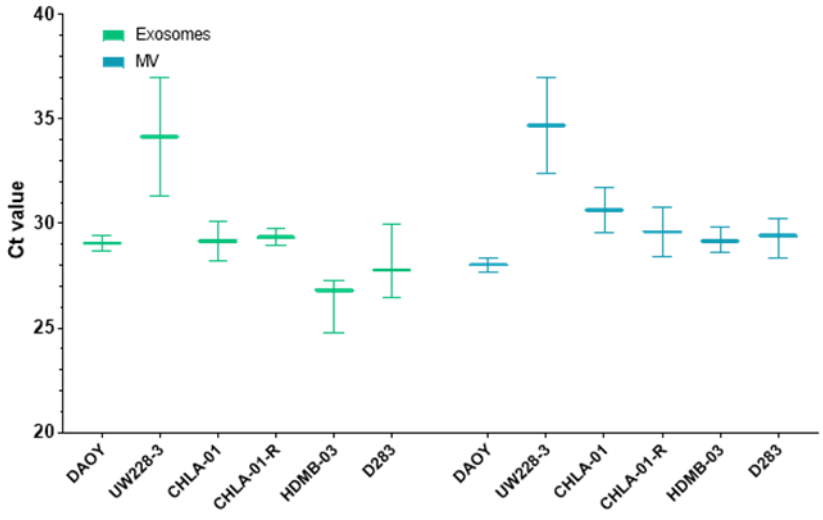

B

Cell line	Exosomes	Microvesicles
DAOY	++++	++++
UW228-3	-	-
CHLA-01	++++	++
CHLA-01-R	++++	++
HDMB-03	+++++	+++
D283	++++	+++

+++++ 25-27.5, ++++ 27.6-29.5, +++ 29.6-31.5, ++ 31.6-33.5 , + 33.6-36.5, - >36.5

Figure 29. c-Met expression in EVs
qRT-PCR was used to determine the relative expression levels of c-Met in extracellular vesicles isolated from six medulloblastoma cell lines with varying migration capabilities, non-metastatic (M0) DAOY, UW228-3 and CHLA-01, metastatic (M+) CHLA-01-R, HD-MB03 and D283. (A) Following qRT-PCR the raw mean Ct values of reactions were acquired. Box plots of exosomes and microvesicles (MV). Boxes denote median values with upper and lower quartiles, and whiskers minimum and maximum outliers with (n=3). (B) Lowest Ct values indicate highest expression of c-Met in extracellular vesicles. Highest expression (+++++) of c-Met was detected in exosomes derived from HD-MB03 cells. No expression (-) of c-Met was detected in exosomes or microvesicles derived from UW228-3 cells.

3.3.2.2 ABCB1 expression

ABCB1 expression was analysed across the different medulloblastoma cell lines with varying migration capacities. ABCB1 expression was highest in metastatic D283 and HD-MB03 cell lines, medium levels of expression were detected in DAOY, CHLA-01 and CHLA-01-R cell lines. ABCB1 was absent in UW228-3 cell lines

(Figure 30). Similar results were seen in extracellular vesicles, results showed that highest expression of ABCB1 was detected in exosomes derived from the metastatic cell line HD-MB03. Low expression levels of ABCB1 were detected in DAOY cell lines and very low levels of expression were detected in D283 cells. No expression of ABCB1 was detected in exosomes or microvesicles derived from UW228-3, CHLA-01 and CHLA-01-R cells. In microvesicles, DAOY and HD-MB03 microvesicles were the only microvesicles expressing ABCB1, but at very low levels (Figure 31).

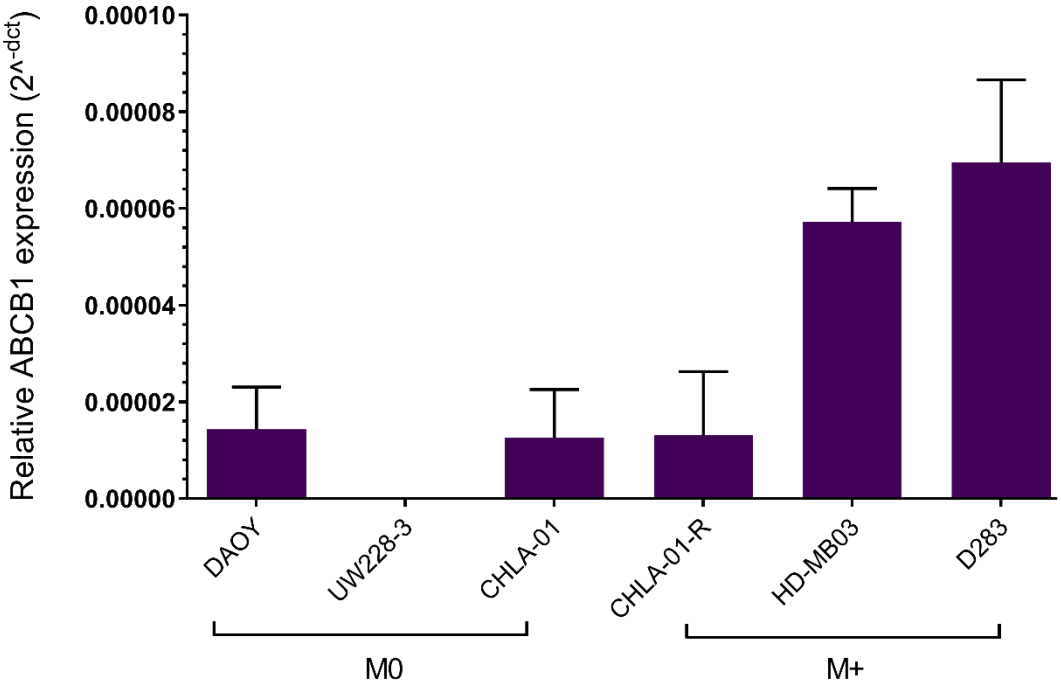

Figure 30. ABCB1 expression in cell lysates
qRT-PCR was used to determine the relative expression levels of ABCB1 in six medulloblastoma cell lines with varying migration capabilities, non-metastatic (M0) DAOY, UW228-3 and CHLA-01, metastatic (M+) CHLA-01-R, HD-MB03 and D283. ABCB1 expression was highest in metastatic D283 and HD-MB03 cell lines, medium levels of expression were detected in DAOY, CHLA-01 and CHLA-01-R cell lines. ABCB1 was absent in UW228-3 cell lines. Gene expression was calculated using 2Δdct relative to GAPDH. Data represents the mean ±SEM with (n=3).

A

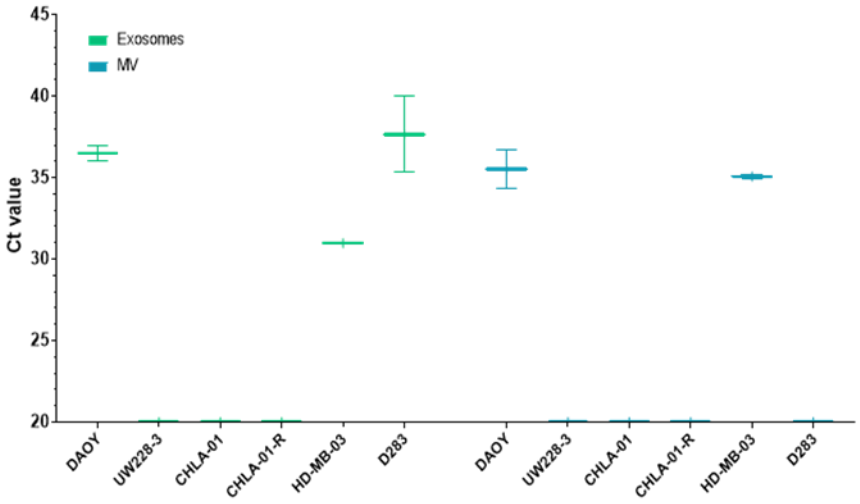

B

Cell line	Exosomes	Microvesicles
DAOY	++	+
UW228-3	-	-
CHLA-01	-	-
CHLA-01-R	-	-
HDMB-03	+++	+
D283	+	-

+++++ 25-27.5, ++++ 27.6-29.5, +++ 29.6-31.5, ++ 31.6-33.5 , + 33.6-36.5, - >36.5

Figure 31. ABCB1 expression in EVs
qRT-PCR was used to determine the relative expression levels of ABCB1 in extracellular vesicles isolated from six medulloblastoma cell lines with varying migration capabilities, non-metastatic (M0) DAOY, UW228-3 and CHLA-01, metastatic (M+) CHLA-01-R, HD-MB03 and D283. (A) Following qRT-PCR the raw mean Ct values of reactions were acquired. Box plots of exosomes and microvesicles (MV). Boxes denote median values with upper and lower quartiles, and whiskers minimum and maximum outliers with (n=3). (B) Lowest Ct values indicate highest expression of ABCB1 in extracellular vesicles. ABCB1 expression was only detected in exosomes derived from HD-MB03 and DAOY cells.

3.3.2.3 ITG-A9 expression

ITG-A9 expression was analysed across the different medulloblastoma cell lines with varying migration capacities. ITG-A9 expression was highest in metastatic CHLA-01-R cells. Medium levels of expression were detected in non-metastatic CHLA-01 and metastatic D283 cell lines, lowest expression was detected in metastatic HD-MB03 cells. ITG-A9 was absent in non-metastatic UW228-3 and

DAOY cell lines (Figure 32). When analysing expression of ITG-A9 in extracellular vesicles, results showed that only metastatic CHLA-01-R and HDBM-03 expressed ITG-A9. Highest expression of ITG-A9 was detected in exosomes derived from HD-MB03 cells. Medium expression of ITG-A9 was detected in CHLA-01-R exosomes and microvesicles. No expression of ITG-A9 was detected in exosomes DAOY, UW228-3, CHLA-01 and D283 cells. ITG-A9 expression was not detected in any microvesicles from any of the cell lines (Figure 33).

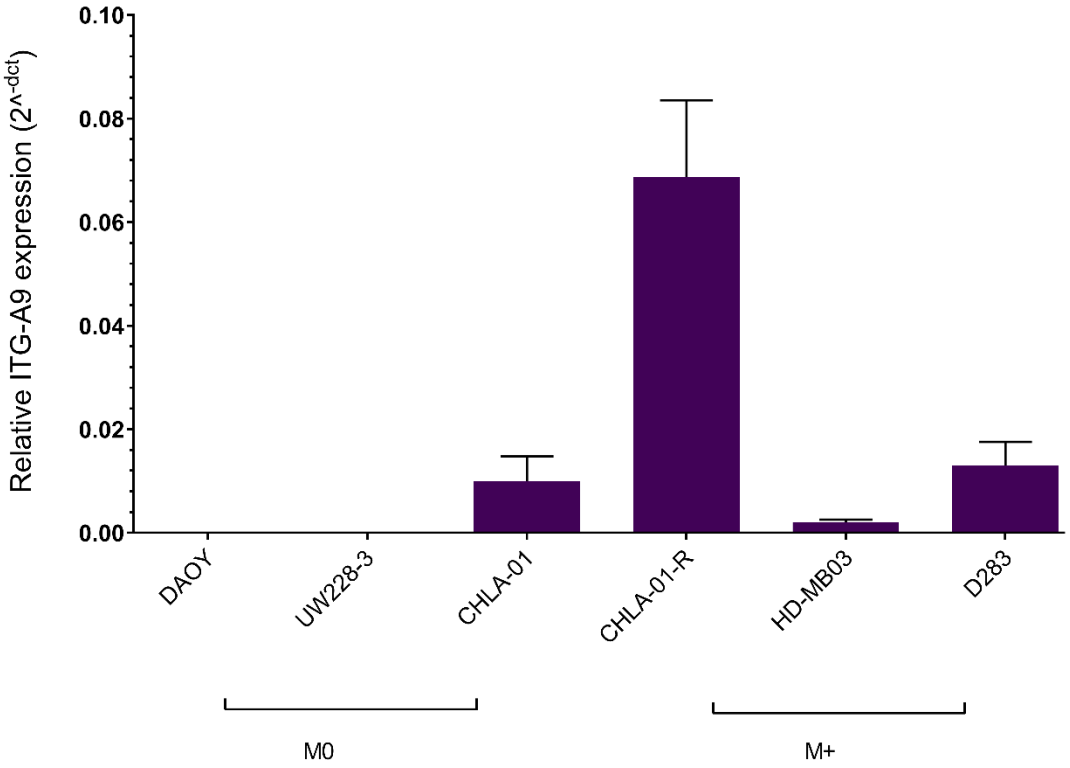

Figure 32. ITG-A9 expression in cell lysates
qRT-PCR was used to determine the relative expression levels of c-Met in six medulloblastoma cell lines with varying migration capabilities, non-metastatic (M0) DAOY, UW228-3 and CHLA-01, metastatic (M+) CHLA-01-R, HD-MB03 and D283. ITG-A9 expression was highest in CHLA-01-R cells. Medium levels of expression were detected in CHLA-01 and D283 cell lines, lowest expression was detected in HD-MB03 cells. ITG-A9 was absent in UW228-3 and DAOY cell lines. Gene expression was calculated using 2Δdct. Data represents the mean ±SEM with (n=3).

A

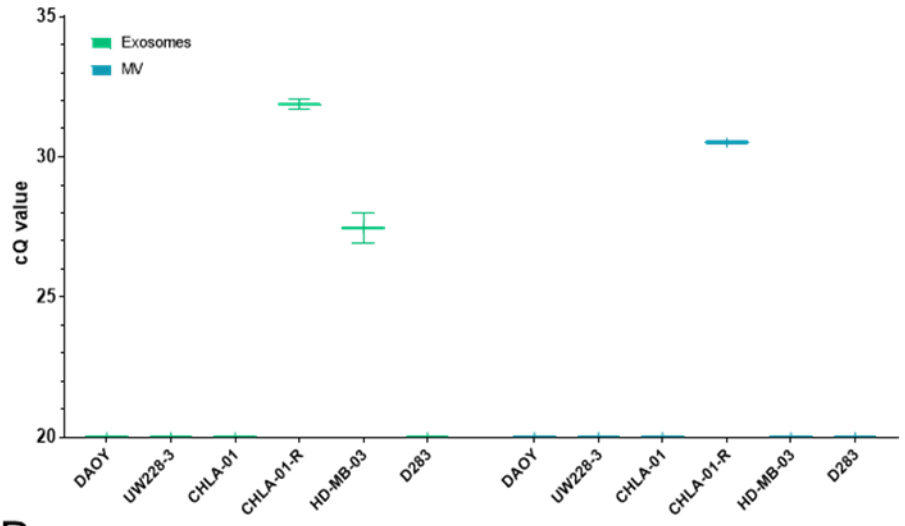

B

Cell line	Exosomes	Microvesicles
DAOY	-	-
UW228-3	-	-
CHLA-01	-	-
CHLA-01-R	+++	+++
HDMB-03	+++++	-
D283	-	-

+++++ 25-27.5, ++++ 27.6-29.5, +++ 29.6-31.5, ++ 31.6-33.5 , + 33.6-36.5, - >36.5

Figure 33. ITG-A9 expression in EVs
qRT-PCR was used to determine the relative expression levels of ITG-A9 in extracellular vesicles isolated from six medulloblastoma cell lines with varying migration capabilities, non-metastatic (M0) DAOY, UW228-3 and CHLA-01, metastatic (M+) CHLA-01-R, HD-MB03 and D283. (A) Following qRT-PCR the raw mean Ct values of reactions were acquired. Box plots of exosomes and microvesicles (MV). Boxes denote median values with upper and lower quartiles, and whiskers minimum and maximum outliers with (n=2). (B) Lowest Ct values indicate highest expression of ITG-A9 in extracellular vesicles. Very high expression (+++++) of ITG-A9 was detected in exosomes derived from HD-MB03 cells, and intermediate expression (+++) was detected in exosomes derived from CHLA-01-R cells.

4. Discussion and future work

Medulloblastoma, the most prevalent malignant paediatric brain tumour, accounts for around 10% of all cancer-related deaths in children (Pizer and Clifford, 2009). Medulloblastomas frequently metastasize, over one-third of patients are metastatic at diagnosis and almost all patients are metastatic at relapse. These patients are categorised as high-/very high-risk (Bailey *et al.*, 1995). Currently there is no curative treatment for patients with metastatic medulloblastoma, any advancements in the underlying biology of medulloblastoma, particularly regarding their metastatic behaviour, could help to improve patient outcome. One area that remains relatively unstudied is medulloblastoma extracellular vesicles.

Extracellular vesicles are a heterogeneous population of nano-sized, cell derived vesicles (Holme *et al.*, 1997; Hess *et al.*, 1999). They can be categorised into three main classes, exosomes, microvesicles and apoptotic bodies. Accumulating evidence indicates that exosomes play vital roles in cancer progression. They have been shown to transfer oncogenic proteins and nucleic acid cargo to recipient cells which modulates their activity and plays a decisive role in tumorigenesis, promoting tumour growth and progression, enhancing tumour cell migration and invasion, developing drug resistance and performing immunosuppressive functions (Graves *et al.*, 2004).

In this project, we optimised a protocol for the isolation of total microvesicles and exosomes from medulloblastoma cells. The second part of this project used this protocol to isolate and characterize exosomes and microvesicles from a series of medulloblastoma cell lines representing different subtypes and metastatic capacity. In the final part of the project, candidate markers of metastasis, identified from the literature, were profiled in cells and their derivative extracellular vesicles.

4.1 Exosomes and microvesicles differ in their morphology and internal cargo

The main aim of my project was to isolate and characterise extracellular vesicles from different medulloblastoma cell lines. Currently, most studies have focused on extracellular vesicles as a mixed population of exosomes and microvesicles, and discrimination between the two has only recently gained consideration (Menck *et al.*, 2013). Using the optimised isolation protocol, I successfully isolated exosomes and microvesicles from six different medulloblastoma cell lines. These include, a matched pair from the same patient, CHLA-01 and CHLA-01-R. CHLA-01 and CHLA-01-R are categorised as Group 4, and originate from a primary tumour and a malignant pleural effusion, respectively (Xu *et al.,* 2012). UW228-3 has been categorised as both SHH and Group 3 and was isolated from a primary tumour of a patient with a non-metastatic medulloblastoma (Keles *et al.*, 1995). The DAOY cell line is also categorised as SHH subgroup and was derived from a patient with a non-metastatic desmoplastic medulloblastoma (Jacobson *et al.*, 1985). HD-MB03 is a Group 3 medulloblastoma cell line isolated from a metastasized medulloblastoma in the cerebellum of a 3-year-old boy (Milde *et al.*, 2012). The final cell line used is D283 which has been classed as both Group 3 and Group 4 and was isolated from metastases in the ascetic fluid (Friedman *et al.*, 1985). Collectively, the six medulloblastoma cell lines used represent 3 out of the 4 molecular subgroups of medulloblastoma.

After isolation of exosomes and microvesicles from all six cell lines, the first step involved characterising the extracellular vesicles. To date, there is no absolute unique protein marker that has been identified to verify that pure preparations of exosome or microvesicle has been obtained. Therefore, a combination of characterisation techniques were required. For this project, I characterised exosome and microvesicle properties by Nanosight, electron microscopy and western blot analysis, showing that their size, morphologies and internal cargo

differ and they can be selectively isolated by differential ultracentrifugation and filtration steps.

Nanoparticle tracking analysis determined the size of exosomes was always <100nm which is consistent throughout the literature (Théry *et al.*, 2006). Microvesicles measured >150nm, which once again was consistent across the six different cell lines and agreed with previous publications (Théry *et al.*, 2006; Menck *et al.*, 2013; Kowal *et al.*, 2016). NTA is an innovative method to determine exosome and microvesicle size and concentration. However, there is no assurance that the particles detected are entirely exosomes/microvesicles. Other particles, such as apoptotic bodies, cell debris or large complexes of proteins, which could be contaminating the sample and lead to false positive signals, could also be included.

An overview of the level of contamination of the sample and therefore its purity can be obtained using transmission electron microscopy (TEM). TEM revealed that samples were not contaminated by cell fragments or apoptotic bodies (Figure 15 and 16). Similar to NTA analysis, TEM results also revealed distinct populations of exosomes and microvesicles. Exosomes were typically spherical in morphology with vesicle diameters never exceeding 100nm. In comparison, microvesicles consisted of a much more heterogenous population of large vesicles with an average diameter of 200nm. These findings are again consistent with previous reports (Colombo, Raposo and Théry, 2014; Zeng *et al.*, 2017) and with our own NTA results.

In addition, the protein content of exosomes can be determined by western blot analysis. As previously mentioned, there are currently no "exosome-specific" markers, but rather "exosome-enriched" proteins. A recently published proteomics study defined novel markers to characterize a heterogenous population of extracellular vesicles (Kowal *et al.*, 2016). They recommended that transmembrane proteins, like tetraspanin CD63 (alongside CD81 and CD9) should

be used as a general exosome marker. Tsg101 was also highlighted as a maker of small exosomes (<100nm). EMMPRIN has also been proposed as a marker for exosomes derived from multiple cancer cell lines (Redzic *et al.*, 2013). Aside from positive markers of exosomes, the International Society for Extracellular Vesicles also recommends negative controls to rule out contaminating cellular material. Examples include endoplasmic reticulum markers such as calnexin, golgi marker GM130 or nuclear markers such as histones (Lötvall *et al.*, 2014).

Our data showed CD63 and Tsg101 were present in exosomes as well as in the cell lysates from all six medulloblastoma cell lines. EMMPRIN was detected in all cell lysates, and was enriched in CHLA-01 and CHLA-01-R cells. EMMPRIN was only detected in exosomes derived from CHLA-01 and CHLA-01-R cells. Importantly, our exosome samples were negative for the nuclear marker, Histone 4 (H4), however all cell lysates were positive for H4, showing that our final pellet was not just nuclear debris (Figure 17). Initially, the aim was to analyse protein from both exosomes and microvesicles by western blot analysis. However, not enough protein was isolated from microvesicles for western blot analysis (Figure 20), and optimisation of protein recovery from microvesicles remains a goal for future work.

To assess the presence of extracellular vesicle impurities derived from FBS, we used DLS analysis of FBS before overnight ultracentrifugation, which revealed an abundance of heterogenous particles. After ultracentrifugation, there was a drastic reduction in these particles. Thus, we were confident that contaminating material did not interfere with our medulloblastoma exosome and microvesicle measurements.

From the extensive characterisation methods, our data clearly shows that the protocol used successfully isolates both exosomes and microvesicles from medulloblastoma samples.

4.2 Metastatic tumour cells secrete higher concentrations of exosomes

Many studies have compared exosomes released from normal cells with exosomes released from tumour cells, revealing that there is an increase in the total number of isolated exosomes from tumour cells. This has been confirmed for exosomes from patients with lung, breast, ovarian and gastric cancer (Baran *et al.*, 2010; Gercel-Taylor *et al.*, 2012). Other studies have found an increase in the protein density in exosomes isolated from cancer patients but not in the amount of extracellular vesicles (Peinado *et al.*, 2012). This led us to investigate the differences between exosomes released from metastatic cells compared to those released by non-metastatic cells. The data demonstrates that three different metastatic medulloblastoma cells secrete markedly more exosomes compared to the non-metastatic cell lines. The reasons for increased numbers of exosomes from metastatic cells are unknown. One theory is that microenvironmental factors which promote metastatic progression also stimulate the release of exosomes (Garcia *et al.*, 2015). Identification of these microenvironmental factors in medulloblastomas is an ongoing line of investigation.

The increase in exosomes secreted from metastatic cells could also support the idea of an expansion of the "seed and soil" hypothesis, in which exosomes travel to distant organs and manipulate the host environment, thus priming a metastatic environment (Paget, 1889). A recent study analysed 28 different cancer types, including melanoma, colorectal, lung and paediatric cancers which metastasize to specific organs, such as brain and lung. They revealed that exosomes from each cancer type reached organs associated with metastasis. The exosomes then reprogrammed the organ sites to support tumour cell growth (Hoshino *et al.*, 2015). These findings strongly support a significant role for exosomes in metastasis and could explain why higher concentrations of exosomes were observed in metastatic cell lines compared to non-metastatic cell lines.

Importantly, we have also observed that the amount of protein and RNA in exosomes from metastatic cell lines is significantly increased, suggesting that differences in exosomal cargo could be involved in medulloblastoma cell metastasis (Figure 20 and Figure 23)

Despite the fact we obtained high particle concentrations and enough exosomal protein and RNA for our project, we required large quantities of starting material. For all cell lines 120mls of conditioned medium was needed for the isolation of exosomes and microvesicles. To translate any of our findings into a clinical environment, results must be reproducible in 3D culture systems and patient samples. This scale of experiment would be prohibitively expensive for current 3D models. However, a recent study by Yagi *et al* isolated exosomes from only 7mls of cerebrospinal fluid (CSF) from normal controls (Yagi *et al.*, 2017). This indicates that patient CSF may produce even higher levels of exosomes. Hence, it may be possible to stimulate cells in 3D models to produce more clinical representative levels. In the future, it would also be desirable to optimise our protocol for the isolation of exosomes and microvesicles from much smaller samples, such as patient CSF and from 3D models.

4.3 RNA from cells is selectively transferred into extracellular vesicles

It has been well established that extracellular vesicles have a role in intercellular communication through the transfer of their cargo to recipient cells. Several studies have also shown that exosomes would be ideal diagnostic biomarkers for cancer as they closely represent the state of their parent cell. Therefore, we evaluated if cell expressed candidate markers of metastasis were also expressed by the extracellular vesicles that they released.

To assess gene expression by qRT-PCR, it was essential to optimise exosomal RNA isolation. The mirVana kit had been standardly used in the past for isolation of

RNA from small samples, however this yielded poor quality exosomal RNA. Therefore, we trialled three other RNA isolation kits (Figure 21). The Qiagen miRNeasy micro kit produced the highest yields and the best quality RNA. Consequently, this kit was taken forward for all future RNA isolations.

Candidate markers of metastasis were identified from the literature. The candidates identified were known to promote cell migration and invasion in medulloblastoma, therefore their expression levels were determined in our six cell lines. The first candidate identified was c-Met. c-Met has been implicated as a significant player in several cancers as it can promote tumorigenesis through proliferation, cell migration and invasion, angiogenesis and prevention of apoptosis. Elevated levels of c-Met mRNA in human medulloblastoma and medulloblastoma cells have been correlated with metastasis and poor patient outcome (Li *et al.*, 2005; Binning *et al.*, 2008). We therefore analysed the expression of c-Met in our six different medulloblastoma cell lines. As predicted, highest c-Met expression was detected in the most aggressive, metastatic cell lines (HD-MB03 and D283). The lowest levels of c-Met expression were detected in two out of three of our non-metastatic cell lines (UW228-3 and CHLA-01) (Figure 26). This further supports findings that c-Met plays an important role in medulloblastoma metastasis and is correlated with poor patient outcome.

c-Met expression was also detected at high expression levels in non-metastatic SHH DAOY cells. This could be explained by the fact that HGF (the ligand which activates c-Met) has been shown to have an enhancing effect on SHH-induced medulloblastoma formation in mice. It was shown that the combination of HGF and SHH significantly increased the incidence of medulloblastoma formation (Binning *et al.*, 2008). This provides an explanation for why c-Met would be expressed at high levels in SHH subtypes.

c-Met abundance was also analysed in extracellular vesicles. Expression of c-Met was detected in all extracellular vesicles apart from extracellular vesicles derived

from non-metastatic UW228-3 cells. The highest expression of c-Met was detected in exosomes derived from metastatic HD-MB03 cells (Figure 29). These findings support that c-Met has an important role in medulloblastoma progression.

Increased expression levels of ABCB1 transporters have been implicated with chemo resistance and poor clinical outcome in medulloblastoma (Chou *et al.*, 1995). This was confirmed in a study by our research group where we showed that a subpopulation of cells from a cancer stem cell model expressed ABCB1 (Hussein *et al.*, 2011). More recently, our research group has also associated ABCB1 with metastasis and high-risk in medulloblastoma tumours using a large patient tissue microarray (Othman *et al.*, 2014). Therefore, the expression of ABCB1 was assessed in medulloblastoma cell lines and extracellular vesicles with varying migration capacities.

ABCB1 is thought to only be expressed in a subpopulation of cells (Hussein *et al.*, 2011), therefore in comparison to c-Met, expression of ABCB1 was detected at lower levels. Despite this, our findings indicate a clear difference in ABCB1 gene expression between non-metastatic and metastatic cell lines. ABCB1 expression was highest in metastatic D283 and HD-MB03 cell lines, medium levels of expression were detected in DAOY, CHLA-01 and CHLA-01-R cell lines. ABCB1 was completely undetected in UW228-3 cell lines (Figure 30). When ABCB1 expression was analysed in extracellular vesicles, highest expression of ABCB1 was detected in exosomes derived from the metastatic cell line HD-MB03. Intermediate expression levels of ABCB1 were detected in DAOY cell lines and low levels of expression were detected in D283 cells. No expression of ABCB1 was detected in exosomes or microvesicles derived from UW228-3, CHLA-01 and CHLA-01-R cells (Figure 31). This data provides further support that ABCB1 expression is important in metastatic tumours.

Several migration and metastasis studies have correlated the expression levels of integrins in human tumours with pathological outcomes. In medulloblastoma,

integrins α9 and β1 have been shown to mediate adhesion to the leptomeningies with the ECM glycoprotein tenascin (Fiorilli *et al.*, 2008). A more recent proteomic study comparing metastatic and non-metastatic medulloblastoma cell lines, revealed that integrin alpha-9 (ITG-A9) was upregulated in metastatic cells compared to non-metastatic cells (Gu *et al.*, 2017). Thus, the expression of ITG-A9 was assessed in our cell lines and derivative extracellular vesicles.

Similar to ABCB1 expression, there was a clear difference in gene expression between non-metastatic and metastatic cell lines observed. ITG-A9 was expressed in all metastatic cell lines, with highest expression being detected in CHLA-01-R cells. ITG-A9 was completely absent in non-metastatic UW228-3 and DAOY cell lines (Figure 32). These findings further support that ITG-A9 expression correlates with metastasis in medulloblastoma cells (Fiorilli *et al.*, 2008; Gu *et al.*, 2017).

When analysing expression of ITG-A9 in extracellular vesicles, results showed that only metastatic CHLA-01-R and HDBM-03 exosomes contained ITG-A9. Highest expression of ITG-A9 was detected in exosomes derived from HD-MB03 cells. No expression of ITG-A9 was detected in exosomes or microvesicles derived from non-metastatic cell lines or in metastatic D283 cells (Figure 33). These findings suggest that ITG-A9 is selectively sorted into exosomes independent of expression levels in the cells. For example, ITG-A9 was detected at medium levels in CHLA-01 cells, however no expression was detected in either exosomes or microvesicles. In contrast, expression was lowest in HDBM-03 cells, however highest expression of ITG-A9 was detected in HD-MB03 exosomes compared to all other cell lines (Figure 33). This supports findings that RNA is selectively packaged into exosomes (Valadi *et al.*, 2007). Our findings also show a clear difference between the matched pair of primary and metastatic cell lines, CHLA-01 and CHLA-01-R. When comparing expression of ITG-A9 in the cells, it was expressed in both cell lines. However, when analysing expression levels in the extracellular vesicles, ITG-A9 was only expressed in the metastatic CHLA-01-R exosomes and microvesicles.

This indicates that ITG-A9 expression in extracellular vesicles correlates with metastasis in medulloblastoma cells.

Exosomal RNA have not only been shown to be stable and accessible biomarkers, they have also been shown to be functionally transferred from parent cells to recipient cells. Therefore, the next step would be to isolate exosomes or microvesicles which have carry high amounts of metastasis-associated RNAs, for example HD-MB03 or CHLA-01-R exosomes, and introduce them into cultures of cells which show very little or no expression of those genes (UW228-3 or CHLA-01 cells). It would then be interesting to test the effect this has on recipient cells, for example their migration and invasion capabilities. This would help clarify whether extracellular vesicles represent a vehicle by which one cell communicates with another, delivering RNA which in turn modulates the recipient cells, with significant implications for our understanding of metastatic medulloblastoma.

Due to the reason that extracellular vesicle cargo can be regulated by the state of the parental cell, all cells assessed in this study were grown under basal conditions, without any prior stimulation of the cells which could alter protein and RNA expression of the extracellular vesicles. For a more comprehensive study, it would be important to alter the tumour microenvironment to represent a more metastatic state. The aim would then be to re-examine the transcriptional contents of the released exosomes or microvesicles. This could be achieved by stimulation of the cells with growth factors. As previously mentioned c-Met has been associated with metastatic medulloblastoma. However, its ligand HGF has also been associated with poor clinical outcome in medulloblastoma patients. A study by Li *et al* showed that treatment of medulloblastoma cells with HGF activates c-Met, and HGF gene transfer to medulloblastoma xenografts caused increased invasion and morphological changes which resembled human LC/A medulloblastoma (subgroup with poorest 5-year survival) (Li *et al.,* 2005). There have also been several migration and metastasis studies which correlated the

expression levels of integrins in human tumours with pathological outcomes and have identified numerous integrins which have an important role in disease progression. A study by Fiorilli *et al* showed that integrins α9 and β1 mediate medulloblastoma adhesion to the leptomeningies with ECM tenascin. Tenascin is a ligand for integrins α9 and β1 and is a component of the ECM (Fiorilli *et al.*, 2008). HGF and tenascin would therefore be natural choices as growth factor stimulants. Cultured medulloblastoma cells could be treated with HGF or tenascin to study if the internal cargo of exosomes or microvesicles are affected by the external microenvironment of medulloblastoma cells.

A limitation with our study was that we were not able to compare expression levels in cells with the expression levels in extracellular vesicles. This is because no housekeeper RNA has been shown to be exclusively and constantly expressed in extracellular vesicles and it is still not known how many vesicles are secreted by a known number of cells. In the future, we plan to normalise the total cell lysates and vesicle fraction to the original cell number, using a "spike-in" of non-human cells, such as *Drosophila* cells. This will allow for the direct comparison of cell and extracellular vesicle gene expression levels.

5. Main conclusions

In conclusion, I have optimised a protocol to for the isolation and characterisation of medulloblastoma extracellular vesicles, exosomes and microvesicles. The results clearly show that medulloblastoma cells secrete two distinct populations of extracellular vesicles, with unique size, morphology and cargo. I have also shown that dependent on the cell type from which they are derived their internal cargo alters. Our data shows that more aggressive, metastatic cell lines produce higher quantities of exosomes compared with less aggressive, non-metastatic cell lines. Finally, I have also shown that RNA of medulloblastoma-associated genes is passed from the parent cells to exosomes and microvesicles.

6. References

Abd Elmageed, Z. Y. *et al.* (2014) 'Neoplastic Reprogramming of Patient-Derived Adipose Stem Cells by Prostate Cancer Cell-Associated Exosomes', *Stem cells*. Wiley Online Library, 32(4), pp. 983–997.

Abounader, R. and Laterra, J. (2005) 'Scatter factor/hepatocyte growth factor in brain tumor growth and angiogenesis', *Neuro-Oncology*, 7(4), pp. 436–451. Available at: http://dx.doi.org/10.1215/S1152851705000050.

Adamson, D. C. *et al.* (2010) 'OTX2 Is Critical for the Maintenance and Progression of Shh-Independent Medulloblastomas', *Cancer Research*, 70(1), p. 181 LP-191. Available at: http://cancerres.aacrjournals.org/content/70/1/181.abstract.

Admyre, C. *et al.* (2007) 'Exosomes with Immune Modulatory Features Are Present in Human Breast Milk', *The Journal of Immunology*, 179(3), p. 1969 LP-1978. Available at: http://www.jimmunol.org/content/179/3/1969.abstract.

Al-Nedawi, K. *et al.* (2009) 'Endothelial expression of autocrine VEGF upon the uptake of tumor-derived microvesicles containing oncogenic EGFR', *Proceedings of the National Academy of Sciences*, 106(10), pp. 3794–3799. doi: 10.1073/pnas.0804543106.

Asea, A. *et al.* (2008) 'Heat shock protein-containing exosomes in mid-trimester amniotic fluids', *Journal of Reproductive Immunology*, 79(1), pp. 12–17. doi: http://dx.doi.org/10.1016/j.jri.2008.06.001.

Atay, S. *et al.* (2014) 'Oncogenic KIT-containing exosomes increase gastrointestinal stromal tumor cell invasion', *Proceedings of the National Academy of Sciences*. National Acad Sciences, 111(2), pp. 711–716.

Bailey, C. C. *et al.* (1995) 'Prospective randomised trial of chemotherapy given before radiotherapy in childhood medulloblastoma. International Society of Paediatric Oncology (SIOP) and the (German) Society of Paediatric Oncology

(GPO): SIOP II.', *Medical and pediatric oncology*. United States, 25(3), pp. 166–178.

Banigan, M. G. *et al.* (2013) 'Differential expression of exosomal microRNAs in prefrontal cortices of schizophrenia and bipolar disorder patients', *PloS one*. Public Library of Science, 8(1), p. e48814.

Bar, E. E. and Stearns, D. (2008) 'New developments in medulloblastoma treatment: the potential of a cyclopamine–lovastatin combination', *Expert Opinion on Investigational Drugs*. Taylor & Francis, 17(2), pp. 185–195. doi: 10.1517/13543784.17.2.185.

Baran, J. *et al.* (2010) 'Circulating tumour-derived microvesicles in plasma of gastric cancer patients', *Cancer Immunology, Immunotherapy*. Springer, 59(6), pp. 841–850.

Beckler, M. D. *et al.* (2013) 'Proteomic analysis of exosomes from mutant KRAS colon cancer cells identifies intercellular transfer of mutant KRAS', *Molecular & cellular proteomics*. ASBMB, 12(2), pp. 343–355.

Bellingham, S. A., Coleman, B. M. and Hill, A. F. (2012) 'Small RNA deep sequencing reveals a distinct miRNA signature released in exosomes from prion-infected neuronal cells', *Nucleic Acids Research*, 40(21), pp. 10937–10949. Available at: http://dx.doi.org/10.1093/nar/gks832.

Bevan, D. *et al.* (2004) 'Diverse and potent activities of HGF/SF in skin wound repair', *The Journal of Pathology*. John Wiley & Sons, Ltd., 203(3), pp. 831–838. doi: 10.1002/path.1578.

Beviglia, L. and Kramer, R. H. (1999) 'HGF induces FAK activation and integrin-mediated adhesion in MTLn3 breast carcinoma cells', *International Journal of Cancer*, 83(5), pp. 640–649. doi: 10.1002/(SICI)1097-0215(19991126)83:5<640::AID-IJC13>3.0.CO;2-D.

Bhagirath, D. *et al.* (2017) 'An exosomal biomarker for prostate cancer'. *Cancer Research.* AACR, 13, pp. 5448. DOI: 10.1158/1538-7445.

Bhoopathi, P. *et al.* (2011) 'MMP-2 mediates mesenchymal stem cell tropism towards medulloblastoma tumors', *Gene therapy*, 18(7), pp. 692–701. doi: 10.1038/gt.2011.14.

Binning, M. J. *et al.* (2008) 'Hepatocyte growth factor and sonic Hedgehog expression in cerebellar neural progenitor cells costimulate medulloblastoma initiation and growth', *Cancer research*. AACR, 68(19), pp. 7838–7845.

Birchmeier, C. and Gherardi, E. (1998) 'Developmental roles of HGF/SF and its receptor, the c-Met tyrosine kinase', *Trends in Cell Biology*, 8(10), pp. 404–410. doi: http://dx.doi.org/10.1016/S0962-8924(98)01359-2.

Bisaro, B. *et al.* (2015) 'Proteomic analysis of extracellular vesicles from medullospheres reveals a role for iron in the cancer progression of medulloblastoma.', *Molecular and cellular therapies*. Molecular and Cellular Therapies, 3(1), p. 8. doi: 10.1186/s40591-015-0045-3.

Bodey, B. *et al.* (2000) 'Matrix metalloproteinase expression in childhood medulloblastomas/primitive neuroectodermal tumors', *In vivo (Athens, Greece)*, 14(5), p. 667—673. Available at: http://europepmc.org/abstract/MED/11212844.

von Bossanyi, P. *et al.* (1997) 'Immunohistochemical expression of P-glycoprotein and glutathione S-transferases in cerebral gliomas and response to chemotherapy', *Acta Neuropathologica*, 94(6), pp. 605–611. doi: 10.1007/s004010050756.

Bracke, M. E., Roy, F. M. Van and Mareel, M. M. (1996) 'The E-cadherin/Catenin Complex in Invasion and Metastasis', in Günthert, U. and Birchmeier, W. (eds) *Attempts to Understand Metastasis Formation I: Metastasis-Related Molecules*. Berlin, Heidelberg: Springer Berlin Heidelberg, pp. 123–161. doi: 10.1007/978-3-

642-61107-0_9.

Bradford, M. M. (1976) 'A rapid and sensitive method for the quantitation of microgram quantities of protein utilizing the principle of protein-dye binding', Anal Biochem. 72, pp. 248–254.

Brugières, L. *et al.* (2012) 'High Frequency of Germline SUFU Mutations in Children With Desmoplastic/Nodular Medulloblastoma Younger Than 3 Years of Age', *Journal of Clinical Oncology*. American Society of Clinical Oncology, 30(17), pp. 2087–2093. doi: 10.1200/JCO.2011.38.7258.

Buonamici, S. *et al.* (2010) 'Interfering with Resistance to Smoothened Antagonists by Inhibition of the PI3K Pathway in Medulloblastoma', *Science Translational Medicine*, 2(51), p. 51ra70 LP-51ra70. Available at: http://stm.sciencemag.org/content/2/51/51ra70.abstract.

Caby, M.-P. *et al.* (2005) 'Exosomal-like vesicles are present in human blood plasma', *International Immunology*, 17(7), pp. 879–887. Available at: http://dx.doi.org/10.1093/intimm/dxh267.

Chambers, A. F., Groom, A. C. and MacDonald, I. C. (2002) 'Metastasis: Dissemination and growth of cancer cells in metastatic sites', *Nature Reviews. Cancer*. London: Nature Publishing Group, 2(8), pp. 563–572. doi: http://dx.doi.org/10.1038/nrc865.

Chang, C. H., Housepian, E. M. and Herbert, C. (1969) 'An Operative Staging System and a Megavoltage Radiotherapeutic Technic for Cerebellar Medulloblastomas', *Radiology*. Radiological Society of North America, 93(6), pp. 1351–1359. doi: 10.1148/93.6.1351.

Chen, K.-C. *et al.* (2011) 'OxLDL up-regulates microRNA-29b, leading to epigenetic modifications of MMP-2/MMP-9 genes: a novel mechanism for cardiovascular diseases', *The FASEB Journal*, 25(5), pp. 1718–1728. doi:

10.1096/fj.10-174904.

Cheung, K. J. *et al.* (2016) 'Polyclonal breast cancer metastases arise from collective dissemination of keratin 14-expressing tumor cell clusters.', *Proceedings of the National Academy of Sciences of the United States of America*. United States, 113(7), pp. E854-63. doi: 10.1073/pnas.1508541113.

Chiou, S.-H. *et al.* (2006) 'Monitoring the growth effect of xenotransplanted human medulloblastoma in an immunocompromised mouse model using in vitro and ex vivo green fluorescent protein imaging', *Child's Nervous System*, 22(5), p. 475. doi: 10.1007/s00381-005-0026-y.

Chou, P. M. *et al.* (1995) 'Multidrug Resistance Gene Expression in Childhood Medulloblastoma: Correlation with Clinical Outcome and DNA Ploidy in 29 Patients', *Pediatric Neurosurgery*, 23(6), pp. 283–292. Available at: http://www.karger.com/DOI/10.1159/000120984.

Colombo, M., Raposo, G. and Théry, C. (2014) 'Biogenesis, Secretion, and Intercellular Interactions of Exosomes and Other Extracellular Vesicles', *Annual Review of Cell and Developmental Biology*. Annual Reviews, 30(1), pp. 255–289. doi: 10.1146/annurev-cellbio-101512-122326.

Coluccia, D. *et al.* (2016) 'Medulloblastoma: Tumor Biology and Relevance to Treatment and Prognosis Paradigm', *Current Neurology and Neuroscience Reports*, 16(5), p. 43. doi: 10.1007/s11910-016-0644-7.

Crescitelli, R. *et al.* (2013) 'Distinct RNA profiles in subpopulations of extracellular vesicles: apoptotic bodies, microvesicles and exosomes', *Journal of Extracellular Vesicles*. Taylor & Francis, 2(1), p. 20677. doi: 10.3402/jev.v2i0.20677.

D'Amico, L. *et al.* (2016) 'C-met inhibition blocks bone metastasis development induced by renal cancer stem cells', *Oncotarget*. Impact Journals LLC, 7(29), pp. 45525–45537. doi: 10.18632/oncotarget.9997.

Danen, E. H. J. (2013) 'Integrin Signaling as a Cancer Drug Target', *ISRN Cell Biology*, 2013, pp. 1–14. doi: 10.1155/2013/135164.

Danzer, K. M. *et al.* (2012) 'Exosomal cell-to-cell transmission of alpha synuclein oligomers', *Molecular neurodegeneration*. BioMed Central, 7(1), p. 42.

Diepenbruck, M. and Christofori, G. (2016) 'Epithelial–mesenchymal transition (EMT) and metastasis: yes, no, maybe?', *Current Opinion in Cell Biology*, 43, pp. 7–13. doi: https://doi.org/10.1016/j.ceb.2016.06.002.

Dudas, J. *et al.* (2017) '9 Matrix remodeling in head and neck squamous cell carcinomais', *Oral Oncology*. Elsevier, 51(5), p. e30. doi: 10.1016/j.oraloncology.2015.02.012.

Duijvesz, D. *et al.* (2013) 'Proteomic profiling of exosomes leads to the identification of novel biomarkers for prostate cancer', *PloS one*. Public Library of Science, 8(12), p. e82589.

Egeblad, M. and Werb, Z. (2002) 'NEW FUNCTIONS FOR THE MATRIX METALLOPROTEINASES IN CANCER PROGRESSION', *Nature Reviews. Cancer*. London: Nature Publishing Group, 2(3), pp. 161–174. doi: http://dx.doi.org/10.1038/nrc745.

Ellison, D. W. (2010) 'Childhood medulloblastoma: novel approaches to the classification of a heterogeneous disease', *Acta Neuropathologica*, 120(3), pp. 305–316. doi: 10.1007/s00401-010-0726-6.

Epple, L. M. *et al.* (2012) 'Medulloblastoma exosome proteomics yield functional roles for extracellular vesicles', *PLoS ONE*, 7(7). doi: 10.1371/journal.pone.0042064.

Février, B. and Raposo, G. (2004) 'Exosomes: endosomal-derived vesicles shipping extracellular messages', *Current Opinion in Cell Biology*, 16(4), pp. 415–421. doi: http://dx.doi.org/10.1016/j.ceb.2004.06.003.

Fidler, I. J. (1970) 'Metastasis: Quantitative Analysis of Distribution and Fate of Tumor Emboli Labeled With 125I-5-Iodo-2' -deoxyuridine23', *JNCI: Journal of the National Cancer Institute*, 45(4), pp. 773–782. Available at: http://dx.doi.org/10.1093/jnci/45.4.773.

Fingleton, B. *et al.* (2010) 'Cleavage of E-cadherin by matrix metalloproteinase-7 promotes cellular proliferation in nontransformed cell lines via activation of RhoA', *Journal of Oncology*, 2010. doi: 10.1155/2010/530745.

Fiorilli, P. *et al.* (2008) 'Integrins mediate adhesion of medulloblastoma cells to tenascin and activate pathways associated with survival and proliferation', *Laboratory investigation; a journal of technical methods and pathology*, 88(11), pp. 1143–1156. doi: 10.1038/labinvest.2008.89.

Friedman, H. S. *et al.* (1985) 'Establishment and characterization of the human medulloblastoma cell line and transplantable xenograft D283 Med', *Journal of Neuropathology & Experimental Neurology*. American Association of Neuropathologists, Inc., 44(6), pp. 592–605.

Frühbeis, C. *et al.* (2013) 'Neurotransmitter-triggered transfer of exosomes mediates oligodendrocyte–neuron communication', *PLoS biology*. Public Library of Science, 11(7), p. e1001604.

Garcia, N. A. *et al.* (2015) 'Glucose starvation in cardiomyocytes enhances exosome secretion and promotes angiogenesis in endothelial cells', *PloS one*. Public Library of Science, 10(9), p. e0138849.

de Gassart, A. *et al.* (2003) 'Lipid raft-associated protein sorting in exosomes', *Blood*, 102(13), p. 4336 LP-4344. Available at: http://www.bloodjournal.org/content/102/13/4336.abstract.

Gassmann, P. *et al.* (2010) 'In vivo tumor cell adhesion in the pulmonary microvasculature is exclusively mediated by tumor cell - endothelial cell

interaction', *BMC Cancer*, 10(1), p. 177. doi: 10.1186/1471-2407-10-177.

Gerber, N. U. *et al.* (2012) 'A long duration of the prediagnostic symptomatic interval is not associated with an unfavourable prognosis in childhood medulloblastoma', *European Journal of Cancer*, 48(13), pp. 2028–2036. doi: 10.1016/j.ejca.2011.11.012.

Gercel-Taylor, C. *et al.* (2012) 'Nanoparticle analysis of circulating cell-derived vesicles in ovarian cancer patients', *Analytical biochemistry*. Elsevier, 428(1), pp. 44–53.

Gottesman, M. M. and Ambudkar, S. V (2001) 'Overview: ABC Transporters and Human Disease', *Journal of Bioenergetics and Biomembranes*, 33(6), pp. 453–458. doi: 10.1023/A:1012866803188.

Graves, L. E. *et al.* (2004) 'Proinvasive Properties of Ovarian Cancer Ascites-Derived Membrane Vesicles', *Cancer Research*, 64(19), p. 7045 LP-7049. Available at: http://cancerres.aacrjournals.org/content/64/19/7045.abstract.

Greenfield, J. P. and Bilsky, M. H. (2005) 'Neurosurgical Interventions for Leptomeningeal Tumor BT - Leptomeningeal Metastases', in Abrey, L. E., Chamberlain, M. C., and Engelhard, H. H. (eds). Boston, MA: Springer US, pp. 107–119. doi: 10.1007/0-387-24199-X_7.

Gruenberg, J. and Stenmark, H. (2004) 'The biogenesis of multivesicular endosomes', *Nature Reviews. Molecular Cell Biology*. London: Nature Publishing Group, 5(4), pp. 317–323. doi: http://dx.doi.org/10.1038/nrm1360.

Gu, S. *et al.* (2017) 'Proteomic profiling of isogenic primary and metastatic medulloblastoma cell lines reveals differential expression of key metastatic factors', *Journal of Proteomics*. Elsevier, 160, pp. 55–63.

Gupta, G. P. and Massagué, J. (2006) 'Cancer Metastasis: Building a Framework', *Cell*, 127(4), pp. 679–695. doi: http://dx.doi.org/10.1016/j.cell.2006.11.001.

Hanahan, D. and Weinberg, R. A. (2000) 'The hallmarks of cancer.', *Cell*, 100(1), pp. 57–70. doi: 10.1007/s00262-010-0968-0.

Haraguchi, N. *et al.* (2006) 'Characterization of a Side Population of Cancer Cells from Human Gastrointestinal System', *STEM CELLS*. John Wiley & Sons, Ltd., 24(3), pp. 506–513. doi: 10.1634/stemcells.2005-0282.

Harding, C., Heuser, J. and Stahl, P. (1983) 'Receptor-mediated endocytosis of transferrin and recycling of the transferrin receptor in rat reticulocytes.', *The Journal of cell biology*. United States, 97(2), pp. 329–339.

HAUG, B. H. *et al.* (2015) 'Exosome-like extracellular vesicles from MYCN-amplified neuroblastoma cells contain oncogenic miRNAs', *Anticancer research*. International Institute of Anticancer Research, 35(5), pp. 2521–2530.

Hess, C. *et al.* (1999) 'Ectosomes Released by Human Neutrophils Are Specialized Functional Units', *The Journal of Immunology*, 163(8), p. 4564 LP-4573. Available at: http://www.jimmunol.org/content/163/8/4564.abstract.

Holme, S. *et al.* (1997) 'The expression of p-selectin during collection, processing, and storage of platelet concentrates: relationship to loss of in vivo viability', *Transfusion*. Blackwell Science Ltd, 37(1), pp. 12–17. doi: 10.1046/j.1537-2995.1997.37197176945.x.

Hoshino, A. *et al.* (2015) 'Tumour exosome integrins determine organotropic metastasis', *Nature*. NIH Public Access, 527(7578), p. 329.

Hu, G., Drescher, K. M. and Chen, X.-M. (2012) 'Exosomal miRNAs: biological properties and therapeutic potential', *Frontiers in genetics*. Frontiers Media SA, 3.

Huang, X. *et al.* (2013) 'Characterization of human plasma-derived exosomal RNAs by deep sequencing.', *BMC genomics*, 14, p. 319. doi: 10.1186/1471-2164-14-319.

Huber, H. J. and Holvoet, P. (2015) 'Exosomes: emerging roles in communication

between blood cells and vascular tissues during atherosclerosis', *Current opinion in lipidology*. Wolters Kluwer Health, 26(5), p. 412.

Hugel, B. *et al.* (2005) 'Membrane Microparticles: Two Sides of the Coin', *Physiology*, 20(1), p. 22 LP-27. Available at: http://physiologyonline.physiology.org/content/20/1/22.abstract.

Hussein, D. *et al.* (2011) 'Pediatric brain tumor cancer stem cells: cell cycle dynamics, DNA repair, and etoposide extrusion', *Neuro-Oncology*, 13(1), pp. 70–83. Available at: http://dx.doi.org/10.1093/neuonc/noq144.

Isaacson, K. J. *et al.* (2017) 'Matrix-metalloproteinases as targets for controlled delivery in cancer: An analysis of upregulation and expression', *Journal of Controlled Release*, 259, pp. 62–75. doi: http://dx.doi.org/10.1016/j.jconrel.2017.01.034.

Ivanov, D. P. *et al.* (2016) 'In vitro models of medulloblastoma: Choosing the right tool for the job', *Journal of Biotechnology*. Elsevier B.V., 236, pp. 10–25. doi: 10.1016/j.jbiotec.2016.07.028.

Jacobson, S. W. *et al.* (1985) 'The effect of intrauterine PCB exposure on visual recognition memory', *Child development*. JSTOR, pp. 853–860.

Janowska-Wieczorek, A. *et al.* (2005) 'Microvesicles derived from activated platelets induce metastasis and angiogenesis in lung cancer', *International Journal of Cancer*. Wiley Subscription Services, Inc., A Wiley Company, 113(5), pp. 752–760. doi: 10.1002/ijc.20657.

Jaworski, E. *et al.* (2014) 'Human T-lymphotropic virus type 1-infected cells secrete exosomes that contain Tax protein', *Journal of Biological Chemistry*. ASBMB, 289(32), pp. 22284–22305.

Kalra, H. *et al.* (2013) 'Comparative proteomics evaluation of plasma exosome isolation techniques and assessment of the stability of exosomes in normal human

blood plasma', *Proteomics*. Wiley Online Library, 13(22), pp. 3354–3364.

Keles, G. E. *et al.* (1995) 'Establishment and characterization of four human medulloblastoma-derived cell lines', *Oncology Research Featuring Preclinical and Clinical Cancer Therapeutics*. Cognizant Communication Corporation, 7(10–11), pp. 493–503.

Kim, W. *et al.* (2011) 'The tumor biology and molecular characteristics of medulloblastoma identifying prognostic factors associated with survival outcomes and prognosis', *Journal of Clinical Neuroscience*, 18(7), pp. 886–890. doi: http://dx.doi.org/10.1016/j.jocn.2011.01.001.

Kimura, Y. *et al.* (2007) 'Cholesterol fill-in model: mechanism for substrate recognition by ABC proteins', *Journal of Bioenergetics and Biomembranes*, 39(5), pp. 447–452. doi: 10.1007/s10863-007-9109-7.

Kogure, T. *et al.* (2013) 'Extracellular vesicle–mediated transfer of a novel long noncoding RNA TUC339: a mechanism of intercellular signaling in human hepatocellular cancer', *Genes & cancer*. SAGE Publications Sage CA: Los Angeles, CA, 4(7–8), pp. 261–272.

Kombogiorgas, D. *et al.* (2011) 'Appraisal of the current staging system for residual medulloblastoma by volumetric analysis', *Child's Nervous System*, 27(12), pp. 2101–2106. doi: 10.1007/s00381-011-1533-7.

Kongkham, P. N. *et al.* (2008) 'An Epigenetic Genome-Wide Screen Identifies SPINT2 as a Novel Tumor Suppressor Gene in Pediatric Medulloblastoma', *Cancer Research*, 68(23), p. 9945 LP-9953. Available at: http://cancerres.aacrjournals.org/content/68/23/9945.abstract.

Kool, M. *et al.* (2008) 'Integrated Genomics Identifies Five Medulloblastoma Subtypes with Distinct Genetic Profiles, Pathway Signatures and Clinicopathological Features', *PLOS ONE*. Public Library of Science, 3(8), p. e3088.

Available at: https://doi.org/10.1371/journal.pone.0003088.

Kool, M. *et al.* (2012) 'Molecular subgroups of medulloblastoma: an international meta-analysis of transcriptome, genetic aberrations, and clinical data of WNT, SHH, Group 3, and Group 4 medulloblastomas', *Acta Neuropathologica*, 123(4), pp. 473–484. doi: 10.1007/s00401-012-0958-8.

Kowal, J. *et al.* (2016) 'Proteomic comparison defines novel markers to characterize heterogeneous populations of extracellular vesicle subtypes', *Proceedings of the National Academy of Sciences*. National Acad Sciences, 113(8), pp. E968–E977.

Kren, A. *et al.* (2007) 'Increased tumor cell dissemination and cellular senescence in the absence of β1-integrin function', *The EMBO Journal*. EMBO Press, 26(12), pp. 2832–2842. doi: 10.1038/sj.emboj.7601738.

Lakkaraju, A. and Rodriguez-Boulan, E. (2008) 'Itinerant exosomes: emerging roles in cell and tissue polarity', *Trends in Cell Biology*, 18(5), pp. 199–209. doi: http://dx.doi.org/10.1016/j.tcb.2008.03.002.

Landreville, S. *et al.* (2011) 'ABCB1 identifies a subpopulation of uveal melanoma cells with high metastatic propensity', *Pigment Cell and Melanoma Research*, 24(3), pp. 430–437. doi: 10.1111/j.1755-148X.2011.00841.x.

Li, L. *et al.* (2016) 'Exosomes derived from hypoxic oral squamous cell carcinoma cells deliver miR-21 to normoxic cells to elicit a prometastatic phenotype', *Cancer research*. AACR, 76(7), pp. 1770–1780.

Li, Y. *et al.* (2005) 'The Scatter Factor/Hepatocyte Growth Factor: c-Met Pathway in Human Embryonal Central Nervous System Tumor Malignancy', *Cancer Research*, 65(20), p. 9355 LP-9362. Available at: http://cancerres.aacrjournals.org/content/65/20/9355.abstract.

Liotta, L. A. and Paweletz, C. P. (2005) 'Invasion and Metastasis', in *The Cancer*

Handbook. John Wiley & Sons, Ltd. doi: 10.1002/0470025077.chap16.

Lötvall, J. *et al.* (2014) 'Minimal experimental requirements for definition of extracellular vesicles and their functions: a position statement from the International Society for Extracellular Vesicles'. Taylor & Francis.

Lotvall, J. and Valadi, H. (2007) 'Cell to Cell Signalling via Exosomes Through esRNA', *Cell Adhesion & Migration*. Taylor & Francis, 1(3), pp. 156–158. doi: 10.4161/cam.1.3.5114.

Louis, D. N. *et al.* (2007) 'The 2007 WHO Classification of Tumours of the Central Nervous System', *Acta Neuropathologica*. Berlin/Heidelberg: Springer-Verlag, 114(2), pp. 97–109. doi: 10.1007/s00401-007-0243-4.

Lu, X. and Kang, Y. (2007) 'Organotropism of Breast Cancer Metastasis', *Journal of Mammary Gland Biology and Neoplasia*, 12(2), p. 153. doi: 10.1007/s10911-007-9047-3.

Masyuk, A. I. *et al.* (2010) 'Biliary exosomes influence cholangiocyte regulatory mechanisms and proliferation through interaction with primary cilia', *American Journal of Physiology - Gastrointestinal and Liver Physiology*, 299(4), p. G990 LP-G999. Available at: http://ajpgi.physiology.org/content/299/4/G990.abstract.

Melo, S. A. *et al.* (2014) 'Cancer exosomes perform cell-independent microRNA biogenesis and promote tumorigenesis', *Cancer cell*. Elsevier, 26(5), pp. 707–721.

Menck, K. *et al.* (2013) 'Induction and transport of WNT 5a during macrophage-induced malignant invasion is mediated by two types of extracellular vesicles', *Oncotarget*. Impact Journals, LLC, 4(11), p. 2057.

Menck, K. *et al.* (2014) 'Tumor-derived microvesicles mediate human breast cancer invasion through differentially glycosylated EMMPRIN', J*ournal of Molecular Cell Biology*. 7, pp. 143-153.

Milde, T. *et al.* (2012) 'HD-MB03 is a novel Group 3 medulloblastoma model

demonstrating sensitivity to histone deacetylase inhibitor treatment', *Journal of neuro-oncology*. Springer, 110(3), pp. 335–348.

Mitchell, K. *et al.* (2001) ' Functional analysis of secreted and transmembrane proteins critical to mouse development', *Nature genetics*. 28, pp. 241 - 249.

Muller, L. *et al.* (2014) 'Isolation of biologically-active exosomes from human plasma', *Journal of immunological methods*. Elsevier, 411, pp. 55–65.

Nelson, W. J. and Nusse, R. (2004) 'Convergence of WNT, beta-catenin, and cadherin pathways.', *Science (New York, N.Y.)*, 303(5663), pp. 1483–7. doi: 10.1126/science.1094291.

van Niel, G. *et al.* (2006) 'Exosomes: A Common Pathway for a Specialized Function', *The Journal of Biochemistry*, 140(1), pp. 13–21. Available at: http://dx.doi.org/10.1093/jb/mvj128.

Northcott, P. A. *et al.* (2011) 'Pediatric and adult sonic hedgehog medulloblastomas are clinically and molecularly distinct', *Acta Neuropathologica*, 122(2), pp. 231–240. doi: 10.1007/s00401-011-0846-7.

Northcott, P.A., Jones, D.T.W., *et al.,* 2012a. Medulloblastomics: the end of the beginning. Nature reviews. Cancer, 12(12), pp.818–34. Available at: http://dx.doi.org/10.1038/nrc3410 [Accessed March 20, 2014].

Ogawa, Y. *et al.* (2011) 'Proteomic Analysis of Two Types of Exosomes in Human Whole Saliva', *Biological and Pharmaceutical Bulletin*, 34(1), pp. 13–23. doi: 10.1248/bpb.34.13.

Ohshima, K. *et al.* (2010) 'Let-7 microRNA family is selectively secreted into the extracellular environment via exosomes in a metastatic gastric cancer cell line', *PloS one*. Public Library of Science, 5(10), p. e13247.

Othman, R. T. *et al.* (2014) 'Overcoming multiple drug resistance mechanisms in medulloblastoma', *Acta Neuropathologica Communications*, 2(1), p. 57. doi:

10.1186/2051-5960-2-57.

Paget, S. (1889) 'The distribution of secondary growths in cancer of the breast.', *The Lancet*, 133(3421), pp. 571–573. doi: http://dx.doi.org/10.1016/S0140-6736(00)49915-0.

Parolini, I. *et al.* (2009) 'Microenvironmental pH is a key factor for exosome traffic in tumor cells', *Journal of Biological Chemistry*. ASBMB, 284(49), pp. 34211–34222.

Paterson, E. K. *et al.* (2017) '814 Tks5 and invadopodia function in melanoma growth and metastasis', *Journal of Investigative Dermatology*. Elsevier, 137(5), p. S140.

Peinado, H. *et al.* (2012) 'Melanoma exosomes educate bone marrow progenitor cells toward a pro-metastatic phenotype through MET', *Nature medicine*. Nature Research, 18(6), pp. 883–891.

Pisitkun, T., Shen, R.-F. and Knepper, M. A. (2004) 'Identification and proteomic profiling of exosomes in human urine', *Proceedings of the National Academy of Sciences of the United States of America* , 101(36), pp. 13368–13373. doi: 10.1073/pnas.0403453101.

Pizer, B. L. and Clifford, S. C. (2009) 'The potential impact of tumour biology on improved clinical practice for medulloblastoma: progress towards biologically driven clinical trials.', *British journal of neurosurgery*. England, 23(4), pp. 364–375. doi: 10.1080/02688690903121807.

van der Pol, E. *et al.* (2012) 'Single vs. swarm detection of microparticles and exosomes by flow cytometry.', *Journal of thrombosis and haemostasis : JTH*. England, 10(5), pp. 919–930. doi: 10.1111/j.1538-7836.2012.04683.x.

Polkinghorn, W. R. and Tarbell, N. J. (2007) 'Medulloblastoma: tumorigenesis, current clinical paradigm, and efforts to improve risk stratification', *Nat Clin Prac*

Oncol. Nature Publishing Group, 4(5), pp. 295–304. Available at: http://dx.doi.org/10.1038/ncponc0794.

Posner, J. B. (1996) 'Brain metastases: 1995. A brief review', *Journal of Neuro-Oncology*, 27(3), pp. 287–293. doi: 10.1007/BF00165486.

Provenzano, P. P., Eliceiri, K. W. and Keely, P. J. (2009) 'Multiphoton microscopy and fluorescence lifetime imaging microscopy (FLIM) to monitor metastasis and the tumor microenvironment', *Clinical & Experimental Metastasis*, 26(4), pp. 357–370. doi: 10.1007/s10585-008-9204-0.

Rao, J. S. *et al.* (2007) 'MMP-9 Short Interfering RNA Induced Senescence Resulting in Inhibition of Medulloblastoma Growth via p16INK4a and Mitogen-Activated Protein Kinase Pathway', *Cancer Research*. American Association for Cancer Research, 67(10), pp. 4956–4964. doi: 10.1158/0008-5472.CAN-07-0380.

Raposo, G. *et al.* (1996) 'B lymphocytes secrete antigen-presenting vesicles.', *The Journal of Experimental Medicine*, 183(3), p. 1161 LP-1172. Available at: http://jem.rupress.org/content/183/3/1161.abstract.

Raposo, G. and Stoorvogel, W. (2013) 'Extracellular vesicles: Exosomes, microvesicles, and friends', *The Journal of Cell Biology*, 200(4), p. 373 LP-383. Available at: http://jcb.rupress.org/content/200/4/373.abstract.

Ratajczak, J. *et al.* (2006) 'Membrane-derived microvesicles: important and underappreciated mediators of cell-to-cell communication', *Leukemia*. London: Nature Publishing Group, 20(9), pp. 1487–1495. doi: http://dx.doi.org/10.1038/sj.leu.2404296.

Redzic, J. S. *et al.* (2013) 'Extracellular vesicles secreted from cancer cell lines stimulate secretion of MMP-9, IL-6, TGF-β1 and EMMPRIN', *PloS one*. Public Library of Science, 8(8), p. e71225.

Reed, J. C. (2000) 'Mechanisms of Apoptosis', *The American Journal of Pathology*, 157(5), pp. 1415–1430. doi: http://dx.doi.org/10.1016/S0002-9440(10)64779-7.

Remke, M. *et al.* (2011) 'Adult Medulloblastoma Comprises Three Major Molecular Variants', *Journal of Clinical Oncology*. American Society of Clinical Oncology, 29(19), pp. 2717–2723. doi: 10.1200/JCO.2011.34.9373.

Rochkind, S. *et al.* (1991) 'Extracranial metastases of medulloblastoma in adults: literature review.', *Journal of Neurology, Neurosurgery & Psychiatry*. BMJ Publishing Group Ltd, 54(1), pp. 80–86. doi: 10.1136/jnnp.54.1.80.

Rong, S. *et al.* (1994) 'Invasiveness and metastasis of NIH 3T3 cells induced by Met-hepatocyte growth factor/scatter factor autocrine stimulation', *Proceedings of the National Academy of Sciences* , 91(11), pp. 4731–4735. Available at: http://www.pnas.org/content/91/11/4731.abstract.

Ronquist, G. and Brody, I. (1985) 'The prostasome: its secretion and function in man', *Biochimica et Biophysica Acta (BBA) - Reviews on Biomembranes*, 822(2), pp. 203–218. doi: http://dx.doi.org/10.1016/0304-4157(85)90008-5.

ROSENTHAL, E. L. *et al.* (1999) 'Role of membrane type 1–matrix metalloproteinase and gelatinase A in head and neck squamous cell carcinoma invasion in vitro', *Otolaryngology - Head and Neck Surgery*, 121(4), pp. 337–343. doi: http://dx.doi.org/10.1016/S0194-5998(99)70217-2.

Rudin, C. M. *et al.* (2009) 'Treatment of Medulloblastoma with Hedgehog Pathway Inhibitor GDC-0449', *New England Journal of Medicine*. Massachusetts Medical Society, 361(12), pp. 1173–1178. doi: 10.1056/NEJMoa0902903.

Sadighi, Z., Vats, T. and Khatua, S. (2012) 'Childhood Medulloblastoma', *Journal of Child Neurology*. SAGE Publications Inc, 27(10), pp. 1302–1307. doi: 10.1177/0883073812449690.

Schorey, J. S. and Bhatnagar, S. (2008) 'Exosome Function: From Tumor Immunology to Pathogen Biology', *Traffic*. Blackwell Publishing Ltd, 9(6), pp. 871–881. doi: 10.1111/j.1600-0854.2008.00734.x.

Scotting, P. J., Walker, D. A. and Perilongo, G. (2005) 'Opinion: Childhood solid tumours: a developmental disorder', *Nature Reviews. Cancer*. London: Nature Publishing Group, 5(6), pp. 481–488. doi: http://dx.doi.org/10.1038/nrc1633.

Sensorn, I. *et al.* (2016) 'ABCB1 and ABCC2 and the risk of distant metastasis in Thai breast cancer patients treated with tamoxifen', *OncoTargets and therapy*. Dove Medical Press, 9, pp. 2121–2129. doi: 10.2147/OTT.S100905.

Skog, J. *et al.* (2008) 'Glioblastoma microvesicles transport RNA and proteins that promote tumour growth and provide diagnostic biomarkers', *Nature Cell Biology*, 10(12), pp. 1470–1476. doi: 10.1038/ncb1800.

Smalley, D. M. *et al.* (2008) 'Isolation and identification of potential urinary microparticle biomarkers of bladder cancer', *Journal of proteome research*. ACS Publications, 7(5), pp. 2088–2096.

Soo, C. Y. *et al.* (2012) 'Nanoparticle tracking analysis monitors microvesicle and exosome secretion from immune cells', *Immunology*. Blackwell Publishing Ltd, 136(2), pp. 192–197. doi: 10.1111/j.1365-2567.2012.03569.x.

Steinbichler, T. B. *et al.* (2017) 'The role of exosomes in cancer metastasis', *Seminars in Cancer Biology*, 44(Supplement C), pp. 170–181. doi: https://doi.org/10.1016/j.semcancer.2017.02.006.

Sternlicht, M. D. and Werb, Z. (2001) 'How Matrix Metalloproteinases Regulate Cell Behavior', *Annual Review of Cell and Developmental Biology*. Annual Reviews, 17(1), pp. 463–516. doi: 10.1146/annurev.cellbio.17.1.463.

Taylor, M. D. *et al.* (2012) 'Molecular subgroups of medulloblastoma: The current consensus', *Acta Neuropathologica*, 123(4), pp. 465–472. doi: 10.1007/s00401-

011-0922-z.

Taylor, R. E. *et al.* (2005) 'Outcome for patients with metastatic (M2–3) medulloblastoma treated with SIOP/UKCCSG PNET-3 chemotherapy', *European Journal of Cancer*, 41(5), pp. 727–734. doi: http://dx.doi.org/10.1016/j.ejca.2004.12.017.

Théry, C. *et al.* (2006) 'Isolation and Characterization of Exosomes from Cell Culture Supernatants and Biological Fluids', in *Current Protocols in Cell Biology*. John Wiley & Sons, Inc. doi: 10.1002/0471143030.cb0322s30.

Thompson, M. C. *et al.* (2006) 'Genomics Identifies Medulloblastoma Subgroups That Are Enriched for Specific Genetic Alterations', *Journal of Clinical Oncology*. American Society of Clinical Oncology, 24(12), pp. 1924–1931. doi: 10.1200/JCO.2005.04.4974.

Toiyama, Y. *et al.* (2016) 'Circulating cell-free microRNAs as biomarkers for colorectal cancer', *Surgery today*. Springer, 46(1), pp. 13–24.

Tong, C. Y. K. *et al.* (2004) 'Detection of oncogene amplifications in medulloblastomas by comparative genomic hybridization and array-based comparative genomic hybridization', *Journal of Neurosurgery: Pediatrics*. Journal of Neurosurgery Publishing Group, 100(2), pp. 187–193. doi: 10.3171/ped.2004.100.2.0187.

Valadi, H. *et al.* (2007) 'Exosome-mediated transfer of mRNAs and microRNAs is a novel mechanism of genetic exchange between cells', *Nature cell biology*. Nature Publishing Group, 9(6), p. 654.

Vella, L. J. *et al.* (2008) 'Enrichment of prion protein in exosomes derived from ovine cerebral spinal fluid', *Veterinary Immunology and Immunopathology*, 124(3), pp. 385–393. doi: http://dx.doi.org/10.1016/j.vetimm.2008.04.002.

Vince, G. H. *et al.* (2001) 'Medulloblastoma Displays Distinct Regional Matrix

Metalloprotease Expression', *Journal of Neuro-Oncology*, 53(2), pp. 99–106. doi: 10.1023/A:1012241031138.

Wirtz, D., Konstantopoulos, K. and Searson, P. P. C. (2011) 'The physics of cancer: the role of physical interactions and mechanical forces in metastasis', *Nat. Rev. Cancer*, 11(7), pp. 512–522. doi: 10.1038/nrc3080.The.

Xu, J. et al. (2012) 'Novel cell lines established from pediatric brain tumors', *Journal of Neuro-Oncology*, 107 (2), pp. 269-280.

Yagi, Y. *et al.* (2017) 'Next-generation sequencing-based small RNA profiling of cerebrospinal fluid exosomes', *Neuroscience letters*. Elsevier, 636, pp. 48–57.

Yu, S. *et al.* (2007) 'Tumor exosomes inhibit differentiation of bone marrow dendritic cells', *The Journal of Immunology*. Am Assoc Immnol, 178(11), pp. 6867–6875.

Zarovni, N. *et al.* (2015) 'Integrated isolation and quantitative analysis of exosome shuttled proteins and nucleic acids using immunocapture approaches', *Methods*. Elsevier, 87, pp. 46–58.

Zeng, A.-L. *et al.* (2017) 'Tumour exosomes from cells harbouring PTPRZ1–MET fusion contribute to a malignant phenotype and temozolomide chemoresistance in glioblastoma', *Oncogene*, (300), pp. 1–13. doi: 10.1038/onc.2017.134.

Zhang, X. *et al.* (2015) 'Exosomes in cancer: small particle, big player.', *Journal of hematology & oncology*. Journal of Hematology & Oncology, 8, p. 83. doi: 10.1186/s13045-015-0181-x.

Zhu, H. *et al.* (2013) 'Mutation of SIMPLE in Charcot–Marie–Tooth 1C alters production of exosomes', *Molecular biology of the cell*. Am Soc Cell Biol, 24(11), pp. 1619–1637.